

© Elsevier 2015

## It's All in the Water: Studies of Materials and Conditions in Fresh and Salt Water Bodies

Journal of  
Materials Research

Volume 30

Edited by Robert F. Heitsch, University of Michigan

Editorial Board: Robert F. Heitsch and Deborah A. Hoelzer

# **It's All in the Water: Studies of Materials and Conditions in Fresh and Salt Water Bodies**



ACS SYMPOSIUM SERIES **1086**

# **It's All in the Water: Studies of Materials and Conditions in Fresh and Salt Water Bodies**

**Mark A. Benvenuto**, Editor

*University of Detroit Mercy, Detroit, Michigan*

**Elizabeth S. Roberts-Kirchhoff**, Editor

*University of Detroit Mercy, Detroit, Michigan*

**Meghann N. Murray**, Editor

*University of Detroit Mercy, Detroit, Michigan*

**Danielle M. Garshott**, Editor

*University of Detroit Mercy, Detroit, Michigan*

**Sponsored by the  
ACS Division of Environmental Chemistry, Inc.**



American Chemical Society, Washington, DC

Distributed in print by Oxford University Press, Inc.



## Library of Congress Cataloging-in-Publication Data

It's all in the water : studies of materials and conditions in fresh and salt water bodies / Mark A. Benvenuto ... [et al.], editor[s] ; sponsored by the ACS Division of Environmental Chemistry, Inc.

p. cm. -- (ACS symposium series ; 1086)

Includes bibliographical references and index.

ISBN 978-0-8412-2634-0 (alk. paper)

1. Water--Analysis. 2. Water--Pollution. I. Benvenuto, Mark. II. American Chemical Society. Division of Environmental Chemistry.

QD142.I85 2011

628.1--dc23

2011046255

The paper used in this publication meets the minimum requirements of American National Standard for Information Sciences—Permanence of Paper for Printed Library Materials, ANSI Z39.48n1984.

Copyright © 2011 American Chemical Society

Distributed in print by Oxford University Press, Inc.

All Rights Reserved. Reprographic copying beyond that permitted by Sections 107 or 108 of the U.S. Copyright Act is allowed for internal use only, provided that a per-chapter fee of \$40.25 plus \$0.75 per page is paid to the Copyright Clearance Center, Inc., 222 Rosewood Drive, Danvers, MA 01923, USA. Republication or reproduction for sale of pages in this book is permitted only under license from ACS. Direct these and other permission requests to ACS Copyright Office, Publications Division, 1155 16th Street, N.W., Washington, DC 20036.

The citation of trade names and/or names of manufacturers in this publication is not to be construed as an endorsement or as approval by ACS of the commercial products or services referenced herein; nor should the mere reference herein to any drawing, specification, chemical process, or other data be regarded as a license or as a conveyance of any right or permission to the holder, reader, or any other person or corporation, to manufacture, reproduce, use, or sell any patented invention or copyrighted work that may in any way be related thereto. Registered names, trademarks, etc., used in this publication, even without specific indication thereof, are not to be considered unprotected by law.

PRINTED IN THE UNITED STATES OF AMERICA

# Foreword

The ACS Symposium Series was first published in 1974 to provide a mechanism for publishing symposia quickly in book form. The purpose of the series is to publish timely, comprehensive books developed from the ACS sponsored symposia based on current scientific research. Occasionally, books are developed from symposia sponsored by other organizations when the topic is of keen interest to the chemistry audience.

Before agreeing to publish a book, the proposed table of contents is reviewed for appropriate and comprehensive coverage and for interest to the audience. Some papers may be excluded to better focus the book; others may be added to provide comprehensiveness. When appropriate, overview or introductory chapters are added. Drafts of chapters are peer-reviewed prior to final acceptance or rejection, and manuscripts are prepared in camera-ready format.

As a rule, only original research papers and original review papers are included in the volumes. Verbatim reproductions of previous published papers are not accepted.

## ACS Books Department

# Preface

“Water, water, every where,  
And all the boards did shrink;  
Water, water, every where,  
Nor any drop to drink.”

When Samuel Taylor Coleridge penned “The Rime of the Ancient Mariner” over two centuries ago, his mariner and sailors were distraught almost to the point of madness over being at sea without fresh water. Like Coleridge’s characters, we rejoice in clean waters today – for a variety of personal, commercial, and industrial uses – and can lament not only brackish water when the need is for fresh, but also the degradation and pollution of our planet’s salt waters. While this problem has existed for millennia, indeed for all the time mankind has lived by water, it has become a matter of great concern within the past fifty years, as the human population of the planet has grown rapidly.

Perhaps only air is more important to life on Earth than water, but even this point may be argued. The analysis of water, specifically fresh and salt water bodies upon which humans depend for daily drinking water, food, transportation, industrial feedstock, resources, and livelihood, becomes more important each year as these bodies are stressed by human interactions, use, and depletion. The quality of fresh water, littoral waters, and even deep ocean waters has thus drawn increasing attention in the recent past from academia, industry, government and the general public (*1*); and this makes it a timely symposium subject, despite an established history of research into the substance (*2–16*), a number of well-written issues of various laymen’s journals (*17–21*), and even growing coverage of the subject in the news media (*22–25*).

To perform the analyses of various waters, and to determine the relative purity of waters and a diverse array of possible contaminants within them, requires numerous different analytical techniques and forms of instrumentation. Researchers who engage in such work often must utilize the talents of those with expertise in fields including: analytical chemistry, biochemistry, inorganic and organic chemistry, microbiology, and botany, as well as chemical and mechanical engineering, to name a few.

The purpose of this volume, based on the symposium of the same name presented at the 241<sup>st</sup> meeting of the American Chemical Society, in Anaheim, California, in the spring of 2011, sponsored by the Environmental Chemistry Division, is to gather into one place the results and findings of current researchers from widely separated laboratories and centers in different areas. Because of the different aims of these researchers’ individual studies, the results gathered here would normally be published in a rather broadly spread out and diversified series

of professional journals. There is definitely a value in presenting these results in a single volume.

We have divided the papers into sections based simply on what water medium was studied, fresh or salt. Barashkov's work on water purity examines the disinfection of drinkable water, as does Hsu's. Shea and Van Engelen each examine plant interactions with fresh water and soil; and Armitage looks closely and keenly at pharmaceuticals in river water.

The chapters concerning salt water include Zhang's study of marine coatings, Tarr's excellent work on the after effects of the Deepwater Horizon spill, and our study of the metals taken up by kelp, which remains in the plant material as it becomes a marketable food supplement.

The study, examination, and monitoring of fresh and salt waters continues, and indeed must continue, so long as humanity continues to need, use, and put stress on existing sources and bodies of water. We believe the papers collected here can be an important part of this larger, continuing study.

## References

1. Jiao, N.; Azam, F.; Sander, S. Microbial carbon pump in the ocean. *Science Supplement*, May 13, 2011.
2. *Saline Water Conversion*; ACS Advances in Chemistry Series 27; American Chemical Society: Washington, DC, 1960.
3. Gould, R. F., Ed.; *Saline Water Conversion—II*; ACS Advances in Chemistry Series 38; American Chemical Society: Washington, DC, 1963.
4. Lustenader, E. L. Saline Water Conversion by the Diffusion Still. In *Saline Water Conversion—II*; ACS Advances in Chemistry Series 38; American Chemical Society: Washington, DC, 1963; Chapter 7, pp 86–98.
5. Dodge, B. F. Review of Distillation Processes for the Recovery of Fresh Water from Saline Waters. In *Saline Water Conversion—II*; ACS Advances in Chemistry Series 38; American Chemical Society: Washington, DC, 1963; Chapter 1, pp 1–26.
6. Kavanaugh, M. C., Leckie, J. O., Eds.; *Particulates in Water: Characterization, Fate, Effects, and Removal*; ACS Advances in Chemistry Series 189; American Chemical Society: Washington, DC, 1980.
7. Baker, A., Ed.; *Environmental Chemistry of Lakes and Reservoirs*; ACS Advances in Chemistry Series 237; American Chemical Society: Washington, DC, 1994.
8. *Letter Report Assessing the USGS National Water Quality Assessment Program's Science Plan*. National Academies Press: Washington, DC, 2011.
9. *Management and Effects of Coalbed Methane Produced Water in the United States*. National Academies Press: Washington, DC, 2010.
10. *Letter Report Assessing the USGS National Water Quality Assessment Program's Science Framework*. National Academies Press: Washington, DC, 2010.
11. *Urban Stormwater Management in the United States*. National Academies Press: Washington, DC, 2009.



12. *Nutrient Control Actions for Improving Water Quality in the Mississippi River Basin and Northern Gulf of Mexico*. National Academies Press: Washington, DC, 2009.
13. Thompson, K. C., Gray, J., Eds.; *Water Contamination Emergencies: Can We Cope?*; Royal Society of Chemistry: London, 2004; ISBN: 9780854046287.
14. Thompson, K. C., Gray, J., Eds.; *Water Contamination Emergencies: Enhancing our Response*, Royal Society of Chemistry: London, 2006; ISBN: 9780854046584.
15. Binnie, C., Kimber, M. *Basic Water Treatment*, 4th ed.; Royal Society of Chemistry: London, 2009, ISBN 9781847558787.
16. Snyder, S., organizer; *The Business of Water: Problems, Solutions, and Opportunities for the Chemical Enterprise*; *Council for Chemical Research*, 30th Anniversary Annual Meeting.
17. Ball, A. P. *Why Water Is Weird*. Royal Society of Chemistry, 2011. [http://www.thereaction.net/events/y2011/weird\\_water.aspx](http://www.thereaction.net/events/y2011/weird_water.aspx).
18. Water: The Power, Promise, and Turmoil of North America's Fresh Water. *National Geographic*, November, 1993.
19. Gorbachev, M., Ed.; Water: The Globe's Most Precious Resource, the World's Most Pressing Problem. *Civilization, A Special Section*, October/November 2000.
20. Water: Our Thirsty World. *National Geographic*, A Special Issue, April 2010.
21. Troubled Waters: Are We Emptying the Oceans? *Virginia Quarterly Review*, Summer, 2011, Volume 87, Number 3.
22. Harvard Medical Advisor, Pharmaceutical and Personal Care Products, *The Detroit Free Press*, July 3, 2011, p D4.
23. Utah Waterways Test Positive for Prescription Drugs. *KSL TV*. <http://www.ksl.com/?nid=148&sid=3959442>
24. Area Tap Water Has Traces of Medicines. *The Washington Post*, March 10, 2008, p B01.
25. The Future of Fish. *Time*, July 18, 2011, pp 28–36.

## Chapter 1

# Formation, Adsorption, and Stability of *N*-Nitrosoatrazine in Water and Soil

Hsin-Ro Wei, Martha G. Rhoades, and Patrick J. Shea\*

School of Natural Resources, University of Nebraska-Lincoln,  
Lincoln, Nebraska 68583

\*E-mail: psheal@unl.edu

The products of xenobiotic reactions may pose risks greater than parent compounds. Products of concern include nitrosamines, which can be carcinogenic, mutagenic, and teratogenic. Nitrosamines may form in soil, lake water, sewage, and agricultural soils after applying nitrogen fertilizer and pesticides containing amine moieties. The herbicide atrazine has secondary amine moieties that react with nitrite to form *N*-nitrosoatrazine (NNAT). We studied NNAT formation, stability, and adsorption in water and soil. NNAT formed most readily in solution at pH 2-4 and in soil at pH  $\leq 5$ . Acetic acid and fulvic acid promoted NNAT formation in water at pH 4-7. In soil NNAT formed after 7 d at pH 4 and 14 d at pH 5, but none was found at pH 6 and 7. No NNAT was detected in oversaturated or anaerobic soil, indicating the importance of oxygen in the reaction. Adsorption  $K_d$  and  $K_{oc}$  values show greater adsorption of NNAT (average  $K_d = 5.93$ ;  $K_{oc} = 495$ ) than atrazine (average  $K_d = 2.71$ ;  $K_{oc} = 123$ ) in Aksarben silty clay loam at agronomic pH. A larger desorption  $K_d$  indicates greater hysteresis of NNAT than atrazine. NNAT half-life in Aksarben soil was approximately 9 d, with degradation to atrazine and other compounds.

The transformation products of xenobiotics in environmental matrices and mammalian systems may pose risks equal to or greater than the parent compounds. Reaction products of concern include nitrosamines, which can be carcinogenic, mutagenic, and teratogenic, and may affect nitric oxide (NO) levels in cells, critical in signaling growth and biological functioning (1, 2). Low concentrations of nitrosamines have been found in food, beverages, sunscreens, cosmetics, pesticide products, cigarette smoke, and automotive exhaust fumes (3, 4).

Previous research indicates that nitrosamines may form in soil, lake water, and sewage, affecting ecosystems (3, 5–10). Nitrosamines can form in agricultural soils treated with pesticides and veterinary pharmaceuticals containing secondary amine moieties and receiving heavy applications of nitrogen fertilizer (3, 5–7, 11–13). The reaction is promoted at acidic pH (3, 11, 14). Nitrosation of organic compounds generally requires conversion of nitrite to nitrous acid (pKa = 2.8, (15)), which explains why nitrosation is catalyzed at acidic pH. Under these conditions the HNO<sub>2</sub> is converted to the nitrous acidium ion (H<sub>2</sub>NO<sub>2</sub><sup>+</sup>), which subsequently forms the nitrosonium ion (NO<sup>+</sup>), a strong nitrosating agent (Figure 1; (3)).

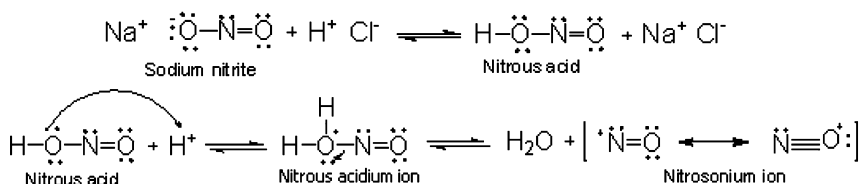


Figure 1. Conversion of nitrite to the nitrosonium ion.

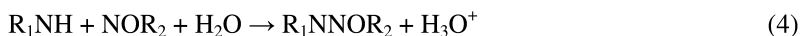
In aqueous solution, HNO<sub>2</sub> is in equilibration with dinitrogen trioxide (N<sub>2</sub>O<sub>3</sub>), which is also a highly effective nitrosating agent (Eq. 1 (4)):



The presence of non-basic nucleophiles (X<sup>-</sup>) can result in the formation of a third nitrosating species, XNO (Eq. 2 (30)):



Secondary amines react with nitrite via the nitrosonium ion (NO<sup>+</sup>) under acidic conditions to form nitrosamine derivatives (Eqs. 3 and 4 and Figure 2 (4)(16)):



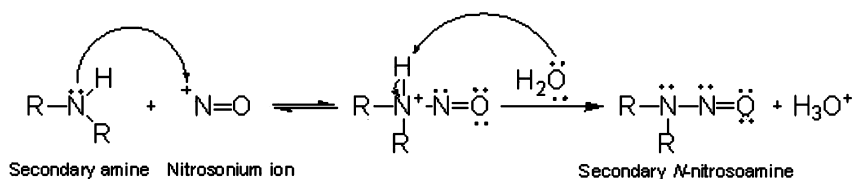


*Figure 2. Formation of N-nitrosamines from secondary amines and the nitrosonium ion.*

The herbicide atrazine, used in agriculture world-wide, is a weak base ( $\text{pK}_a = 1.68$ ; (17)) with two secondary amine groups and is nitrosatable (16). Little is known about the formation, availability and fate of N-nitrosoatrazine (NNAT) in soil. NNAT was slightly less mobile than atrazine in four soils tested by Kearney et al. (6). Young et al. (18) found that NNAT was relatively stable in solution and soil, although Wolfe et al. (19) reported rapid decomposition under light and acidic conditions in water to atrazine and DEA. Kearney et al. (6) found denitrosation was a primary mechanism of NNAT transformation, because atrazine was the major product identified in the soil extracts. However, Oliver et al. (20) and Tate and Alexander (9) reported that biodegradation was primarily responsible for the degradation of nitrosamines in soil.

The objective of this research was to characterize the formation, adsorption, and stability of NNAT in water and soil.

## Experimental

### Herbicides, Soils, and Reagents

Herbicides not available in our laboratory inventory were purchased from Chem Service (West Chester, PA). NNAT was prepared following the procedure of Mirvish et al. (3). Soil (Table I) was available in our laboratory inventory. Sodium nitrite ( $\text{NaNO}_2$ ) and humic acid were obtained from Sigma-Aldrich (*St. Louis, MO*). Sodium hydroxide ( $\text{NaOH}$ ), hydrochloric acid ( $\text{HCl}$ ), and acetic acid were obtained from Fisher Scientific (Fair Lawn, NJ). Fulvic acid was prepared following the procedure of Black (21). Unrefined, dissolved organic matter was prepared by mixing 10 mL deionized, distilled (DD) water with 1 mg Histosol soil (98% organic matter, obtained from North Carolina, U.S.A) and filtering to remove the solids.

**Table I. Properties of the soils used in the experiments**

<i>Property</i>	<i>Aksarben</i>	<i>Valentine</i>	<i>Rosebud</i>
Sand (%)	11	88	40
Silt (%)	58	6	50
Clay (%)	31	6	10
organic matter (%)	2.2	0.6	2.7
pH	6.3	5.6	7.6
CEC (cmol+/kg)	20.3	8	22.2
K (% base saturation)	3.2	5.3	6.9
Mg (% base sat.)	23.6	12.4	4.8
Ca (% base sat.)	62.9	58.1	88.3

### Formation of *N*-Nitrosoatrazine in Water and Soil

The 'nitrosation assay procedure' (NAP test; (22)) was used to determine nitrosation of atrazine in aqueous solution. In the NAP test the secondary amine is reacted with sodium nitrite at a 1:4 molar ratio in deionized, distilled (DD) water at room temperature. In our experiments 10 mL of 0.4 mM sodium nitrite was mixed with 10 mL of a 0.1 mM solution of atrazine in a Teflon tube and pH was adjusted to 2-7 with 1.0 M HCl and 0.1 M NaOH. Samples were removed for HPLC analysis to monitor NNAT formation and loss of atrazine during two weeks of incubation at room temperature under aerobic and anaerobic conditions. In some tests, acetic acid or humic acid (100  $\mu$ L of 100 mg/L solution), fulvic acid (100  $\mu$ L of aqueous extract from organic matter), or unrefined dissolved organic matter (100  $\mu$ L) were added to evaluate their impact on nitrosation of atrazine.

For soil experiments, Aksarben soil was prepared by adding 10 mL DD water to 10 g air-dried soil and allowing it to drain by gravity (to determine soil water-holding capacity). After 24 h, the soil contained 7.5 mL water, and this amount was added to air-dry soil in subsequent experiments. The pH of the soil was adjusted to 4, 5, 6, and 7 with 1.0 M HCl and 0.1 M NaOH. Sodium nitrite (5.26 mg) and 0.02 mg of atrazine (nitrite:atrazine molar ratio of 156:1) were added in 7.5 mL DD water and the tubes were incubated for 3, 7, 14, and 28 d, following the general procedures of Kearney et al. (6) and Khan and Young (12). The soil was extracted for 1 h twice with 10 mL of acetonitrile, extracts were centrifuged at 5000 rpm for 15 min, and 1 mL of supernatant was removed for HPLC analysis. This experiment was repeated in oversaturated soil under aerobic conditions and in an anaerobic chamber (Coy Laboratory Products Inc., Grass Lake, MI) to determine the influence of soil oxygen on nitrosation. "Oversaturated" soil was prepared by adding 15 mL water to 10 g of air-dried soil in a Teflon tube. For anaerobic chamber experiments, the water was degassed with nitrogen.

## Adsorption of *N*-Nitrosoatrazine in Soil

Soil adsorption of NNAT was determined by adding 2 g air-dried Aksarben soil to Teflon tubes with 10 mL DD water and 12  $\mu\text{g}$  NNAT (6 mg/kg Aksarben soil). The pH was adjusted to 3-8 with 1M HCl and 0.1M NaOH, and the tubes were shaken for 24 h at 25°C. The suspensions were centrifuged and concentrations of NNAT in the supernatant were determined by HPLC. Desorption was determined by decanting the remaining supernatant, adding 10 mL DD water to the soil, shaking for 24 h at 25°C, and determining the concentrations of the compounds by HPLC. The experiment was repeated with atrazine for comparison with NNAT.

Adsorption and desorption distribution coefficients ( $K_d$ ) and organic carbon partition coefficient ( $K_{oc}$ ) were calculated as follows (Eqs. 5 and 6):

$$K_d = q / C \quad (5)$$

$$K_{oc} = K_d / f_{oc} \quad (6)$$

where  $q$  is atrazine or NNAT adsorbed ( $\mu\text{mol}/\text{kilogram}$  soil),  $C$  is micromoles of atrazine or NNAT per liter of supernatant after equilibration, and  $f_{oc}$  is the organic carbon fraction of the soil.

## Stability in Solution and Soil

For solution experiments, 10 mL of 45  $\mu\text{M}$  NNAT was placed in Teflon tubes and incubated under dark (tubes wrapped in foil) and light (laboratory/natural daylight) conditions. Solution pH was adjusted to 4, 6, and 8 with 1.0 M HCl and 0.1 M NaOH. The solution was subsampled on 2, 4, 7, 10, 14, 21, 31, 37, 50, and 60 d and analyzed by HPLC over a two week period.

In soil experiments, 10 g air-dried Aksarben soil was placed in Teflon tubes containing 6.5 mL DD water and 50  $\mu\text{g}$  parent compound or nitrosated product. Samples were incubated for 3, 5, 7, 9, and 14 d under aerobic conditions at 25 °C. Extractions were performed by shaking equal amounts of moist soil with 20 mL acetonitrile for 1 h twice. The extracts were centrifuged at 5000 rpm for 15 min and analyzed by HPLC. This experiment was repeated, following the same procedure, after adjusting soil pH to 4, 6, and 7 with 1.0 M HCl and 0.1 M NaOH.

## HPLC Analysis

Parent compounds and nitrosated products were quantified by HPLC (Shimadzu Scientific Instruments, Inc., Columbia, MD) using a Keystone Betasil NA column (25 cm  $\times$  4.6 mm) and UV detection at 235 nm (atrazine) and 246 nm (nitrosoatrazine). The mobile phase was acetonitrile and water (50:50 v/v) at a flow rate of 1.0 mL/min. Retention times for atrazine and NNAT were 6.3 and 9.6 min, respectively.

## Results and Discussion

### *N*-Nitrosoatrazine Formation

#### *Formation in Solution*

In a 14-d solution experiment (Figure 3), NNAT was formed only at pH 2 to 4. Rapid production of NNAT in solution at low pH was likely due to conversion of  $\text{NO}_2^-$  to  $\text{HNO}_2$  ( $\text{pK}_a = 2.8$ ) and reaction of subsequent nitrosating species with unprotonated atrazine ( $\text{pK}_a = 1.68$ ). The  $\text{HNO}_2$  is in equilibrium with dinitrogen trioxide ( $\text{N}_2\text{O}_3$ ), a nitrosating species Eq. 1 (4). Under highly acidic conditions  $\text{HNO}_2$  is also converted to  $\text{H}_2\text{NO}_2^+$  ( $\text{pK}_a = 1.7$ ; (15)), which forms the strongly nitrosating  $\text{NO}^+$  species. Although NNAT was rapidly formed in solution at pH 2, it was transformed to atrazine and hydroxyatrazine (HA) after 6 h (data not shown). NNAT formed more slowly but was more stable at pH 3 than 2 (Figure 3). Atrazine initially decreased then increased as NNAT formed and was denitrated in a 48-h experiment. NNAT stability in solution decreased with increasing acidity.

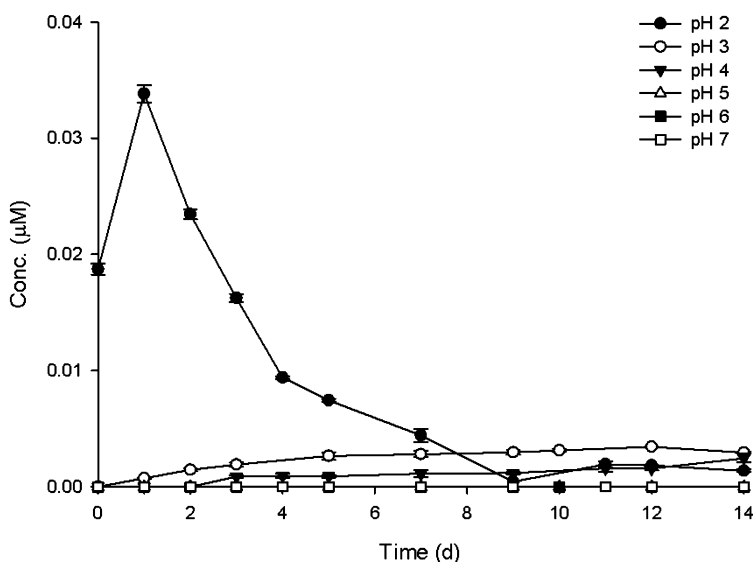
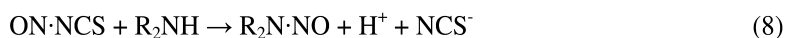
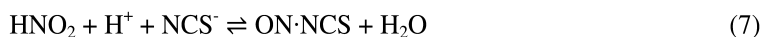


Figure 3. Formation of NNAT from reaction of atrazine and nitrite (1:4 molar ratio) in solution at pH 2 to 7 (no NNAT was detected at pH 5-7). Bars indicate standard deviations of the means; where absent bars fall within symbols.

Adding acetate resulted in NNAT formation at pH 5 to 7 and also appeared to increase NNAT stability (Figure 4). Cova et al. (23) similarly reported formation of *N*-nitrosocurzate in solution containing 350 mM acetate at pH higher than without acetate. Mirvish et al. (24) observed that thiocyanate (NCS<sup>-</sup>) increased the nitrosation reaction ten-fold at pH 2.5. The acetate anion may increase the productivity of the reaction in a manner similar to NCS<sup>-</sup>, which involves formation of nitrosyl thiocyanate (ON·NCS) and subsequent reaction with the secondary amine (Eqs. 7 and 8; (3)):



The presence of fulvic acid (extracted from soil organic matter) also promoted NNAT formation (Figure 4). Weerasooriya and Dissanayake (25) showed the rate of dibutylamine (DBA) nitrosation doubled when fulvic acid was present and nitrosation occurred under less acidic conditions. This may be primarily due to the presence of more strongly acidic polycarboxylate groups in fulvic acid ( $\text{pK}_a \leq 3.0$ ; (26, 27)), which may have a catalytic effect similar to acetate. Weerasooriya and Dissanayake (25) reported that the nitrosation reaction rate depended on fulvic acid concentration and suggested that fulvic acid lowered the activation energy of the amine-nitrosamine ion complex. Keefer and Roller (28) also showed that nitrosation was catalyzed by formaldehyde, suggesting that the importance of carbonyl groups in the mechanism of catalysis.

In contrast to fulvic acid, humic acid did not promote NNAT formation (data not shown). Humic acid contains the higher molecular weight organic fractions and will precipitate under acidic conditions. Adding unrefined dissolved organic matter to the reaction solution produced results similar to fulvic acid (data not shown). At pH 2, NNAT formation was very similar in all treatments. NNAT reached a maximum concentration within several days, after which the atrazine concentration increased as NNAT gradually decreased. No NNAT was detected in deoxygenated solution at pH 4 or higher (data not shown). These observations indicate the importance of oxygen in the reaction (4).

Simazine ( $\text{pK}_a = 1.62$ ; (17)) also formed *N*-nitrososimazine in solution containing nitrite (molar ratio 1:4) (data not shown). It is likely that cyanazine ( $\text{pK}_a = 1.6$ ; (17)) similarly formed *N*-nitrosocyanazine, but the product peak was not readily resolved from the parent under the HPLC conditions used. Nitrosation of cyanazine, as well as terbuthylazine, terbuthryn, and terbutmeton (all s-triazines with secondary amine moieties), was demonstrated in previous research (10, 13, 29).



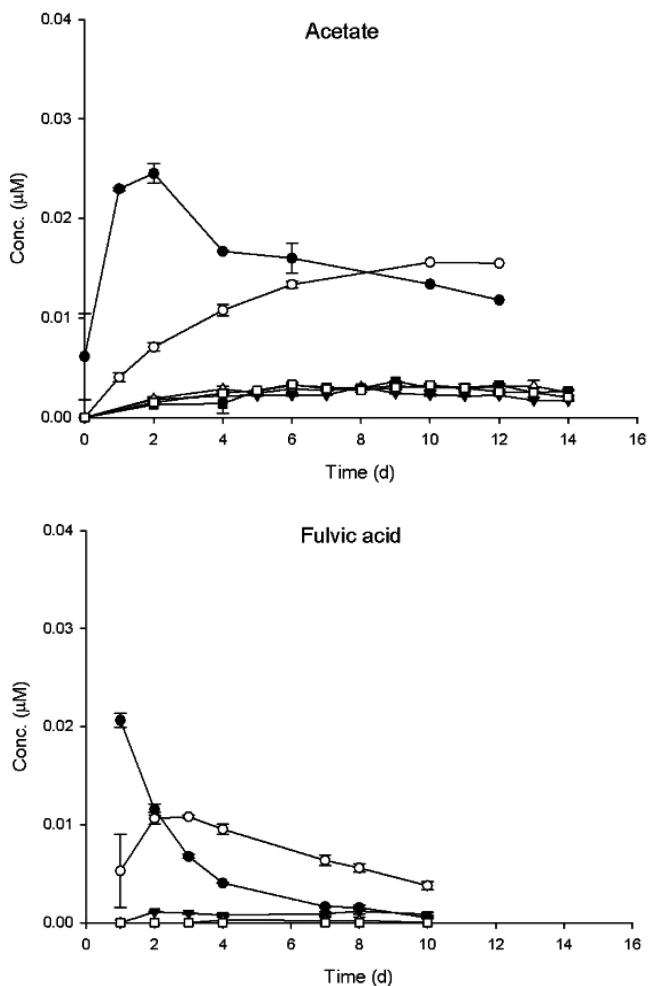


Figure 4. Formation of NNAT from reaction of atrazine and nitrite (1:4 molar ratio) with acetate or fulvic acid (100 mg/L) in solution at pH 2 to 7. (● = pH 2, ○ = pH 3, ▼ = pH 4, △ = pH 5, ■ = pH 6, □ = pH 7). Bars indicate standard deviations of the means; where absent bars fall within symbols.

## Formation in Soil

NNAT formed in soil after 7 d at pH 4 and after 14 d at pH 5, but no NNAT was found in soil at pH 6 and 7 (Figure 5). At pH 4, NNAT slowly degraded to atrazine, HA, and other compounds. NNAT formation in soil at pH 4 and 5 soil may be due to increased acidity at particulate surfaces and the presence of organic matter, which has been associated with nitrosamine formation (25, 30). Padhye et al. (31) showed that adsorption of dimethylamine (DMA) to activated carbon promoted its transformation to NDMA in the presence of oxygen, and a similar mechanism may be occurring at soil surfaces.

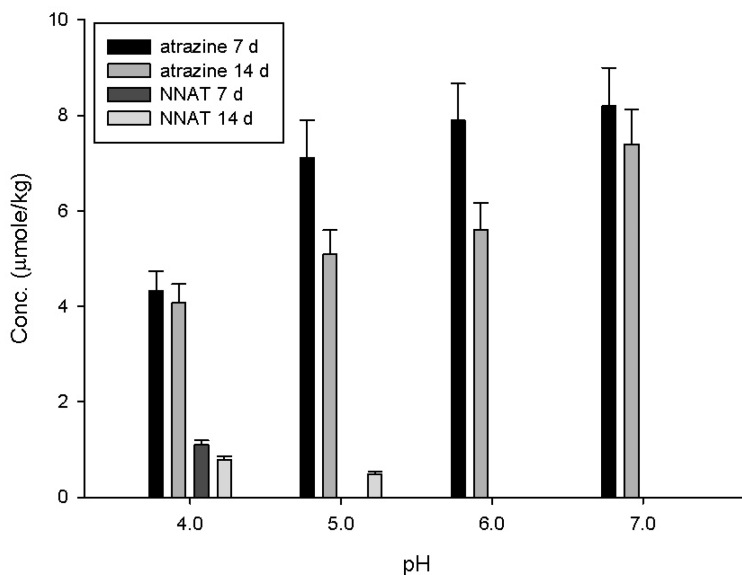


Figure 5. Formation of NNAT from atrazine and nitrite (1:156 molar ratio) in soil at pH 4 to 7. Error bars indicate standard deviations of the means.

To obtain more information about NNAT formation in soil at pH 4, the same experiment was repeated and concentrations monitored more frequently. NNAT reached a maximum at 7 d and the amount remained constant until 21 d (Figure 6). After 21 d the rate of nitrification may be exceeding nitrosation, resulting in loss of the nitrite and further slowing the reaction. Atrazine also may be degrading. No NNAT was detected in pH 4 soil under oversaturated or anaerobic conditions (data not shown), again indicating the importance of oxygen for nitrosation (4). Decomposition of nitrous acid in the absence of oxygen further slows nitrosation reactions (4).

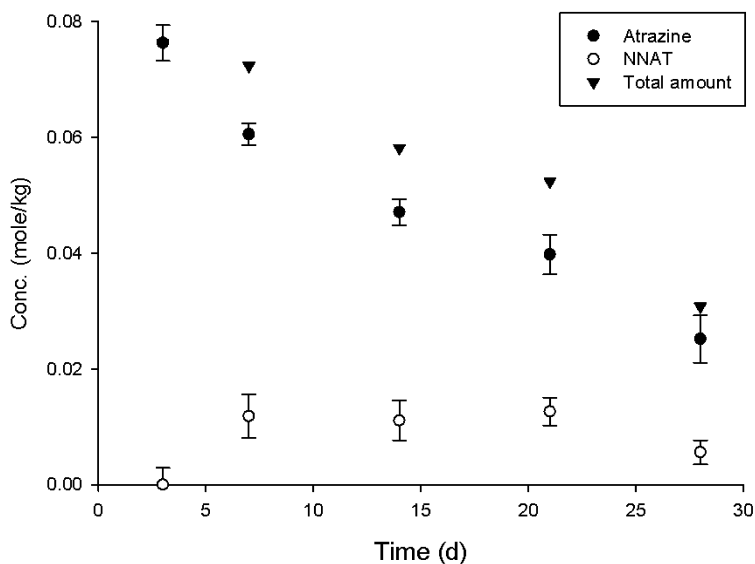


Figure 6. NNAT formation from reaction of atrazine with nitrite (1:156 molar ratio) in soil at pH 4. Bars indicate standard deviations of the means; where absent bars fall within symbols.

### Adsorption of N-Nitrosoatrazine in Soil

NNAT and atrazine adsorption and desorption coefficients ( $K_d$ ) were determined in Aksarben silty clay loam at different pH levels in a two-day experiment (Figure 7). No effect of soil pH (ranging from 3 to 8) on NNAT and atrazine adsorption and desorption was observed. Adsorption  $K_d$  and  $K_{oc}$  values (Table II) indicated that NNAT was more strongly adsorbed (average  $K_d = 5.9$  and  $K_{oc} = 495$ ) than atrazine (average  $K_d = 2.71$  and  $K_{oc} = 123$ ) average over all soil pH levels. Larger differences between adsorption and desorption  $K_d$  values indicated more hysteresis of NNAT than atrazine.

NNAT and atrazine adsorption isotherms were obtained for Aksarben, Rosebud, and Valentine soils (Figure 8). Adsorption decreased in the order: NNAT in Aksarben > NNAT in Rosebud > atrazine in Aksarben > atrazine in Rosebud > NNAT in Valentine > atrazine in Valentine soil. NNAT showed greater adsorption than atrazine in the Aksarben silty clay loam and Rosebud silt loam soils. Adsorption of NNAT and atrazine was very low and similar in the sandy Valentine soil. Soil texture affected NNAT and atrazine adsorption in soil. As expected, adsorption of NNAT and atrazine was much less in the Valentine sand (which contains fewer adsorption sites) than in the Aksarben (silty clay loam) and Rosebud (silt loam) soils.

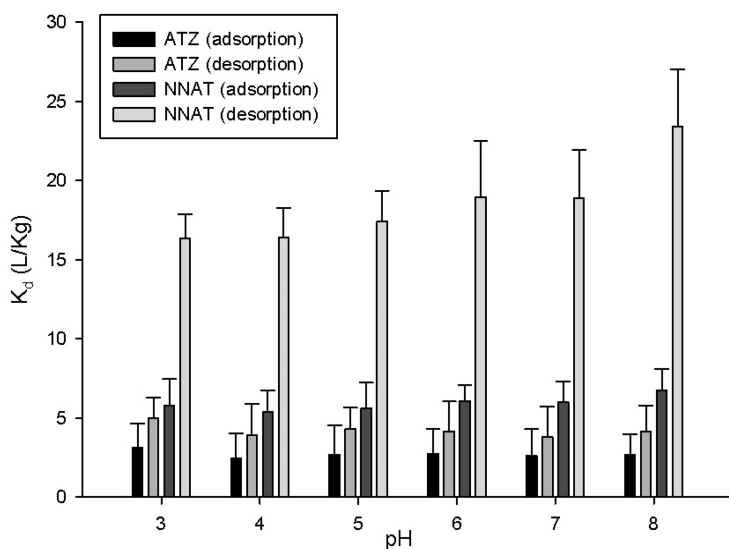


Figure 7. Atrazine and NNAT adsorption and desorption in soil at different pH levels. Error bars indicate standard deviations of the means.

**Table II. Organic carbon partition coefficients ( $K_{oc}$ ) for atrazine and N-nitrosoatrazine based on  $K_d$  measurements in Aksarben silty clay loam soil containing 2.2% organic matter**

<i>pH</i>	<i>atrazine</i> $K_{oc}$ ( $\pm SD$ )	<i>NNAT</i> $K_{oc}$ ( $\pm SD$ )
3	141 ( $\pm 2$ )	481 ( $\pm 2$ )
4	111 ( $\pm 2$ )	448 ( $\pm 1$ )
5	122 ( $\pm 2$ )	466 ( $\pm 2$ )
6	124 ( $\pm 2$ )	508 ( $\pm 1$ )
7	119 ( $\pm 2$ )	503 ( $\pm 1$ )
8	122 ( $\pm 1$ )	561 ( $\pm 1$ )
Average	123	495

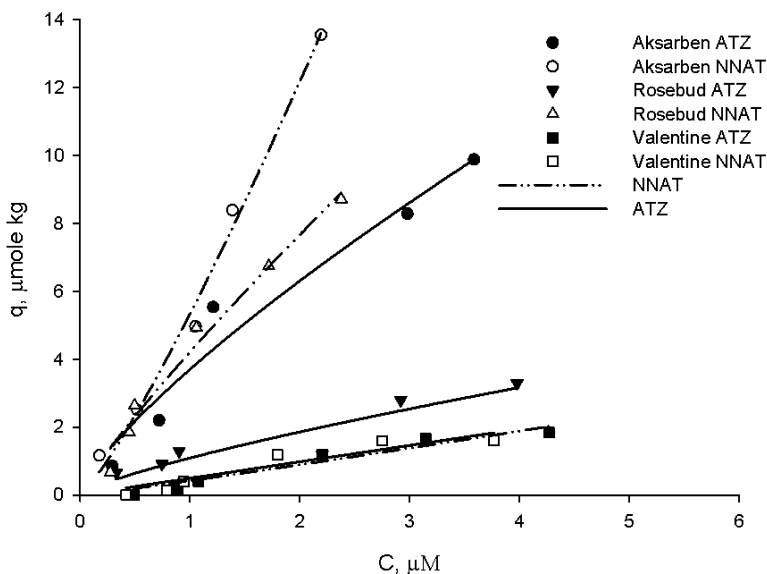


Figure 8. Adsorption Isotherms for NNAT and atrazine in three soils (● = atrazine on Aksarben, ○ = NNAT on Aksarben, ▼ = atrazine on Rosebud, Δ = NNAT on Rosebud, ■ = atrazine on Valentine, □ = NNAT on Valentine).

## N-Nitrosoatrazine Stability in Solution and Soil

### Aqueous Solution

In the absence of light, NNAT was relatively stable in aqueous solution, with only small decreases in concentration in a two-month experiment (Figure 9). The small increase in atrazine concentration during this period can be attributed to NNAT denitrosation. The stability of NNAT in solution was not affected by the presence of acetate, humic acid, or fulvic acid (not shown). Under light, NNAT rapidly degraded in solution (pH = 7) and atrazine concentration increased (Figure 10). Lee et al. (32, 33) similarly found that exposing aqueous solutions of NDMA to UV light resulted in production of DMA, in addition to methylamine, nitrite, and nitrate. DMA production was favored at high NDMA concentrations and greatest at pH 4-5.

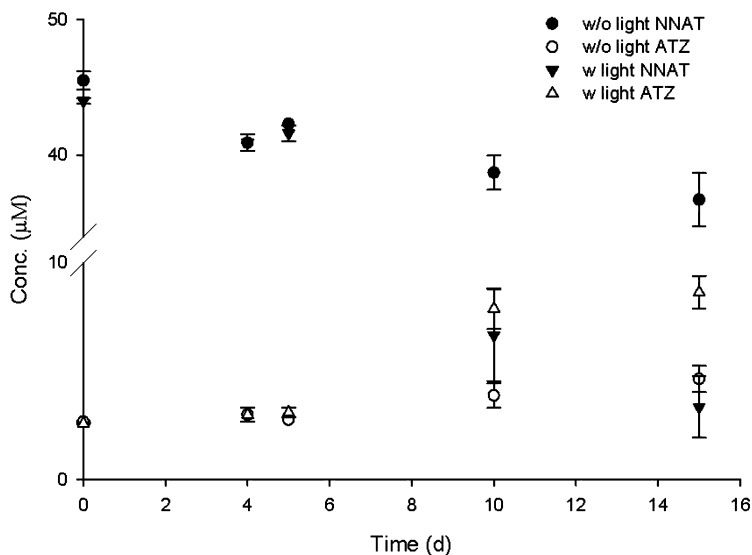


Figure 9. Stability of NNAT in solution ( $pH = 6.7$ ) with and without light. Bars indicate standard deviations of the means; where absent bars fall within symbols.

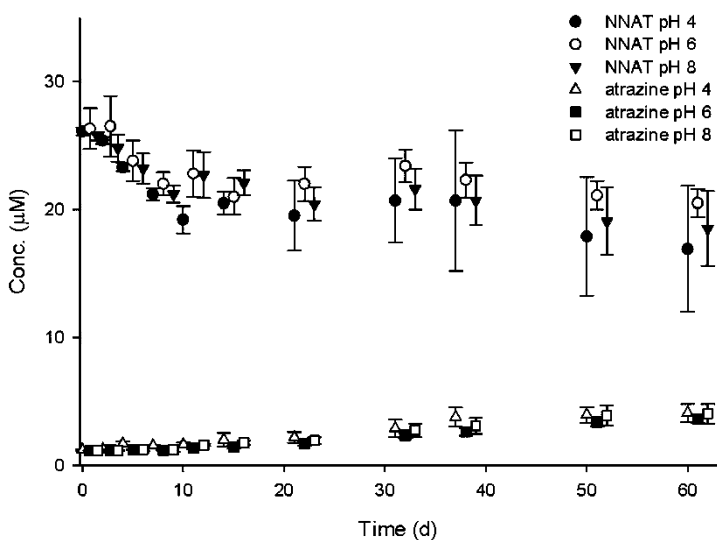


Figure 10. Stability of NNAT in solution at  $pH 4, 6,$  and  $8$ . Bars indicate standard deviations of the means; where absent bars fall within symbols.

In Aksarben soil (pH = 6.3), NNAT half-life was about 9 d (Figure 11). NNAT denitrosated to atrazine and HA was detected with time. NNAT degradation in soil was similar at pH 6 and 7, with greater loss after 15 d at pH 4 (Figure 12). Some atrazine was detected as NNAT degraded, and the amount was somewhat greater at pH 4. Biodegradation is likely the major degradation mechanism at pH 6 and 7. Hydrolysis (denitrosation) may be contributing to the observed loss of NNAT at pH 4 and some of the resulting atrazine would be expected to form HA.

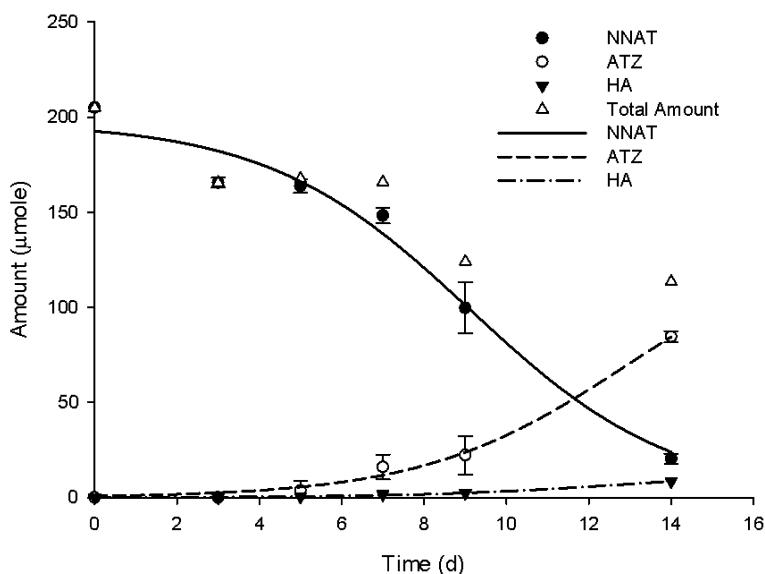


Figure 11. NNAT degradation in soil at pH 6.3. Bars indicate standard deviations of the means; where absent bars fall within symbols.

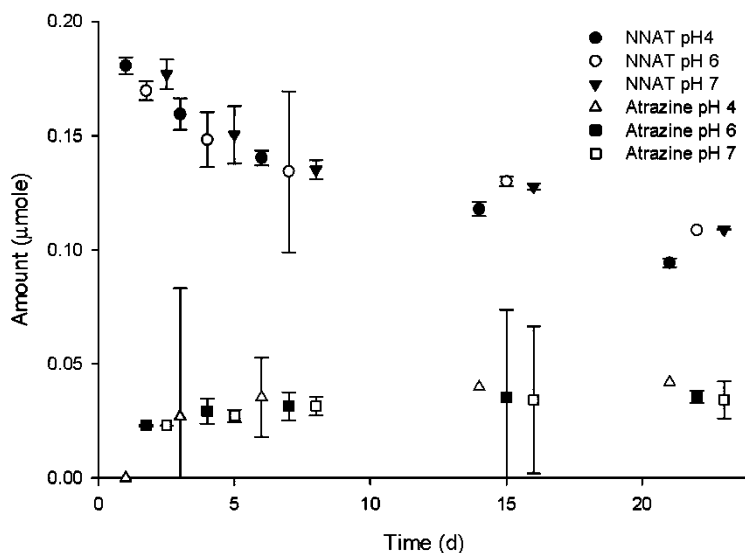


Figure 12. Degradation of NNAT in soil at pH 4, 6, and 7. Bars indicate standard deviations of the means; where absent bars fall within symbols.

## Conclusions

Atrazine is a widely used herbicide which can react with nitrite to form a potentially toxic nitrosamine product, *N*-nitrosoatrazine (NNAT). NNAT formation and stability are both affected by pH. NNAT is formed in solution at pH 2 to 4, and in soil at pH 4 and 5. The reaction is likely promoted at acidic pH because  $\text{NO}_2^-$  forms  $\text{HNO}_2$ , which becomes  $\text{H}_2\text{NO}_2^+$ , potentially producing the strongly nitrosating  $\text{NO}^+$  species. However, in aqueous solution,  $\text{HNO}_2$  is in equilibration with  $\text{N}_2\text{O}_3$ , also a highly effective nitrosating agent. In addition, the presence of non-basic nucleophiles ( $\text{X}^-$ ) can result in the formation of a third nitrosating species,  $\text{XNO}$ . The latter mechanism may explain catalysis of NNAT formation by acetate acid and fulvic acid in water at pH 5 to 7.

NNAT formation in soil at pH 4 and 5 may be due to increased acidity at particulate surfaces and promotion by organic matter. No NNAT was detected in pH 4 soil under oversaturated or anaerobic conditions, indicating the importance of oxygen in the nitrosation reaction.

Adsorption  $K_d$  and  $K_{oc}$  values show greater soil adsorption of NNAT than atrazine at all agronomic pH levels. Soil texture affected NNAT and atrazine adsorption in soil. As expected, NNAT and atrazine adsorption was lower on the Valentine sand than on Aksarben silt clay loam and Rosebud silt loam soils. Larger desorption  $K_d$  values indicate greater hysteresis of NNAT than atrazine.

NNAT was relatively stable in solution, with only small decreases in concentration in a two-month experiment under dark conditions, but rapidly transformed to atrazine when exposed to light. In soil, NNAT degradation was similar at pH 6 and 7, with greater loss after 15 d at pH 4. Some atrazine was



detected as NNAT degraded, and the amount was somewhat greater at pH 4. The half-life of NNAT in Aksarben silt clay loam was about 9 d, with degradation to atrazine and other compounds.

The information obtained from this research is important when evaluating atrazine fate and impacts in soil-water environment. NNAT may form when atrazine and nitrite are present in acidic waters and soils. Although oxygen is important for nitrosation, the presence of acetate, a fermentation product, will promote nitrosation under near-neutral conditions. Thus NNAT may be found in some locations where agrichemical runoff accumulates following application of atrazine and nitrogen fertilizers. NNAT may also be present in wetlands and riparian zones receiving agricultural runoff. The relatively high affinity for clay and organic matter would reduce NNAT availability for further movement, but it may persist in some ground waters. While exposure to light would promote NNAT degradation in surface water, sediment-adsorbed NNAT may be ingested by bottom feeders. The potential toxicity of NNAT warrants monitoring for the compound in environmental media where atrazine and nitrite are found.

## Acknowledgments

Support for this research was provided through the USDA Multistate Research Program, project W1082/2082, and the School of Natural Resources, University of Nebraska-Lincoln Institute of Agriculture and Natural Resources.

## References

1. Turjanski, A. G.; Leonik, F.; Estrin, D. A.; Rosenstein, R. E.; Doctorovich, F. *J. Am. Chem. Soc.* **2000**, *122*, 10468–10469.
2. Lai, C-H.; Chou, P-T. *Theor. Chem. Acc.* **2008**, *119*, 453–462.
3. Mirvish, S. S. *Toxicol. Appl. Pharmacol.* **1975**, *31*, 325–351.
4. Williams, D. L. H. *Nitrosation Reactions and the Chemistry of Nitric Oxide*, 1st ed.; Elsevier: London, 2004.
5. Ayanaba, A.; Verstraete, W.; Alexander, M. *Soil Sci. Soc. Am. Proc.* **1973**, *37*, 565–568.
6. Kearney, P. C.; Oliver, J. E.; Helling, C. S.; Isensee, A. R.; Kontson, A. J. *J. Agric. Food Chem.* **1977**, *25*, 1177–1181.
7. Oliver, J. E.; Kontson, A. *Bull. Environ. Contam. Toxicol.* **1978**, *20*, 170–173.
8. Pancholy, S. K. *Soil Biol. Biochem.* **1978**, *10*, 27–32.
9. Tate, R. L.; Alexander, M. *J. Natl. Cancer Inst.* **1975**, *54*, 327–330.
10. Trevisan, M.; Graviani, E.; Del Re, A. M.; Arnoldi, A.; Bassoli, A.; Cova, D.; Rossignoli, A. *J. Agric. Food Chem.* **1998**, *46*, 314–317.
11. Khan, S. U. *J. Am. Chem. Soc.* **1981**, *174*, 275–287.
12. Khan, S. U.; Young, J. C. *J. Agric. Food Chem.* **1977**, *25*, 1430–1432.
13. Zwickelpflug, W.; Richter, E. *J. Agric. Food Chem.* **1994**, *42*, 2333–2337.
14. Mallik, M. A.; Tesfai, K.; Pancholy, S. K. *Proc. Okla. Acad. Sci.* **1981**, *61*, 31–35.

15. Riordan, E.; Minogue, N.; Healy, D.; O'Driscoll, P.; Sodeau, J. R. *J. Phys. Chem.* **2005**, *109*, 779–786.
16. Mirvish, S. S.; Gannett, P.; Babcook, D. M.; Williamson, D.; Chen, S. C.; Weisenburger, D. D. *J. Agric. Food Chem.* **1991**, *39*, 1205–1210.
17. *Herbicide Handbook*, 9th ed.; Senseman, S. A., Ed.; Weed Science Society of America: Lawrence, KS, 2007.
18. Young, J. C.; Khan, S. U.; Marriage, P. B. *J. Agric. Food Chem.* **1977**, *25*, 918–922.
19. Wolfe, N. L.; Zepp, R. G.; Gordon, J. A.; Fincher, R. C. *Bull. Environ. Contam. Toxicol.* **1976**, *15*, 342–347.
20. Oliver, J. E.; Kearney, P. C.; Kontson, A. *J. Am. Chem. Soc.* **1979**, *27*, 887–891.
21. Black, C. A. In *Methods of Soil Analysis, Part 1–2*; Black, C. A., Ed.; Amer. Soc. Agronomy, Inc.: Madison, WI, 1965; pp 1414–1417.
22. Coulston, F.; Dunne, J. F. *The Potential Carcinogenicity of Nitrosatable Drugs*; WHO Symposium; World Health Organization: Geneva, 1978; Vol. 1, p 9.
23. Cova, D.; Nebuloni, C.; Arnoldi, A.; Bassoli, A.; Trevisan, M.; Del Re, A. A. M. *J. Agric. Food Chem.* **1996**, *44*, 2852–2855.
24. Mirvish, S. S.; Sams, J.; Fan, T. Y.; Tannenbaum, S. R. *J. Natl. Cancer Inst.* **1973**, *51*, 1833–1840.
25. Weerasooriya, S. V. R.; Dissanayake, C. B. *Toxicol. Environ. Chem.* **1989**, *25*, 57–62.
26. Leenheer, J. A.; Weershaw, R. L.; Reddy, M. *Environ Sci. Technol.* **1995a**, *29*, 393–398.
27. Leenheer, J. A.; Weershaw, R. L.; Reddy, M. *Environ Sci. Technol.* **1995b**, *29*, 399–405.
28. Keefer, L. K.; Roller, P. P. *Science* **1973**, *181*, 1245–1247.
29. Janzowski, C.; Klein, R.; Preussmann, R. *IARC Sci. Publ.* **1980**, *31*, 329–339.
30. Mills, A. L.; Alexander, M. *J. Environ. Qual.* **1976**, *5*, 437–440.
31. Padhye, L.; Wang, P.; Karanfil, T.; Huang, C-H. *Environ. Sci. Technol.* **2010**, *44*, 4161–4168.
32. Lee, C.; Choi, W.; Kim, Y. G.; Yoon, J. *Environ. Sci. Technol.* **2005a**, *39*, 2101–2106.
33. Lee, C.; Choi, W.; Kim, Y. G.; Yoon, J. *Environ. Sci. Technol.* **2005b**, *39*, 9702–9709.

## Chapter 2

# Chlorine-Free Electrochemical Disinfection of Water Contaminated with *Salmonella typhimurium* and *E. coli B*

N. N. Barashkov,<sup>\*,1</sup> D. A. Eisenberg,<sup>1</sup> and I. S. Irgibaeva<sup>2</sup>

<sup>1</sup>Micro-Tracers, Inc., 1370 Van Dike Avenue, San Francisco, CA 94124

<sup>2</sup>Eurasian National University, 5 Munaitpasova St., Astana, Kazakhstan

\*E-mail: Nikolay@microtracers.com

Deionized (DI) water contaminated with *Salmonella typhimurium* (*S. typhimurium*) or *E. coli B* bacteria was disinfected by alternating current. Ammonium sulfate, sodium nitrate and phosphate buffer were used as electrolytes. Disinfection was carried out in the circulation system including an electrochemical cell with three types of electrodes; stainless steel, titanium and nickel. The process efficiency was estimated and the number of killed bacteria was directly proportional to the water treatment time and concentration of hydroxyl radicals generated by electrolysis. The presence of OH radicals was detected with N,N-dimethyl-p-nitrosoaniline (RNO) used as a spin trap. Similar experiments were carried out with water remaining after poultry washing at poultry farms and additionally contaminated with *S. typhimurium* bacteria. Measures were recommended to increase the process efficiency and decrease the water treatment time.

## Introduction

Sewage water contains numerous microorganisms. There are numerous methods to reduce the number of infection components to an acceptable level for drainage to any water pools (*I*). Earlier, the chlorination method was traditionally used; in recent years, ozone treatment, ultraviolet irradiation, and various electrochemical processes are applied. Selection of the disinfection method

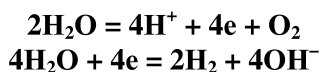
significantly depends upon the cost of required energy, especially in the cases, where large quantities of water should be treated.

*S. typhimurium* and *E. coli* bacteria are classified as the most dangerous microorganisms causing serious intestinal disorders of humans. Food products of animal and vegetable origin are often infected with both types of bacteria. Water remaining after poultry washing at poultry farms (rinsing water) is also often infected with these bacteria. Recently, poultry water was disinfected by such chemical methods as chlorination (2), ozonation (3), and others (4). The disadvantages of these methods include potential formation and accumulation of toxic chemical products as, for example, in the case of chlorination or high cost as in the case of ozonation (5).

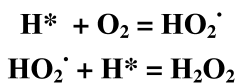
Electrochemical treatment of water, including rinsing water became interesting relatively recently (1, 6–12). The authors of study (1) found that effective electrolytic water treatment using NaCl electrolyte is accompanied by generating significant quantities of elementary chlorine, hypochlorite, and, probably, chlorate and requires a high initial concentration of NaCl (over 0.15%). At such concentration, chloride anions cause corrosion of any bimetal parts of water systems, for example, water distributors, cooling towers, etc. Replacement of chloride anions with phosphates, nitrates, sulfates, or carbonates, which do not cause corrosion, is more favorable with respect to the equipment operation costs and increases profitability of the electrochemical water sterilization process.

The mechanism of electrochemical disinfection depends upon numerous parameters, including the nature of electrolyte. Calculations of the number of *S. typhimurium* bacteria in NaCl, Na<sub>2</sub>SO<sub>4</sub>, and Na<sub>3</sub>PO<sub>4</sub> solutions subjected to low voltage and low current electrolysis were performed (6, 13, 14). Already in five minutes, this treatment was shown to reduce the concentration of live *S. typhimurium* bacteria by one or two orders of magnitude.

The authors of (15–17) studied the electrochemical disinfection mechanism for *E. coli* B bacteria in NaCl, NaNO<sub>3</sub>, and Na<sub>2</sub>SO<sub>4</sub> solutions. The disinfection efficiency of electrolysis was close to that of ozonation, i.e., much higher than that of ordinary chlorination. Electrochemical disinfection was shown to kill bacteria not by electric field. In the opinion of the authors of (18), the major contribution to the disinfection effect is made by generation of hydroxyl radicals. The formation mechanism of OH radicals in electrolysis of aqueous solutions was discussed in studies (19–21). They authors showed, in particular, that the generally accepted schemes of anodic oxidation and cathodic reduction are simplified for the reactions:



Formation of atomic hydrogen (H\*) is one of the intermediate stages in the course of molecular hydrogen formation in the reaction of cathodic reduction. Here a part of atomic hydrogen initiates the following sequence of reactions:



In the cases, where electrodes are made of metal (M), hydrogen peroxide takes part in the reaction generating hydroxyl radicals:



The life time of hydroxyl radicals is too short for their identification by ESR method. Nevertheless, an effective method for detection of hydroxyl radicals was suggested by the authors of (21). They analyzed the interaction products of hydroxyl radicals with *tert*-butylnitron in electrolysis of potassium chlorate solutions. The generated long-living radicals were detected by ESR method.

In addition to hydroxyl radicals, the disinfection process may involve also other intermediate highly active compounds such as  $\cdot\text{O}_2^-$  anion radicals. In the case of sulfate electrolyte (22), there may be persulfate and sulfate radicals. In electrolysis of phosphate buffer (23, 24), bacteria are killed due to formation of hydrogen peroxide.

Our earlier studies represent the results from electrochemical disinfection of deionized (DI) water contaminated with *E. coli B* (25) and *S. typhimurium* (26) containing  $(\text{NH}_4)_2\text{SO}_4$  as electrolyte. We suggested a kinetic model for elimination of bacteria and a quantitative method describing the rate of interaction between hydroxyl radicals and bacteria and considered the effects of such parameters as treatment time, electrolyte concentration, and initial concentration of bacteria. In this work, we analyzed the results of a similar study carried out for DI water and poultry water containing three different types of electrolytes contaminated with a high concentration of *S. typhimurium* and *E. coli B* bacteria.

## Experimental

We used N,N-dimethyl-p-nitrosoaniline (RNO) which is known (15) as a spin trap for hydroxyl radicals. The concentration of OH radicals resulting from electrolysis was estimated with a spectrophotometer by the change in the RNO optical absorption spectral intensity with the peak at 440 nm. The solutions of DI water contained the  $(\text{NH}_4)_2\text{SO}_4$   $\text{NaNO}_3$  or phosphate buffer ( $\text{NaH}_2\text{PO}_4 + \text{Na}_2\text{HPO}_4$ ) electrolyte concentration of 0.025 to 0.5% and RNO concentration of 0.0027 to 0.003% ( $1.8 \times 10^{-6}$  to  $2.0 \times 10^{-6}$  M). The poultry rinsing water was provided by the experimental poultry plant at the University of Arkansas (Fayetteville, Arkansas). Before electrolysis, this water was diluted with the same volume of DI water containing the necessary quantities of electrolyte and RNO. According to the results of microbiological analysis, the population of *S. typhimurium* bacteria in the prepared solution was below the detection level. We prepared the solutions of *S. typhimurium* bacteria with various concentrations by dilution of water with highly concentrated suspension containing approximately  $42 \times 10^6$  cfu/ml of bacteria.

Our experimental water disinfection device is represented in Figure 1. We found that alternating current of 0.21 A (50 Hz frequency) corresponding to the current density of 60 mA/cm<sup>2</sup> does not cause corrosion of steel electrodes in the selected range of electrolyte concentrations.

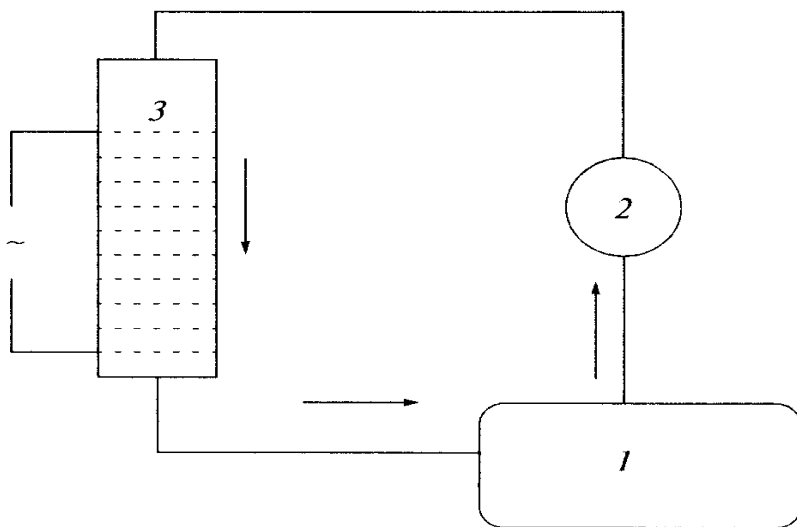


Figure 1. Laboratory electrochemical water disinfection device: (1) pump, (2) water flow meter, (3) plastic electrochemical cell; parallel set of ten stainless steel net electrodes (5.5 cm diameter) with 3 mm intervals. (Reproduced with permission from reference (26). Copyright 2010 Pleiades Publishing, Ltd).

We maintained the constant current density by selecting the initial voltage in the range from 40 to 170 V with respect to the electrolyte concentration. Before starting each experiment, the laboratory device was disinfected for 20 min with hot water flow at the temperature of 75 to 80°C. The initial temperature of the treated water was 20°C. The water flow rate through the electrochemical cell was 10 Gallon/min. The portions of 10 ml were sampled through the open cover of electrochemical cell and stored at 4°C for microbiological analysis. The colonies of *S. typhimurium* and *E. coli* B were counted after incubation for 48 h at 35°C.

## Results and Discussion

Figure 2 represents a typical curve of live bacteria concentration in solution vs. electric current treatment time. Our analysis of experimental data enables to make to conclusions. First, without electric current, no addition of electrolyte and RNO to DI water contaminated with *S. typhimurium* causes any significant bactericidal effect. Second, if electric current is applied, the number of live bacteria vs. treatment time can be described with a linear logarithmic curve. To describe the process of electrolysis, we used a modified kinetic model designed for the disinfection of natural water contaminated with coliforms (15).

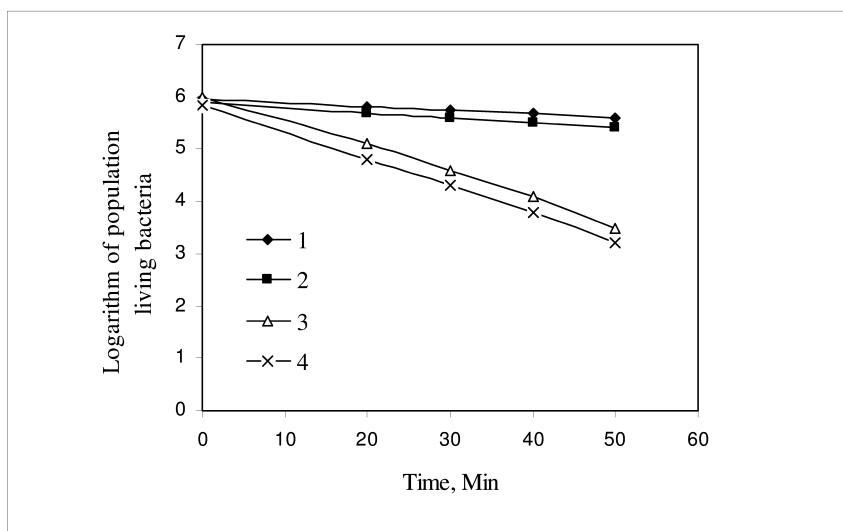


Figure 2. Live *S. typhimurium* bacteria count vs. disinfection time in  $(\text{NH}_4)_2\text{SO}_4$  solutions with concentrations of 0.025% (1, 3) and 0.05% (2, 4) without electrolysis (1, 3) and with electrolysis (3, 4).

According to this model, the initial number of bacteria ( $n_0$ ) and the current number of bacteria ( $n$ ) at time moment  $t$  are interrelated as follows:

$$\text{Log } n = \text{log } n_0 - kt \quad (1)$$

where  $k$  is the factor depending on the current density for the constant volume of water to be disinfected and constant surface area of the electrodes.

The diagram in Figure 2 enables to calculate factor  $k$  and to determine such essential parameter of disinfection process as the minimum time  $t_d$ , which is necessary to decrease the concentration of bacteria to  $n = 1$ . With respect to calculation of the bacteria population in the selected dimension, such low concentration should be considered as negligibly small. Therefore,  $t_d$  can be referred to as the time required for complete elimination of bacteria. It corresponds to the intersection point of the experimental line with the time axis. Table I represents the parameters of  $k$  and  $t_d$  calculated for each concentration of electrolyte.

The contaminated water flow through the electrochemical cell without the applied voltage slightly decreases the population of bacteria, which becomes noticeable after 30 min experiment. A similar effect was earlier noted for DI water contaminated with *E. coli* B (26) and seems to be accounted for by the known biocide effect of cavitation to microorganisms (27).

Our electrochemical experiments with poultry rinsing water contaminated with *S. typhimurium* bacteria were carried out under the same conditions as our experiments with DI water. First, as in the case of DI water, electrochemical

disinfection of rinsing water takes place far more effectively than water flow through electrodes under no voltage. Second, the live bacteria count *vs.* water treatment time is described with logarithmic curve. Table I shows a comparison between factor  $k$  and time  $t_d$  for poultry water with the corresponding data for DI water. One can see that achievement of complete disinfection by electrochemical treatment of *S. typhimurium* bacteria in poultry water requires more time than in the case of DI water.

**Table I. Factor  $k$  and complete disinfection time  $t_d$ , calculated for linear model (equation 1) for electrolysis of aqueous *S. typhimurium* solutions. (Reproduced with permission from reference (26). Copyright 2010 Pleiades Publishing, Ltd)**

Concentration of $(NH_4)_2SO_4$ , %	Disinfection media	Log $n_o$ [cfu/ml]	$k$	$t_d$ , min
0.025	DI water	6.01	0.0499	120.2
	Poultry water	5.76	0.0448	128.6
0.05	DI water	6.06	0.0550	110.1
	Poultry water	5.68	0.0464	122.3
0.2	DI water	6.13	0.0565	108.5
	Poultry water	5.63	0.0472	119.2
0.5	DI water	6.21	0.0634	98.0
	Poultry water	5.59	0.0503	111.2

Generation of OH radicals by electrochemical treatment of contaminated water was successfully used for oxidation of organic compounds, for example, phenols (28). The advantages of RNO used as a spin trap are accounted for by high selectivity of the reaction of interaction between RNO and OH radicals. Consider the reactions of OH radicals spending in the course of electrolysis. The interaction scheme can be represented as follows:

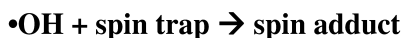


Figure 3 shows the change in the absorption spectra of RNO in  $(NH_4)_2SO_4$  aqueous solution contaminated with *S. typhimurium* under the conditions of electrolysis.

As one can see, a solution flow through the zero current electrolytic cell only slightly decreases the optical density at 440 nm (Figure 3). Under the conditions of electrolysis, the optical density changes rapidly. It decreases far more rapidly if electrolysis takes place in the bacteria free solution. These results apparently evidence formation of OH radicals.



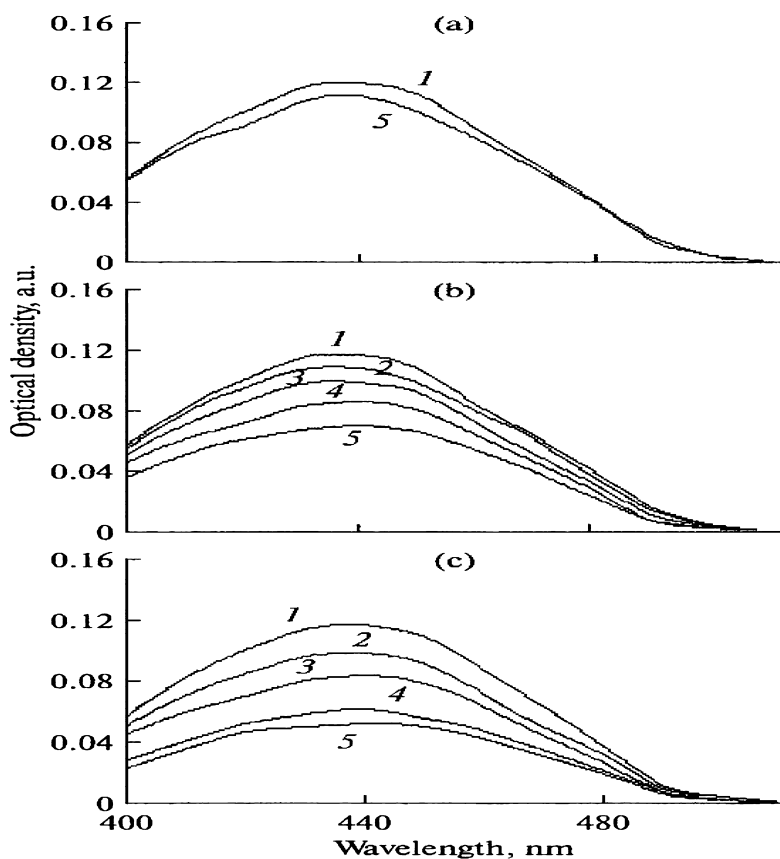
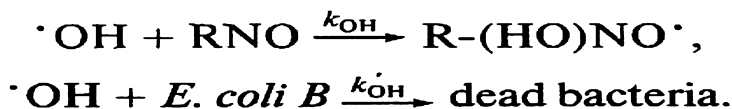


Figure 3. Absorption spectra of RNO in 0.2% solution of  $(\text{NH}_4)_2\text{SO}_4$  in DI water contaminated with *S. typhimurium* before (1) and after flow through electrochemical cell for 5 (2), 20 (3), 40 (4), 60 (5) min; water treated without voltage (a), under voltage (b), under voltage in bacteria free solution (c). (Reproduced with permission from reference (26). Copyright 2010 Pleiades Publishing, Ltd).

One can neglect potential occurrence of other reactions involving hydroxyl radicals, excepting elimination of bacteria and interaction with RNO. Then expenditure of OH radicals in electrochemical treatment can be described as follows (26):



We use the kinetic model suggested for description of two competing reactions (28):

$$1/G_t = 1/G_o \times \{ 1 + (k'_{OH} [B]) / (k_{OH} [RNO]) \} \quad (2)$$

where  $G_t$  is the bleaching rate of RNO in the presence of bacteria;  $G_o$  is the bleaching rate of RNO in the absence of bacteria;  $[B]$  is the bacteria concentration in the electrolyte;  $[RNO]$  is the concentration of RNO in the electrolyte;  $k'_{OH}$  and  $k_{OH}$  are the rate constants of the corresponding reactions.

Like in the case of DI water, voltage applied to poultry rinsing water sharply decreases the RNO optical density at 440 nm. Compare the kinetic characteristics of RNO interaction with hydroxyl radicals in DI water and poultry water. For this calculation, we selected the  $(NH_4)_2SO_4$  concentration of 0.2% and various initial concentrations of *S. typhimurium* (Table II).

The RNO concentration was measured after 40 min treatment of water. The  $1/G_t$  vs.  $[B]/[RNO]$  is a linear relationship with the slope of  $1/G_o (k'_{OH} / k_{OH})$ . The radical-bacteria interaction rate constant was calculated on the assumption the RNO-OH radical reaction rate constant is  $1.2 \times 10^{10} \text{ mol}^{-1} \text{ s}^{-1}$  (4). Thus calculated values of  $k'_{OH}$  for DI water and poultry water are represented in Table II along with the values of constant  $k$  and time  $t_d$  for both kinds of water as calculated by equation (1). One can see that the bacteria elimination rate in DI water is higher than that in poultry water.

**Table II. Factor  $k$  and complete disinfection time  $t_d$ , calculated by equation (1) and *S. typhimurium* elimination rate constants calculated by equation (2). (Reproduced with permission from reference (26). Copyright 2010 Pleiades Publishing, Ltd)**

Disinfection media	Log $n_o$ [cfu/ml]	$k$	$t_d$ , min	$k'_{OH}$ [cfu/sec]
DI water	6.13	0.057	109	3.9 x 10 <sup>6</sup>
DI water	6.32	0.055	116	
DI water	6.43	0.053	122	
DI water	6.85	0.055	125	
Poultry water	5.63	0.047	119	1.7 x 10 <sup>6</sup>
Poultry water	5.76	0.047	124	
Poultry water	5.89	0.046	127	
Poultry water	6.05	0.046	130	

Therefore, disinfection of poultry water is a slower process than disinfection of DI water. This conclusion follows from comparison of the bacteria elimination rate and agrees with the determined time  $t_d$  required for complete disinfection of water. As follows from (29), the bacteria elimination rate under electrochemical treatment of *S. typhimurium* suspensions is higher in DI water than that in poultry water. This difference was accounted for by the fact that poultry water contains additionally blood cells, fat micelles, and other organic substances, which can coat the cells of bacteria and thus protect them from the effect of radicals. Such explanation seems to be true also for interpretation of the results represented in this work.

Table III represents the results from electrochemical treatment of DI water contaminated with bacteria of two species. All the measurements were carried out with the same electrolyte in the same concentration under the same conditions of AC treatment. Apparently, for approximately the same initial concentration of bacteria (deviation not exceeding 3%), complete disinfection in the case of *E. coli B* needs less time than in the case of *S. typhimurium*.

Our conclusion that disinfection of *S. typhimurium* is a slower process as compared to that of *E. coli B* is confirmed with the bacteria elimination rate constants  $k'_{OH}$ . These constants were calculated in (26) as  $3.91 \times 10^6$  and  $6.01 \times 10^6$  cfu/s, respectively.

The efficiency of electrochemical disinfection can be enhanced also by varying such parameters as water volume and flow rate through electrochemical cell as well by changing the nature of the electrode materials. Data presented in Figure 4 and Table IV are obtained during electrolysis with two different types of electrodes for DI water containing two different electrolytes at concentration 0.5% contaminated with *S. typhimurium*.

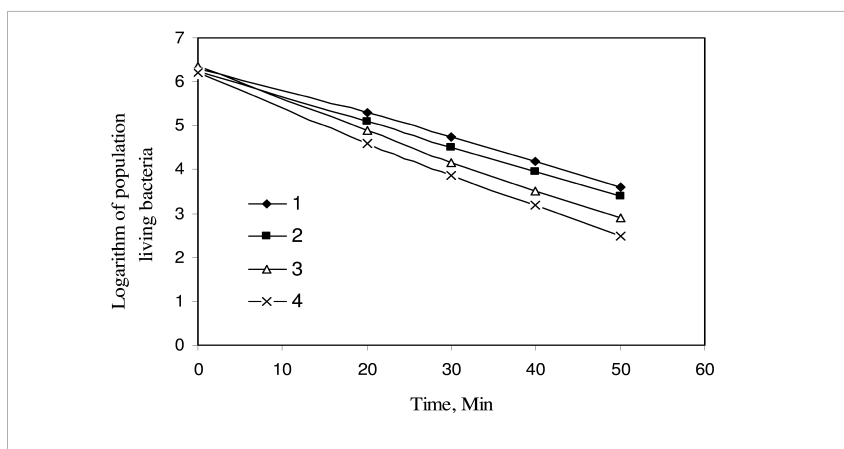


Figure 4. Live *S. typhimurium* bacteria count vs. disinfection time in ammonium sulfate solution (1,3) and phosphate buffer solution (2,4) with two different types of electrodes: titanium (1, 2) and stainless steel (3, 4).

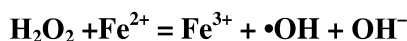
**Table III. Complete water disinfection time  $t_d$  for various initial concentrations of *S. typhimurium* and *E. coli B* bacteria (stainless steel electrodes are used)**

Nature of electrolyte	Nature of bacteria	Log $n_0$ [cfu/ml]	$k$	$t_d, \text{min}$
Ammonium sulfate	<i>E. coli B</i>	6.23	0.0698	89.3
	<i>S. typhimurium</i>	6.21	0.0634	98.0
Sodium nitrate	<i>E. coli B</i>	6.19	0.0674	91.9
	<i>S. typhimurium</i>	6.34	0.0626	101.3
Phosphate buffer	<i>E. coli B</i>	6.16	0.0727	84.7
	<i>S. typhimurium</i>	6.28	0.0706	88.9

**Table IV. Complete water disinfection time  $t_d$  for various initial concentrations of *S. typhimurium* with three different types of electrodes**

Material of electrodes	Nature of electrolyte (concentration 0.5%)	Log $n_0$ [cfu/ml]	$k$	$t_d, \text{min}$
Stainless steel	(NH <sub>4</sub> ) <sub>2</sub> SO <sub>4</sub>	6.21	0.0634	98.0
	Phosphate buffer	6.28	0.0706	88.9
Titanium	(NH <sub>4</sub> ) <sub>2</sub> SO <sub>4</sub>	6.30	0.0587	107.3
	Phosphate buffer	6.27	0.0596	105.1
Nickel	(NH <sub>4</sub> ) <sub>2</sub> SO <sub>4</sub>	6.38	0.0589	108.3
	Phosphate buffer	6.40	0.0599	106.8

It was found that the AC electrolysis of phosphate buffer solution leads to formation of hydrogen peroxide, which was confirmed by using Hochanadel's colorimetric method (30). According to this method, the concentration of hydrogen peroxide is proportional to absorbance at 350 nm related to presence of anions I<sub>3</sub><sup>-</sup> in product of interaction between H<sub>2</sub>O<sub>2</sub>, KI, NaOH, KHC<sub>8</sub>H<sub>4</sub>O<sub>4</sub> and (NH<sub>4</sub>)<sub>6</sub>Mo<sub>7</sub>O<sub>24</sub> x4H<sub>2</sub>O. It is known that hydrogen peroxide can easily react with ferrous ions giving very active hydroxyl radicals (Fenton reaction):



The experimental confirmation of this hypothesis was obtained in following test. The low concentration of ferrous sulfate (0.05%) was added to phosphate buffer during electrolysis of aqueous *S. typhimurium* solution with titanium electrodes: complete water disinfection time  $t_d$  in this case was decreased from 105.1 min (the same system, but with no ferrous sulfate addition) to 89.3 min.

The energy loss of this process decrease at a lower electric resistance of the electrolyte solution, for example, for a shorter distance between electrodes, larger surface area, or higher electrolyte concentration. The process cost can be essentially decreased by selecting the electrolyte, for example, if  $(\text{NH}_4)_2\text{SO}_4$  is replaced with less expensive  $\text{Na}_2\text{SO}_4$ .

## Conclusions

(1) Chlorine-free AC electrochemical disinfection with chloride-free electrolyte such as ammonium sulfate, sodium nitrate and phosphate buffer is an effective method for disinfection of DI water contaminated with *S. typhimurium* and *E. coli B* bacteria.

(2) If all other conditions are the same, disinfection of *S. typhimurium* in poultry rinsing water requires more time than disinfection of *S. typhimurium* of DI water.

(3) If all other conditions are the same, disinfection of *S. typhimurium* of DI water in electrolytic cell with stainless steel electrodes is more effective than disinfection in electrolytic cell with titanium or nickel electrodes.

(4) Use of N,N-dimethyl-p-nitrosoaniline as a spin trap experimentally confirmed formation of hydroxyl radicals in electrolysis of aqueous ammonium sulfate solutions. Hydroxyl radicals make an essential impact to the bactericidal process.

(5) Under the same electrolytic conditions, disinfection of DI water contaminated with *S. typhimurium* bacteria takes more time than in the case of DI water contaminated with *E. coli B*. This conclusion is confirmed with the kinetic calculations for expenditure of hydroxyl radicals.

## Acknowledgments

This work was partially supported by EPA SBIR Program (Project EP-D-11-052). The authors are grateful to L. Lam and G. Shegebaeva for microbiological tests of bacteria concentration, as well as R. E. Wolfe for providing the poultry rinsing water.

## References

1. Sampson, R. L.; Sampson, A. H. U.S Patent 6,416,645,2002.
2. Lillard, H. S. The impact of commercial processing procedures on the bacterial contamination and cross-contamination of broiler carcasses. *J. Food Prot.* **1990**, *53*, 202–204.
3. Sheldon, B. W.; Brown, A. L. Efficacy of ozone as a disinfectant for poultry carcasses and chiller water. *J. Food Sci.* **1986**, *51*, 305–309.
4. Izat, A. L.; Griffis, C. Incidence and level of *Campylobacter jejuni* in broiler processing. *Poult. Sci.* **1988**, *67*, 1568–1572.
5. Slavik, M. F.; Griffis, C. L.; Li, Y.; Engler, P. V. Effect of electrical stimulation on bacterial contamination of chicken legs. *J. Food Prot.* **1991**, *54*, 508–513.

6. Li, Y.; Walker, J. T.; Slavik, M. F.; Wang, H. Electrical treatment of poultry chiller water to destroy *Campylobacter jejuni*. *J. Food Prot.* **1995**, *58*, 1330–1334.
7. Chauvier, D. J. U.S. Patent 6,827,847, 2004.
8. Hecking, W. U.S. Patent 6,849,178, 2005.
9. Gillham, R. W. U.S. Patent 5,868,941, 1999.
10. Snee, T. M. U.S. Patent 6,113,779, 2000.
11. Hernlem, B. J.; Tsai, L. S. Chlorine generation and disinfection by electroflotation. *J. Food Sci.* **2000**, *65*, 834–837.
12. Tsai, L. S.; Hernlem, B. J.; Huxsoll, C. C. Disinfection and solids removal of poultry chiller water by electroflotation. *J. Food Sci.* **2002**, *67*, 2160–2164.
13. Li, Y.; Kim, J. W.; Slavik, M. F.; Griffis, C. L.; Walker, J. T. *Salmonella typhimurium* Attached to chicken skin reduced using electrical stimulation and inorganic salts. *J. Food Sci.* **1994**, *59*, 23–25.
14. Slavik, M. F.; Kim, J. W.; Li, Y.; Walker, J. T.; Wang, H. Morphological changes of *Salmonella typhimurium* caused by electrical stimulation in various salt solutions. *J. Food Prot.* **1995**, *58*, 375–378.
15. Patermarakis, G.; Fountoukidis, E. Disinfection of water by electrochemical treatment. *Water Res.* **1990**, *24*, 1491–1496.
16. Shinohara, H.; Kojima, J.; Yaoita, M.; Aizawa, M. Electrically stimulated rupture of cell membranes with a conducting polymer-coated electrode. *Bioelectrochem. Bioenerg.* **1989**, *22*, 23–35.
17. Grahl, T.; Markl, H. Killing of microorganisms by pulsed electric fields. *Appl. Microbiol. Biotechnol.* **1996**, *45*, 148–157.
18. Li, X. Y.; Diao, H. F.; Fan, F. X. J.; Gu, J. D.; Ding, F.; Tong, A. S. F. Electrochemical wastewater disinfection: Identification of its principal germicidal actions. *J. Environ. Eng.* **2004**, *130*, 1217–1221.
19. Amadelli, R.; Samiolo, Velichenko, A. B.; Knysh, V. A.; Luk'yanenko, T. V.; Danilov, F. I. Composite PbO<sub>2</sub>–TiO<sub>2</sub> materials deposited from colloidal electrolyte: Electrosynthesis, and physicochemical properties. *Electrochim. Acta* **2009**, *54*, 5239–5245.
20. Kazi, A.; Hays, R. L.; Buckley, J. W. U.S. Patent 6,270,650, 2001.
21. Kasai, P. H.; McLeod, D. Detection by spin trapping of H and OH radicals generated during electrolysis of water. *J. Phys. Chem.* **1978**, *82*, 619–624.
22. Hepel, M.; Luo, J. Photoelectrochemical mineralization of textile diazo dye pollutants using nanocrystalline WO<sub>3</sub> electrodes. *Electrochim. Acta* **2001**, *48*, 729–740.
23. Shimada, K.; Shimahara, K. Factors affecting the surviving factors of resting *Escherichia coli* B and K-12 cells exposed to alternating current. *Agric. Biol. Chem.* **1981**, *45*, 1589–1595.
24. Palaniappan, S.; Sastry, S. K. Effects of electricity on microorganism: a review. *J. Food Process. Preserv.* **1990**, *14*, 393–414.
25. Barashkov, N. N.; Irgibaeva, I. S.; Shegebaeva, G. Sh.; Myrkhaidarov, K. B. Chlorine-free electrochemical AC disinfection of water contaminated with *Escherichia coli* B. *Vestnik ENU* **2008**, *6*, 134–140, in Russian.
26. Barashkov, N. N.; Eisenberg, D.; Eisenberg, S.; Shegebaeva, G. Sh.; Irgibaeva, I. S.; Barashkova, I. I. Electrochemical chlorine-free AC

- disinfection of water contaminated with *Salmonella typhimurium* bacteria. *Elektrokhimiya* **2010**, *46*, 320–325, in Russian.
27. Carter, S. D.; Cunefare, K. A. U.S. Patent 6,447,718, 2002.
  28. Comninellis, Ch. Electrocatalysis in the electrochemical conversion/combustion of organic pollutants for waste water treatment. *Electrochim. Acta* **1994**, *39*, 1857–1862.
  29. Ma, L.; Yanf, Z.; Li, Y.; Griffis, C. Microbial, chemical and physical changes in chill water treated with electrochemical method. *J. Food Process Eng.* **2000**, *23*, 57–72.
  30. Hochanadel, C. J Photolysis of dilute hydrogen peroxide solution in the presence of dissolved hydrogen and oxygen. *Radiat. Res.* **1962**, *17*, 286–301.

## Chapter 3

# Effect of Calcium and EDTA on the Uptake of Cadmium and Lead by *Brassica juncea* in Hydroponic Growth Medium

D. L. Van Engelen,\* J. S. Boyd, and K. Ekbia

Department of Chemistry, University of Redlands,  
Redlands, California 92373, United States

\*E-mail: [debra\\_vanengelen@redlands.edu](mailto:debra_vanengelen@redlands.edu)

Uptake by *Brassica juncea* of nutrient and toxic metals was studied using hydroponic growth media in some experiments with 200 mg Ca<sup>2+</sup> L<sup>-1</sup> compared to other experiments without added calcium ion. The absence of adequate Ca<sup>2+</sup> alone resulted in very unhealthy plants and low biomass. In other treatment experiments, 10 mg Cd<sup>2+</sup> L<sup>-1</sup> and/or 50 mg Pb<sup>2+</sup> L<sup>-1</sup> and/or 150 mg EDTA L<sup>-1</sup> were added. Addition of EDTA increased plant biomass, protected against phytotoxicity, and increased total uptake of heavy metals. Addition of even very low levels of Pb<sup>2+</sup> improved the plant health produced by either low Ca<sup>2+</sup> availability or Cd<sup>2+</sup> toxicity. *B. juncea* produced extremely high bioconcentration (BC) factors for lead and good BC factors for cadmium. Reductions of 10 ppm Cd<sup>2+</sup> and 50 ppm Pb<sup>2+</sup> in the treatment solutions over time indicate that contamination would be removed after 3.8 and 3.6 growth cycles, respectively.

## Introduction

Metal uptake by the roots of higher plants is mediated by a number of factors including the solubility in the external rhizosphere and the chemical form of the cation. There are also a number of complex inter-metal effects which regulate the relative concentrations of metals in plants. Calcium ion, Ca<sup>2+</sup>, has a regulatory role in mediating transpiration rates and the balance of metals such as magnesium ion and sodium ion in the cell. Calcium ion has been shown to affect a favorable ratio between Na<sup>+</sup> and K<sup>+</sup> for cells as well as other metals (1). An example of



membrane transport is the sodium-potassium pump, Na<sup>+</sup>-K<sup>+</sup> ATPase, which is gated by calcium ions, Ca<sup>2+</sup> (2).

Plants known as hyperaccumulators have developed efficient mechanisms for protection from non-nutrient metals such as cadmium or lead ion and have an increased tolerance for toxic metals within the plant tissue itself. The type IB ATPases evolved very early in plants to sequester or transfer heavy metals out of cells and are used to resist toxic effects and maintain metal homeostasis (3). Most plants protect themselves from toxic metals using exclusion mechanisms to precipitate heavy metals in external pathways of roots (4, 5) or by sequestering mechanisms which encapsulate heavy metal deposits in the xylem external to cells, in vacuoles within the cell, or in external leaf structures (6, 7). Toxic metal cations often decrease plant growth by inhibiting accumulation of nutrient metals such as Fe and Mn (8).

Fe-transporting chelators, called phytosiderophores, that are released from roots have been shown to have a direct effect on cadmium accumulation and can be fairly nonspecific for transport of divalent ions (9). These natural chelators also appear to have a protective role against toxic metals (10). It has been shown that complexed forms of metal ions facilitate transport across the root membrane and also translocation of the complexed metal to the green shoots (stems and leaves) of *Brassica juncea* or Indian mustard (7, 11). Synthetic chelating agents such as ethylenediaminetetraacetic acid (EDTA) and other synthetic chelating agents also increase the uptake of heavy metals from soils by Indian mustard (12–14). EDTA-complexed Cd or Pb may also offer the same type of protective benefits as natural chelators to plants grown in contaminated media.

*B. juncea* has a unique ability to hyperaccumulate a large number of heavy metals at normally phytotoxic levels. Indian mustard reacts to the presence of toxic metals by rapidly releasing phytochelatins to protect the plants (11) but also changes the lipid composition of the cell membrane for protection (15). Hyperaccumulation by *B. juncea* can be a concern for foodstuffs that are grown in metal-contaminated soils (16). This species has also been studied as possible sources of phytoremediation of contaminated soil (12, 13, 17, 18) or contaminated water (5, 6, 8, 11, 14, 19).

## Experimental Methods

### Hydroponic Growth Experiments with “High Ca” or “Low Ca”

The hydroponic nutrient solutions were prepared based upon a procedure by Reiss (20). Growth experiments were repeated up to four times with different variations. As shown in Table I, two different concentration levels of Ca(NO<sub>3</sub>)<sub>2</sub>·4H<sub>2</sub>O were added to the thirteen tanks with either a final tank concentration of approximately zero called “Low Ca” (i.e. none added to Tanks 1, 4 and 11–13) or at the normal hydroponic concentration of 200 ppm Ca<sup>2+</sup> (i.e. mg Ca<sup>2+</sup> L<sup>-1</sup>) called “High Ca” (resulting in an added final concentration of 5.0 × 10<sup>-3</sup> M Ca(NO<sub>3</sub>)<sub>2</sub>·4H<sub>2</sub>O added to tanks 2, 3, and 5–10). To the “Low calcium” tanks was added 5.0 × 10<sup>-3</sup> M NaNO<sub>3</sub> to balance the ionic strength. Other final

nutrient concentrations added to all thirteen tanks were  $5.0 \times 10^{-3}$  M of  $\text{KNO}_3$  (or 196 ppm  $\text{K}^+$  per tank),  $2.0 \times 10^{-3}$  M  $\text{MgSO}_4$  (or 49 ppm  $\text{Mg}^{2+}$  per tank) and  $1.0 \times 10^{-3}$  M  $\text{KH}_2\text{PO}_4$  (or 39 ppm  $\text{K}^+$  and 95 ppm  $\text{PO}_4^{3-}$  per tank). To each tank was added 20 mL of a filtered saturated solution containing 5 g of  $\text{FeSO}_4 \cdot 7\text{H}_2\text{O}$  in 1.0 L of water (exact final concentration unknown). To each tank was then added 20 mL of a 1 L micronutrient solution containing 2.88 g  $\text{H}_3\text{BO}_3$ , 1.81 g  $\text{MnCl}_2 \cdot 4\text{H}_2\text{O}$  (J.T. Baker, Phillipsburg NJ), 0.22 g  $\text{ZnSO}_4 \cdot 7\text{H}_2\text{O}$ , 0.08 g  $\text{CuSO}_4 \cdot 5\text{H}_2\text{O}$  and 0.02 g  $(\text{NH}_4)_6\text{Mo}_7\text{O}_{27} \cdot 4\text{H}_2\text{O}$  (J.T. Baker). All reagents were purchased from Aldrich (St. Louis, Mo.) unless otherwise noted. The average measured pH of the hydroponic solutions in the thirteen tanks was 6.9. Each of 13 growth tanks were filled to a total volume of 10 L of hydroponic nutrient solution and aerated by airstones connected to air pumps. A permanent mark on the outside of each 20 gallon aquarium tank was made to show the 10 L volume level and deionized water was added weekly to maintain a constant tank volume. The tanks were illuminated constantly by both 40 watt warm and cool white fluorescent lighting and held at a constant temperature of 23 °C and relative humidity of 50% in controlled-environment growth rooms. The tanks' hydroponic solutions were allowed to equilibrate for three days before the cups with transplanted plants were placed in them.

A mixture of 1 part vermiculite to 2 parts perlite by volume, was support for the seedlings in the growth cups, eight 9 oz. plastic growth cups with 4 punctured holes at bottom were floated atop Styrofoam sheets in each experiment tank. *Brassica juncea* or Indian mustard seeds (Johnny's Selected Seeds, Albion, ME, Cat. No. 377.26) were germinated in covered Petri dishes on paper towels soaked with deionized water for 14 days. The seedlings were then transplanted into the growth cups, at 4-5 seedlings per cup. After the cups were floated in the hydroponic growth tanks, the plants were given 9 additional days to recover from the transplanting before any treatment compounds ( $\text{Cd}^{2+}$ ,  $\text{Pb}^{2+}$ , and/or EDTA) were added to the tanks

### Treatment Growth Period with Added $\text{Cd}^{2+}$ , $\text{Pb}^{2+}$ , and/or EDTA

Tank treatment variations for each experiment are also given in Table I. Ethylenediaminetetraacetic acid (EDTA) was added to tanks 1-3, 8, 10, 12 and 13 at a final concentration of 150 ppm EDTA (or 150 mg EDTA  $\text{L}^{-1}$ ) or  $5.17 \times 10^{-4}$  M EDTA final tank concentration. This concentration of EDTA is sufficient to complex trace amounts of divalent ions and thus make them more available in the hydroponic solution without damaging the plants by adding too much chelating agent. It has previously been reported that levels over 200 ppm EDTA can be toxic to plants (14). No chelating agent was added to the other tanks. To tanks 7-12 was added  $\text{Cd}(\text{NO}_3)_2 \cdot 4\text{H}_2\text{O}$  to an initial treatment concentration of 10 ppm  $\text{Cd}^{2+}$  (or 10 mg  $\text{Cd}^{2+}$   $\text{L}^{-1}$ ) in each tank solution. To tanks 2, 5, 9-10 and 12-13 was added  $\text{Pb}(\text{NO}_3)_2$  to make an initial tank concentration of 50 ppm (i.e. 50 mg  $\text{Pb}^{2+}$   $\text{L}^{-1}$ ).

**Table I. Hydroponic tank experiments for growth experiments with *Brassica juncea* (conditions for 4<sup>th</sup> trial)**

<i>Tank #</i>	<i>10 mg Cd<sup>2+</sup> L<sup>-1</sup></i>	<i>50 mg Pb<sup>2+</sup> L<sup>-1</sup></i>	<i>150 mg EDTA L<sup>-1</sup></i>	<i>Low Ca<sup>2+</sup>, (i.e. none added)</i>	<i>High Ca<sup>2+</sup>, added 200 mg Cd<sup>2+</sup> L<sup>-1</sup></i>
1 [Control +EDTA Low Ca]	-	-	+	+	-
2	-	+	+	-	+
3 [Control + EDTA High Ca]	-	-	+	-	+
4 [Control Low Ca]	-	-	-	+	-
5	-	+	-	-	+
6 [Control High Ca]	-	-	-	-	+
7	+	-	-	-	+
8	+	-	+	-	+
9	+	+	-	-	+
10	+	+	+	-	+
11	+	-	-	+	-
12	+	-	+	+	-
13	-	+	+	+	-

### **Observations and Sampling of Hydroponic Solutions during the Growth Period**

The plants were grown for 75 additional days after the treatment period began (or a total growth period of 93 days from day 1 of germination). During the treatment period observations about plant health and average heights were recorded and 25 mL samples of the nutrient solution were taken on treatment days 17, 36, 54 and 74 and acidified with 2 mL 3 M HNO<sub>3</sub> for later analysis.

## Plant Harvest, Sample Preparation, and Analysis

At the end of the growth period, the plants were carefully removed from their support medium, rinsed with deionized water, and blotted. It was very difficult to separate the roots from the perlite/vermiculate growth support so very little root matter was available for analysis (root data not presented here). The harvested plant shoots (leaves and stems) were oven-dried for 24 hours at 80 °C. The dried plant matter was then separated into 3 replicate subsamples of 0.2-0.5 g each depending upon the total amount of dried plant material available.

Each weighed sample of dried plant matter above was cut to small pieces with scissors, pulverized with a mortar and pestle, and placed in 70 mL polyethylene vials of a ModBlock digestion apparatus (CPI International, Santa Rosa, Ca). The plant samples were digested with concentrated trace-metal-grade nitric acid and 30% hydrogen peroxide according to a USEPA procedures (21, 22). To each vial were added 6 mL of HNO<sub>3</sub> and 2 mL of 30% H<sub>2</sub>O<sub>2</sub>, and allowed to sit for 30 min to 1 h until the foaming subsided. The samples were then refluxed with occasional swirling on the hot block for approximately 1 h that was preheated to 80 °C and gradually increased to 140 °C or until 2-3 mL of solution was left in the vial. The refluxing was repeated two more times at 140 °C for 30-45 min, each time after adding 3 mL of HNO<sub>3</sub> and 1 mL of H<sub>2</sub>O<sub>2</sub> to each sample. In the final step of the digestion, the walls of the vials were washed with 10 mL of 10% HNO<sub>3</sub>, 5 mL of concentrated HCl and 10 mL of deionized water were added, and refluxed for another 15 min. Depending upon the initial mass of the sample, 0.5, 0.3, or 0.2 g, the total volume was adjusted to 50, 30 or 20 mL, respectively. All digested samples were filtered with a 0.45 μm pore nylon syringe filters and re-filtered with a 0.20 μm pore nylon syringe filters.

Tanks solutions samples and the digested plant samples were analyzed using a Shimadzu AA-6300 atomic absorption spectrophotometer (AAS) (Baltimore, Md) using either an air-acetylene flame nebulizer for ppm concentrations or Shimadzu GFA-EX71 graphite furnace for ppb levels of lead. Tank solution samples collected over the growth period were analyzed for Cd<sup>2+</sup> ( $\lambda = 228.8$  nm), Pb<sup>2+</sup> ( $\lambda = 217.0$  nm for furnace or 283.3 nm for flame), Ca<sup>2+</sup> ( $\lambda = 422.7$  nm), and Mg<sup>2+</sup> ( $\lambda = 285.2$  nm). Ions analyzed in dried plant samples included Cd<sup>2+</sup> and Pb<sup>2+</sup>.

## Results and Discussion

### Measurement of Selected Ions in Hydroponic Growth Solutions

Hydroponic nutrient and treatment solutions are easy to sample and determine the exact concentrations of soluble metal ions available for uptake during the growth period. In normal hydroponic growth solution (“high Ca”), calcium was measured at 150-170 mg Ca<sup>2+</sup> L<sup>-1</sup>. Other tanks indicated as “low Ca” had the same hydroponic nutrient solutions except no added calcium ion was added and they had a measured background level of Ca<sup>2+</sup> of 3-7 mg Ca<sup>2+</sup> L<sup>-1</sup> solution (see Table II). In experiments not described here, the low background level of calcium ion was found to originate from the perlite/vermiculite root support in the growth cups.

Cd<sup>2+</sup> and Pb<sup>2+</sup> added to tanks without EDTA were partially or nearly completely precipitated as the phosphate salts. Care was taken to add no other precipitating anions (e.g. CO<sub>3</sub><sup>2-</sup>) to the growth solutions.

### Summary of Plant Growth and Biomass in Different Experiments and Treatments

Table III summarizes the plant growth characteristics, appearance, and biomass of the total plant matter in each tank experiment. In experiments with low calcium, the low Ca<sup>2+</sup> condition alone (even without added Cd<sup>2+</sup> or Pb<sup>2+</sup>) had a very adverse effect on plant growth and biomass with stunted growth and small, yellow leaves. Many “low Ca” plants died during the growth period. Addition of EDTA in related experiments improved the plant of the low calcium plants and increased the total biomass by fourfold and improved the plant health.

**Table II. Measurements by AAS of four ion concentrations in tank nutrient solutions on day 17 of the treatment period**

<i>Ion measured</i>	<i>No EDTA</i>				<i>+ 150 ppm EDTA</i>			
	<i>Low Ca</i>		<i>High Ca</i>		<i>Low Ca</i>		<i>High Ca</i>	
	<i>mg ion/L</i>	<i>SD</i>	<i>mg ion/L</i>	<i>SD</i>	<i>mg ion/L</i>	<i>SD</i>	<i>mg ion/L</i>	<i>SD</i>
Ca <sup>2+</sup>	3.3	0.1	150	31	7.5	5.1	170	6
Mg <sup>2+</sup>	17	4	43	5	33	4	41	2
Cd <sup>2+</sup>	0.39	---	1.2	0.6	8.6	---	8.6	0.2
Pb <sup>2+</sup>	2.0 × 10 <sup>-4</sup>	---	4.4 × 10 <sup>-3</sup>	---	58 <sup>a</sup>	---	45	5

<sup>a</sup> Slightly high value for Pb<sup>2+</sup> in tank 13 was consistent in later tank sample measurements. “Low Ca” = none added; “High Ca” = normal nutrient level of 200 ppm Ca<sup>2+</sup> added. Mg<sup>2+</sup> added at 50 ppm. No standard deviation, SD, given where only one sample analyzed.

In additional treatment hydroponic experiments, toxic levels of 10 µg/mL Cd<sup>2+</sup> and/or 50 µg/mL Pb<sup>2+</sup> were added to some nutrient solutions in order to study the uptake of these heavy metals in relation to added calcium or EDTA. Cadmium ion is quite toxic to Indian mustard but treatment experiments with Pb<sup>2+</sup> showed little phytotoxic effect of lead alone. When the normal hydroponic growth solutions with measured soluble of 150-170 mg Ca<sup>2+</sup> L<sup>-1</sup> were treated with phytotoxic of cadmium (soluble at 3-9 mg Cd<sup>2+</sup> L<sup>-1</sup> without EDTA), the Indian mustard plants showed signs of poor health and markedly reduced biomass. In Cd treatment tank 7 with normal, high-Ca<sup>2+</sup> and no EDTA, cadmium toxicity alone produced plants that were very unhealthy and small (comparable to the low-Ca<sup>2+</sup> plants in tank 4). In other experiments, the addition of EDTA alleviated the detrimental effects of cadmium to the plants somewhat when it was added to the growth medium. Tank 8 had the same exact growth medium and Cd-treatment

as tank 7 except EDTA was added, and the plants were a healthy green color with over three times greater biomass.

Interestingly, the addition of either  $\text{Cd}^{2+}$  and/or  $\text{Pb}^{2+}$  to the experimental hydroponic growth medium in the presence of EDTA improved the adverse effects of low- $\text{Ca}^{2+}$ . In cases of low- $\text{Ca}^{2+}$  but with the addition both of  $\text{Cd}^{2+}$  and EDTA, the plant total biomass increased over sevenfold higher (in tank 12). Likewise, when  $\text{Pb}^{2+}$  was added to the low calcium medium with EDTA (in tank 13), the biomass increased nearly eightfold over the low- $\text{Ca}^{2+}$  control in tank 4. This might indicate that in cases of low calcium in the presence of EDTA, the divalent cations cadmium and lead are replacing some regulatory functions of calcium ion in the plants when calcium ion is not present at sufficient levels.

**Table III. Plant health and total biomass per tank**

TANK	Conditions	Plant health, appearance	Total plant	
			Mass (g)	Ave. Ht (cm)
6	High Ca control	good, green	5.4	19
3	High Ca + EDTA control	very good, green	6.2	27
4	Low Ca control	poor, yellow	0.94	4
1	Low Ca + EDTA control	good, green	3.8	17
5	High Ca + Pb	good, green	5.8	17
2	High Ca + Pb + EDTA	good, green	4.7	17
13	Low Ca + Pb + EDTA	very good, green	8.1	23
7	High Ca + Cd	poor, yellow	0.7	4
8	High Ca + Cd + EDTA	OK. Green	2.3	13
11	Low Ca + Cd	poor, yellow	1.9	6
12	Low Ca + Cd + EDTA	good, green	7.6	21
9	High Ca + Cd + Pb	OK. Green	1.8	13
10	High Ca + Cd + Pb + EDTA	v. good, green	12.8	23

In growth experiments with normal high levels of  $\text{Ca}^{2+}$  and EDTA present, adding both  $\text{Cd}^{2+}$  and  $\text{Pb}^{2+}$  simultaneously in the growth medium as in tanks 9 and 10 resulted in double the biomass of dried plant shoots over the non-treated control plants with similar conditions but with the heavy metals added individually. This might indicate that some compensatory protection mechanism in the plants

towards heavy metals was acting to improve overall growth of the plant. For example, the presence of a second toxic metal might be stimulating release of more natural phytosiderophores or other plant protective mechanisms. In the normal  $\text{Ca}^{2+}$  and  $\text{Cd}^{2+}$  treatment tanks without EDTA added, addition of  $\text{Pb}^{2+}$  also improved the health of plants adversely affected by  $\text{Cd}^{2+}$  toxicity.

### **$\text{Cd}^{2+}$ and $\text{Pb}^{2+}$ in Dried Plant Samples**

After the plants in each tank were harvested and dried, the leaves and shoots (or green parts) of the plants were digested and analyzed by AAS for concentrations of cadmium and lead. The results of these measurements of plant shoots are shown in Figure 1A and 1B for added cadmium and added lead treatments, respectively. It is expected that the concentrations of toxic ions would be much greater in roots than those measured in green shoots because as noted above most heavy metals are immobilized on root surfaces. EDTA addition normally increased the dried plant concentrations of  $\text{Cd}^{2+}$  in this trial although we did not find this trend to be entirely reproducible in all experiments.

The concentration of toxic ions in dried samples does not necessarily reflect or even correlate with the total uptake of  $\text{Cd}^{2+}$  or  $\text{Pb}^{2+}$  because of the much greater health and biomass of plants grown with EDTA present. For example, even if the dried plant samples for a particular experiment contain a lower toxic metal concentration, a much larger plant biomass could result in a greater total uptake for that experiment. As seen in Table III, Tank 10 (high- $\text{Ca}^{2+}$  +  $\text{Cd}^{2+}$  +  $\text{Pb}^{2+}$  + EDTA) and tank 12 (low- $\text{Ca}^{2+}$  +  $\text{Cd}^{2+}$  + EDTA) had the largest biomass for Cd-treated tanks. Tank 10 (high- $\text{Ca}^{2+}$  +  $\text{Cd}^{2+}$  +  $\text{Pb}^{2+}$ ) and tank 13 (low- $\text{Ca}^{2+}$  +  $\text{Pb}^{2+}$  + EDTA) had the greatest biomass for Pb-treatment tanks. These are the conditions in which the greatest remediation of toxic metals by Indian mustard occurs. Figure 2A and 2B show the experimental tanks with the greatest total uptake of  $\text{Cd}^{2+}$  and  $\text{Pb}^{2+}$  in plant shoots, respectively. As stated previously, the concentrations of these toxic metals are expected to be much greater in the plant roots.

### **Effect of EDTA on Plant Uptake of Toxic Ions, Health, and Biomass**

Addition of EDTA to any growth medium experiment increased the total biomass of the shoots relative to the same experiment without EDTA. EDTA greatly increases the solubility of divalent ions when precipitated in insoluble salts or bound to soil matrix. For Cd-treatment tanks, adding EDTA did not greatly increase the soluble  $\text{Cd}^{2+}$  present nor did it greatly increase the concentration of  $\text{Cd}^{2+}$  in the dried shoot samples. This is unlike plants grown in soil where addition of the chelating agent significantly increases the solubility of  $\text{Cd}^{2+}$  and thus has a marked effect on the concentration in plant tissues (13). Addition of EDTA to  $\text{Pb}^{2+}$  treatments greatly increased the concentration in plant samples because the EDTA complex released the  $\text{Pb}^{2+}$  from insoluble phosphate precipitate and therefore, increased the soluble concentration of lead in the growth solution.

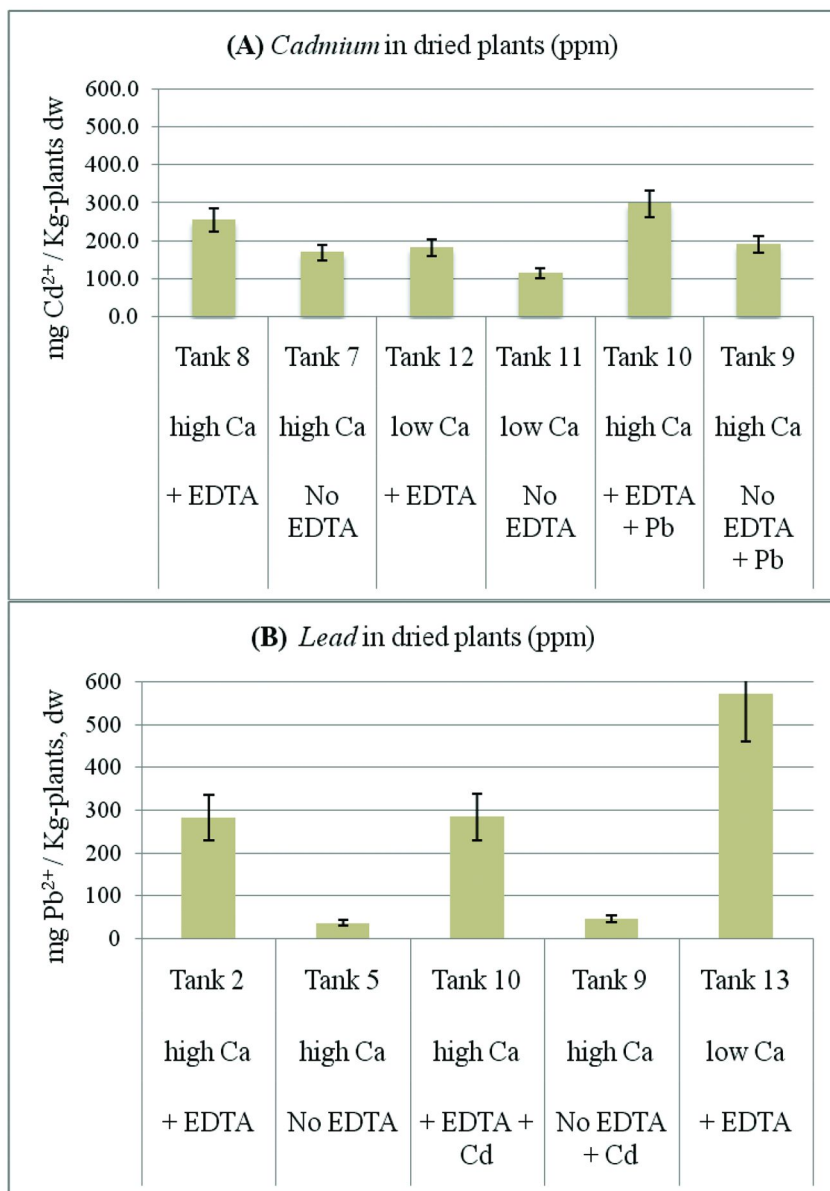


Figure 1. Ion concentration in plant shoots (leaves and stems) samples, dry weight (d.w.) for (A) Cd<sup>2+</sup> or (B) Pb<sup>2+</sup>; N = 3, Error bars in RSD.



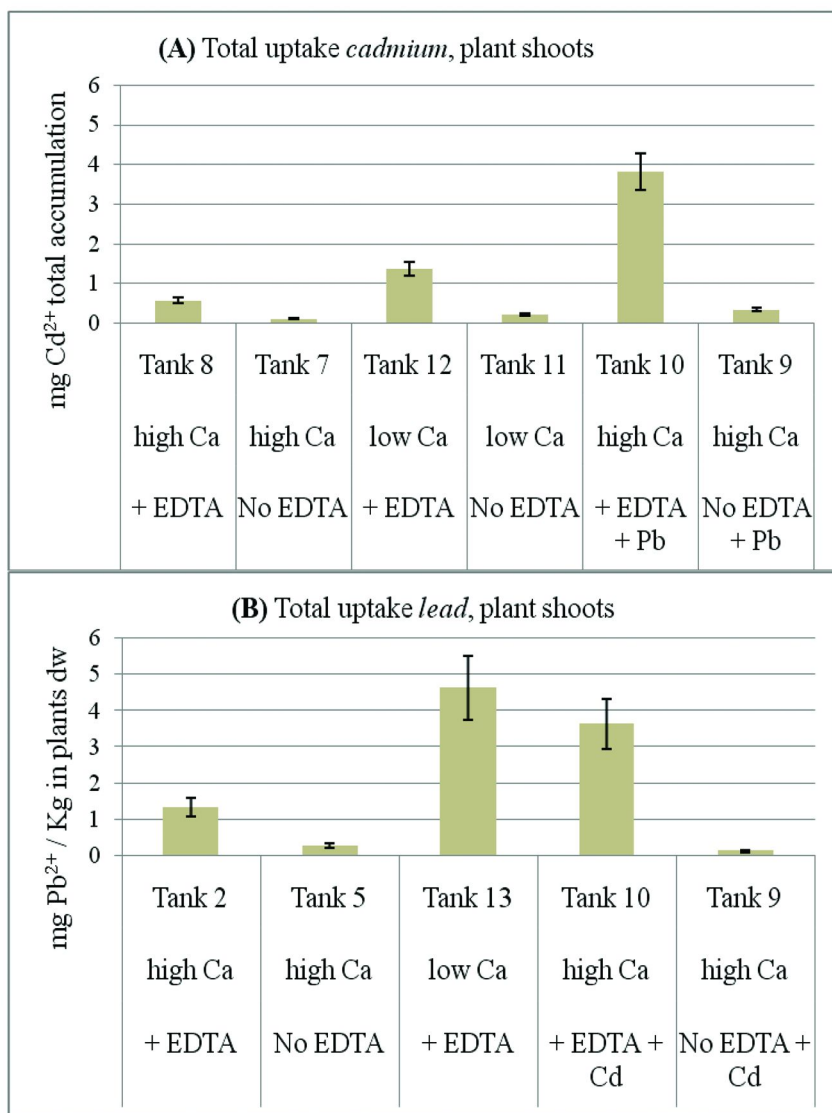


Figure 2. Total uptake in plant shoots of toxic metals per tank for (A) Cd<sup>2+</sup> and (B) Pb<sup>2+</sup>; N = 3, Error bars in RSD.

In hydroponic growth solutions, EDTA has a complex effect on the dried plant concentration of a particular ion after harvesting depending upon the particular conditions and plant health in a tank. EDTA complexes with some divalent metal ions and may increase their solubility and availability for uptake into the plant. On the other hand, some metals are very tightly bound to the EDTA ligand, and the large complex might not as readily cross the symplast for transport into the plant stems and leaves. However, once the EDTA-complexed cation is in the xylem, it is more water soluble and more easily translocates from plant roots to green stems and leaves. Therefore, with particular cations under different conditions, the addition of EDTA increases the dried plant concentration of ions in the plant shoots but in other cases, the concentration of a particular cation will decrease when EDTA is added to the hydroponic nutrient solution.

### **Bioconcentration Factors and Phytoremediation Potential**

The bioconcentration factors (BCF) calculated for this research are defined as the concentration of a specific cation in the plant green shoots over the concentration of that same cation in tank growth solutions. As shown in Table IV, *B. juncea* has extremely high bioconcentration (BC) factors values for lead showing that it is able to remove and concentrate  $\text{Pb}^{2+}$  even from water with extremely low ppb contamination. It also has good BC factors for cadmium. Note that in all cases, addition of EDTA dramatically lowers the BCF because the complexed form of these ions has a greater solubility in the growth solution.

Measured reductions of 10 ppm  $\text{Cd}^{2+}$  and 50 ppm  $\text{Pb}^{2+}$  in the treatment growth solutions over time in different tanks are shown in Figures 3A and 3B. All tanks graphed in Figure 3A contained 10 ppm  $\text{Cd}^{2+}$  and 150 ppm EDTA, initially. The rate of decrease in tank concentration of  $\text{Cd}^{2+}$  are similar for all three experiments. Averaging the slopes from those three experiments and assuming a constant uptake rate for subsequent repeated plantings and harvests of *B. juncea*, all  $\text{Cd}^{2+}$  would be removed from Cd-treated tanks after 3.8 growth cycles. Likewise, three 50 ppm Pb-treated experiments with added EDTA are shown in Figure 3B. The rates of uptake of  $\text{Pb}^{2+}$  are somewhat more varied for the three experiments shown than for cadmium. However, assuming a constant average uptake rate (average linear decrease of measured ion of the three tanks shown) all contamination from lead would be removed after 3.6 growth cycles.

**Table IV. Calculated BCF for Cd<sup>2+</sup> and Pb<sup>2+</sup> treatments**

TANK	Experiment Conditions	Bioconcentration Factor (BCF)	
		Cd <sup>2+</sup>	Pb <sup>2+</sup>
2	High Ca +Pb +EDTA	N/A	5.82
5	High Ca +Pb	N/A	8.74 × 10 <sup>3</sup> <sup>a</sup>
7	High Ca + Cd	218	N/A
8	High Ca +Cd +EDTA	27.2	N/A
9	High Ca +Cd +Pb	477	2.33 × 10 <sup>5</sup> <sup>a</sup>
10	High Ca +Cd+Pb+EDTA	33.3	6.77
11	Low Ca + Cd	67.9	N/A
12	Low Ca + Cd +EDTA	19.8	N/A
13	Low Ca +Pb +EDTA	N/A	9.76

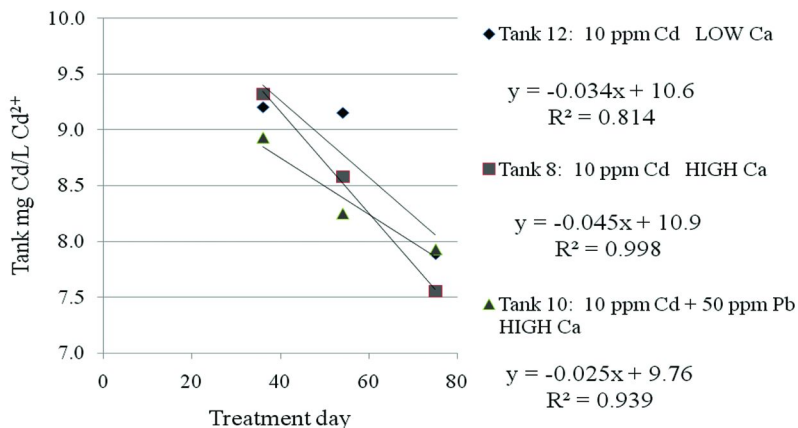
<sup>a</sup> In Pb<sup>2+</sup> treatments without added EDTA, virtually all Pb<sup>2+</sup> is precipitated as Pb<sub>3</sub>(PO<sub>4</sub>)<sub>2</sub>. Soluble Pb<sup>2+</sup> measured by AAS was 4.4 × 10<sup>-3</sup> mg/L and 2.0 × 10<sup>-4</sup> mg/L in Tanks 5 and 9 solutions, respectively. The bioconcentration values in Table IV were calculated using

$$BCF = \frac{(\text{mg M}^{n+} / \text{Kg plant tissue})}{(\text{mg M}^{n+} / \text{L growth solution})}$$

<sup>a</sup> In Pb<sup>2+</sup> treatments without added EDTA, virtually all Pb<sup>2+</sup> is precipitated as Pb<sub>3</sub>(PO<sub>4</sub>)<sub>2</sub>. Soluble Pb<sup>2+</sup> measured by AAS was 4.4 × 10<sup>-3</sup> mg/L and 2.0 × 10<sup>-4</sup> mg/L in Tanks 5 and 9 solutions, respectively. The bioconcentration values in Table IV were calculated using

$$BCF = \frac{(\text{mg M}^{n+} / \text{Kg plant tissue})}{(\text{mg M}^{n+} / \text{L growth solution})}$$

(A) Decrease in tank ppm Cd over time,  
 all these tanks contain EDTA



(B) Decrease in tank ppm Pb over time,  
 all these tanks contain EDTA

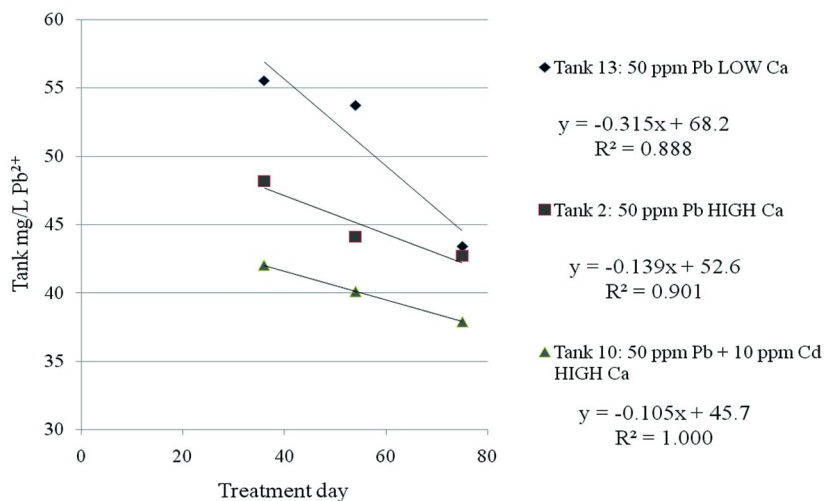


Figure 3. Measured ion concentration of tank solution over time for (A)  $Cd^{2+}$  or (B)  $Pb^{2+}$ .

## Conclusions

Hydroponically grown *B. juncea* with low calcium conditions (measured background at 3-7 ppm  $\text{Ca}^{2+}$  in growth solutions) resulted in poor plant growth and health. Adding cadmium-EDTA complex to the growth solution, slightly improved plant health and biomass. Adding lead-EDTA complex greatly improved plant health and increased the biomass of low calcium plants eight-fold. It may be possible that these chelated forms of  $\text{Cd}^{2+}$  or  $\text{Pb}^{2+}$  may compensate for some of the regulatory functions of the missing  $\text{Ca}^{2+}$  ion such as the improving the balance between  $\text{Na}^+$  and  $\text{K}^+$ .

When hydroponically grown *B. juncea* is grown in normal high calcium conditions without EDTA, cadmium treatment was highly toxic to the plants but lead showed little phytotoxicity. Adding EDTA Cd-treated plants, improved the health and biomass of plants. For  $\text{Cd}^{2+}$ , the BCF was in the range of 218 to 477 without EDTA, and 27 to 33 with EDTA. For  $\text{Pb}^{2+}$ , BCF were  $8.7 \times 10^3$  to  $2.3 \times 10^4$  without EDTA, and was 5.2 to 6.8 with EDTA. The greater biomass with EDTA resulted in a greater total uptake of toxic metals in experiments containing EDTA, and these results indicate that virtually all of the heavy metals would be removed from the growth solutions in approximately 4 growth cycles of *B. juncea* assuming a constant uptake rate.

While EDTA does not appear to have a consistent effect on the concentration of  $\text{Cd}^{2+}$  or  $\text{Pb}^{2+}$  in dried plant samples grown in hydroponic growth medium, it is possible that the chelated form of these metals are more readily incorporated into vacuoles in plant cells as a protection mechanism resulting in healthier plants. Plants that were treated with  $\text{Cd}^{2+}$ ,  $\text{Pb}^{2+}$ , and EDTA simultaneously had the greatest biomass and heavy metal uptake of all experiments. This may indicate that the plants have developed mechanisms to protect themselves and promote growth in the presence of multiple toxic metal species.

## Acknowledgments

University of Redlands Student Summer Research Fellowships

## References

1. Huang, J.; Redmann, R. E. Physiological responses of canola and wild mustard to salinity and contrasting calcium supply. *J. Plant Nutr.* **1995**, *18* (9), 1931–1949.
2. Møller, J. V.; Juul, B.; le Maire, M. Structural organization, ion transport, and energy transduction of P-type ATPases. *Biochim. Biophys. Acta* **1996**, *1286*, 1–51.
3. Axelsen, K. B.; Palmgren, M. G. Evolution of substrate specificities in the P-type ATPase superfamily. *J. Mol. Evol.* **1998**, *46*, 84–101.
4. Hall, J. L. Cellular mechanisms for heavy metal detoxification and tolerance. *J. Exp. Bot.* **2002**, *53*, 1–11.

- Salt, D. E.; Benhamou, N.; Leszczyniecka, M.; Raskin, I.; Chet, I. A. Possible role for rhizobacteria in water treatment by plant roots. *Int. J. Phytorem.* **1999**, *1* (1), 67–79.
- Meyers, D. E. R.; Auchterlonie, G. J.; Webb, R. I.; Wood, B. Uptake and localization of lead in the root system of *Brassica juncea*. *Environ. Pollut.* **2008**, *153*, 323–332.
- Salt, D. E.; Prince, R. C.; Pickering, I. J.; Raskin, I. Mechanisms of cadmium mobility and accumulation in Indian mustard. *Plant Physiol.* **1995**, *109*, 1427–1433.
- Ebbs, S. D.; Kochian, L. V. Toxicity of zinc and copper to *Brassica* species: Implications for phytoremediation. *J. Environ. Qual.* **1997**, *26*, 776–781.
- Cohen, C. K.; Fox, T. C.; Garvin, D. F.; Kochian, L. V. The role of iron-deficiency stress responses in stimulating heavy-metal transport in plants. *Plant Physiol.* **1998**, *116*, 1063–1072.
- Hill, K. A.; Lion, L. W.; Ahner, B. A. Reduced Cd accumulation in *Zea mays*: A protective role for phytosiderophores? *Environ. Sci. Technol.* **2002**, *36*, 5363–5368.
- Salt, D. E.; Pickering, I. J.; Prince, R. C.; Gleba, D.; Dushenkov, S.; Smith, R. D.; Raskin, I. Metal accumulation by aquacultured seedlings of Indian mustard. *Environ. Sci. Technol.* **1997**, *31*, 1636–1644.
- Blaylock, M. J.; Salt, D. E.; Dushenkov, S.; Zakharova, O.; Gussman, C.; Kapulnik, Y.; Ensley, B. D.; Raskin, I. Enhanced accumulation of Pb in Indian mustard by soil-applied chelating agents. *Environ. Sci. Technol.* **1997**, *31* (3), 860–865.
- Van Engelen, D. L.; Sharpe-Pedler, R. C.; Moorhead, K. K. Effect of chelating agents and solubility of cadmium complexes on uptake from soil by *Brassica juncea*. *Chemosphere* **2007**, *68*, 401–408.
- Vassil, A. D.; Kapulnik, Y.; Raskin, I.; Salt, D. E. The role of EDTA in lead transport and accumulation by Indian mustard. *Plant Physiol.* **1998**, *117*, 447–453.
- Nouairi, I.; Ammar, W. B.; Youssef, N. B.; Daoud, D. B. M.; Ghorbal, M. H.; Zarrouk, M. Comparative study of cadmium effects on membrane lipid composition of *Brassica juncea* and *Brassica napus* leaves. *Plant Sci.* **2006**, *170*, 511–519.
- Xiong, S.-L.; Xiong, Z.-T.; Chen, Y.-C.; Huang, H. Interactive effects of lanthanum and cadmium on plant growth and mineral element uptake in crisped-leaf mustard under hydroponic conditions. *J. Plant Nutr.* **2006**, *29*, 1889–1902.
- Marchiol, L.; Sacco, P.; Assolari, S.; Zerbi, G. Reclamation of polluted soil: phytoremediation potential of crop-related *Brassica* species. *Water, Air, Soil Pollut.* **2004**, *158*, 345–356.
- Jiang, X. J.; Luo, Y. M.; Zhao, Q. G.; Baker, A. J. M.; Christie, P.; Wong, M. H. Soil Cd availability to Indian mustard and environmental risk following EDTA addition to Cd-contaminated soil. *Chemosphere* **2003**, *50*, 813–818.
- Dushenkov, V.; Kumar, P. B. A. N.; Motto, H.; Raskin, I. Rhizofiltration: The use of plants to remove heavy metals from aqueous streams. *Environ. Sci. Technol.* **1995**, *29*, 1239–1246.

20. Reiss, C. *Experiments in Plant Physiology*; Prentice Hall: Engelwood Cliffs, NJ, 1994.
21. *Evaluating Solid Waste*; USEPA Publication Vol. SW-846; U.S. Environmental Protection Agency: Cincinnati, OH, 1996.
22. *Standard Operating Procedures for Lead in Paint by Hotplate- or Microwave-Based Acid Digestion and Atomic Absorption or Inductively Coupled Plasma Emission Spectrometry*; USEPA Publication Vol. PB 92-114172; U.S. Environmental Protection Agency: Research Triangle, NC, 1991.

## Chapter 4

# A Creative Scientific Inquiry Experience in Organic Chemistry and Quantitative Analysis: Pharmaceuticals in the River Raisin

Ruth Ann Armitage,\* Jennifer Bates, Amy Flanagan Johnson,  
and Harriet Lindsay

Chemistry Department, Eastern Michigan University,  
Ypsilanti, Michigan 48197

\*E-mail: rarmitage@emich.edu

The Creative Scientific Inquiry Experience program at Eastern Michigan University supports connecting courses in science, technology, and math through a common theme to improve student persistence and success. Quantitative Analysis and Organic Chemistry I were offered as a cluster with an environmental theme, focusing on analysis of non-steroidal anti-inflammatory drugs in water. The lab experience emphasized lecture concepts of acid-base chemistry, pKa, derivatization reactions, and mass spectrometry. The results led to a research project on the correlation between population and NSAID concentration in the nearby River Raisin. Assessments of student learning were used to determine if and how students were making connections between the material taught in the two lectures and the experiences in the laboratory. We report here on the outcomes from bringing together these two disparate courses into a themed experience where students learned about what was in the water.

## Introduction

The Creative Scientific Inquiry Experience project, funded in 2005 by the National Science Foundation, has provided opportunities for faculty to collaborate across science, technology, and mathematics disciplines to develop themed course clusters that aim to increase student performance and persistence in these fields.



These clusters were focused primarily on the first-year courses during the initial phases of the project. One of us (HL) saw the opportunity to expand this in the Chemistry Department to the second year, when chemistry majors and minors take Organic Chemistry I (Chem 371), immediately after completing the second General Chemistry course (Chem 123).

For many college students in the sciences, undergraduate organic chemistry poses a difficult challenge. The two-course sequence requires the mastery of a large body of knowledge that is presented in a unique language using a system of representation that is significantly different from that used in introductory chemistry courses.

The daunting nature of the course has been widely recognized. Indeed, Hewitt and Seymore (1) place it on a short list of classes that act as “filters” to the science pipeline. The actual difficulties of the course as well as its negative reputation present a challenge to those interested in recruiting and retaining chemistry students.

Learning communities such as those offered by the CSIE program at EMU have been demonstrated to improve student persistence in college in general (2) and in chemistry in specific (3). Consequently, we anticipated incorporating first semester organic chemistry into a CSIE course cluster might improve persistence in the chemistry program at EMU. To test our hypothesis, we targeted students who would be enrolling in the off-sequence section of organic, which, anecdotally, we believe to be at higher risk academically.

The vast majority of students who complete the two-semester organic chemistry sequence are also required to take Quantitative Analysis (Chem 281) to complete their programs, but tend to put it off until they have completed the organic sequence. This leads to poor performance, particularly from chemistry minors who put Chem 281 off until the final term of their senior year. The course material is a direct continuation of the acid-base equilibrium chemistry covered in second semester general chemistry; unfortunately students have forgotten many of these key concepts by the time they reach Quantitative Analysis one to three years later. To prevent this problem and to allow students to make better use of important concepts from Chem 281 as they progress through their undergraduate curriculum, we believe that Chem 281 and 371 should be taken at the same time, during a student’s third semester. This is a total of 11 credit hours (three lecture hours in Chem 371, two lecture hours and six lab hours in Chem 281); anecdotal evidence indicates that students wait to take Chem 281 to “focus on organic.” Unfortunately, rather than leading to better performance in either course, students were generally underperforming in both courses. We envisioned that combining Organic Chemistry I and Quantitative Analysis using the CSIE program format of bringing together content from clustered courses through a shared seminar might provide an opportunity to improve recruitment and retention of chemistry students. Not only would students enroll in Quantitative Analysis at the appropriate time in their undergraduate careers, they might develop a greater appreciation for the importance of organic chemistry within the undergraduate curriculum as they applied organic chemistry concepts in Quantitative Analysis to solve “real world” problems. Thus we developed a cluster that brought Chem 371

and 281 together with the theme of environmental analysis with the hypothesis that performance and persistence could be improved for participating students..

Students were recruited from second semester general chemistry (Chem 123) to take the course cluster, which was scheduled for two days per week, beginning with Chem 371 lecture, then a one hour seminar course (CSIE 377), followed by Chem 281 lecture, and then laboratory. The seminar time was used for group work, outside speakers, demonstrations, and lab planning. The environmental theme was selected for the ease of connecting concepts from the two courses in a way that students would find interesting. Several concepts were selected for emphasis: acid strength and pKa (to bring explanations from organic and analytical courses in line with one another); the organic chemistry transformations leading to changes in acid-base indicator colors, ocean acidification and its effect on marine life that produces biologically important natural products; and finally structure, derivatization, gas chromatography, and mass spectrometry.

In addition to making connections between organic and analytical chemistry, the CSIE program provided the opportunity to revitalize the Quantitative Analysis laboratory. The non-CSIE quantitative analysis laboratory consisted almost entirely of titrations, with some spectroscopic methods. Samples were either powder unknowns that were water soluble, or solutions made by the GA to known concentrations. Grades were based solely on accuracy and precision, with some labs requiring graphs that made up a portion of the overall grade. For the CSIE lab, one of us (RAA) developed several new experiments to emphasize analysis of water and soil. Hard water titrations were supplemented with calcium ion selective electrodes, to emphasize selectivity differences. The existing spectroscopy experiments were replaced with analysis of archaeological soils for phosphorus, calcium, and potassium, to demonstrate how humans have affected the environment in ways that can provide useful information to non-scientists. The most significant change to the quant lab curriculum was a multi-week group project on the analysis of surface waters for environmental contaminants utilizing gas chromatography-mass spectrometry.

## Water Analysis Project

The group project goal was to have students prepare and analyze realistic samples in a context that they would care about and do well at. In the first CSIE cluster in 2008, we used DDT and its metabolites as the analytes of interest in the water samples, but no DDT was detected, which students – somewhat disturbingly – found disappointing. Although completing the group project as a culminating experience for the CSIE cluster broadened the students' understanding of and interest in scientific research, they just were not able to integrate the information from the courses together in a meaningful way. One student summed up the experience as such: "The two topics that we are dealing with are kind of on the opposite ends of the spectrum... they [RAA and HL] certainly do a lot to tie the two together, but it has been really tough to try and exactly put the two together."

In order to help students more readily make the connections between quant and organic for the second iteration of the course in 2010, we chose to focus on

the common over the counter non-steroidal anti-inflammatory drugs (NSAIDs) ibuprofen, aspirin, and naproxen in surface and drinking water. The NSAIDs project was potentially easier for the students to relate to their everyday lives and it offered several connection points between the courses, such as pKa, derivatizing agents, and steric effects. We included drinking water samples to bring in discussion of how wastewater treatment facilities do not remove pharmaceuticals and personal care products, which are discharged into our lakes and rivers. We discussed in class the historical reasons for water treatment – focusing on removal of pathogens – and the recent emphasis on proper disposal of medications and household products to keep them out of the wastewater stream. Projects involving aquatic sources are particularly of interest in the state of Michigan because of our abundance of fresh water, and the value that is placed on remediation of our industrial past.

NSAIDs are widely used as pain relievers and fever reducers. Roughly \$1.8 billion is spent on over the counter NSAIDs every year (4). Unfortunately much of the consumed dose gets excreted unchanged into sewage. The effects of these substances on the aquatic life in our lakes and rivers are not well understood. The River Raisin is a waterway in southeastern Michigan that had not been previously studied for pharmaceuticals, located not far from EMU. An earlier study in 2002 (5) did not detect ibuprofen in the Detroit River, but parts per trillion levels were detected in the Huron River by others (6).

The CSIE class project consisted of three samples from the River Raisin and one drinking water sample from the town of Dundee. Students were studying the samples to detect one or more of the drugs; quantitation was not possible due to limitations of sample size, time, and instrument access. One of the students (JB) chose to pursue the quantitative analysis as a research project. In particular, her hypothesis was that there would be a strong correlation between population and downstream NSAID concentration. The River Raisin flows through five counties in southeastern Michigan, with a population of more than 140,000 within its mainly agricultural watershed (7). Some of the population centers along the river have a history of storm sewer overflows during heavy rain events. According to the Michigan Department of Environmental Quality, the city of Adrian (midway along the River Raisin) had seven sanitary sewer overflow events in 2008 and five in 2009, leading to a total of 4.3 million gallons of sewage discharged directly into the river (8, 9). A single sanitary sewer overflow in the village of Dundee in 2009 released 3.9 million gallons of partially treated sewage (9). These overflows may lead to increased concentrations of personal care products and pharmaceuticals in the river water.

## Materials and Methods

For the research project, water samples were collected (1 liter, in HDPE bottles) from twelve locations along River Raisin, listed in Table 1. Locations marked with an asterisk were also included in the CSIE class project; an additional sample was collected between the Dundee and Raisinville Twp locations. Sampling locations were selected as points downstream from the water treatment

facilities of each population center, when applicable. Each water sample was stored at 0°C until prepared for analysis. Standards of aspirin (ASA), ibuprofen (IBU), and naproxen (NAP) were prepared in 500 mL deionized water (18 MΩ, Barnstead Nanopure); mecoprop was used as an internal standard (IS). Standards and solvents were of USP or residue analysis grade, and were obtained from Fisher Scientific.

## Sample Preparation

Water samples were collected when the River Raisin was at its highest flow of the season, and significant particulate matter was present. All water samples were vacuum filtered through quantitative cellulose filter paper to remove large particulates. Standards were filtered as well for consistency. Samples were acidified to pH 2.6 with concentrated HCl (ACS grade, Fisher Scientific). The acidic compounds, which included the NSAIDs, were isolated with solid phase extraction using Strata-X polymeric reversed phase SPE columns (Phenomenex, 500 mg packing, 6 mL volume).

**Table 1. Sampling Locations along River Raisin for Research Project**

<i>Location</i>	<i>Population (10)</i>	<i>Gage height, Ft (11)</i>	<i>Discharge, Ft<sup>3</sup>/s (11)</i>
Onsted	813	3.5 <sup>a</sup>	170 <sup>a</sup>
Brooklyn	1176	"	"
Sharon Hollow	1678	"	"
Manchester	2160	"	"
Clinton	2293	5.2 <sup>a</sup>	350 <sup>a</sup>
Tecumseh	8574	3.5 <sup>a</sup>	170 <sup>a</sup>
Adrian	21574	6.5 <sup>b</sup>	450 <sup>b</sup>
Blissfield	3223	"	"
Petersburg	1157	14 <sup>b</sup>	>5000 <sup>b</sup>
Dundee*	3522	"	"
Raisinville Twp*	4896	4.7 <sup>c</sup>	1800 <sup>c</sup>
Monroe	22076	"	"

<sup>a</sup> Measured at Manchester, MI. <sup>b</sup> Measured at Adrian, MI. <sup>c</sup> Measured at Monroe, MI.

The SPE columns were conditioned first with methanol (residue analysis grade, Fisher Scientific), then with pH 2.6 deionized water. The acidified sample was then passed through the column, followed by a rinse with 2% acetic acid (in 5:95 methanol:DI water). Rinsed columns were dried for 15 min under vacuum, then immediately eluted with 3 mL 2% ammonium hydroxide in methanol. The

eluate was dried down under a gentle flow of nitrogen, and frozen for storage. Prior to analysis, the thawed samples were reconstituted with 100  $\mu\text{l}$  25% tetramethylammonium hydroxide (TMAH) in methanol. The project utilized this derivatizing agent for its ease of use: methylation of the carboxylic acid functionality occurs upon injection of the sample into the gas chromatograph. In the CSIE course, silylation was carried out offline, using both MTBSTFA and BSTFA, to emphasize the importance of organic reactions in environmental analysis.

## GC-MS Analysis

Analyses were carried out on a Varian 3800 gas chromatograph equipped with a Saturn 2000 ion trap mass spectrometer. This instrument was donated to EMU by the Environmental Chemistry laboratory at BASF's Wyandotte (MI) facility. A one microliter injection was made at a 50% split ratio and 250  $^{\circ}\text{C}$  onto a VF5-ms column (Varian, 30 m long x 0.25 mm i.d., 0.25  $\mu\text{m}$  film thickness). The GC temperature program consisted of an initial hold of 2 minutes at 70 $^{\circ}\text{C}$ , followed by an increase to 250 $^{\circ}\text{C}$  at a rate of 10 $^{\circ}\text{C}/\text{minute}$ , which was held for 20 minutes. The mass spectrometer had a 5 min solvent delay, after which electron impact ionization (at 70 eV) was turned on automatically. Masses in the range from 35-650  $m/z$  were monitored throughout. The ion trap was held at 150  $^{\circ}\text{C}$ , the transfer line at 120  $^{\circ}\text{C}$ , and the manifold at 70  $^{\circ}\text{C}$ . For the research project, NSAIDs in the water samples were identified as their methyl esters, while the CSIE class samples were investigated as tri-*t*-butylsilyl and trimethylsilyl esters, as well as methyl esters.

## Results of Class/Research Projects

The CSIE class project yielded only qualitative traces of NSAIDs in the tested water samples. Total ion chromatograms did not show peaks for aspirin, ibuprofen, or naproxen. Selected ion chromatograms did show, in some cases, small peaks that could be identified as ibuprofen. For the research projects, selected ion chromatograms were used to qualitatively identify each NSAID compound: ASA at  $m/z$  135, IBU at  $m/z$  161, and NAP at  $m/z$  244, with the mecoprop (IS) at  $m/z$  228. Table 2 shows which compounds were found in the water samples from the River Raisin samples from the research project.

Total ion chromatograms showed that other compounds were also present in the water. These included N,N-diethyl-*m*-toluamide (DEET) insect repellent from the collector, and compounds characteristic of humic acids from the suspended organic matter in the water. TMAH hydrolyzes humic substances into smaller fragments (12); methyl esters of hexadecanoic and octadecanoic acids observed in the samples are likely derived from the humic substances in the water.

Aspirin could only be identified as a decomposed salicylate; quantitation of ASA was not attempted. Naproxen was observed in three of the samples: the two with the highest population and one where the river was flooding. Selected ion chromatograms were utilized to identify NAP in the samples. The lower limit of

quantitation was determined to be 5 parts per billion ( $\mu\text{g/L}$ ). All of the River Raisin samples containing NAP fell just below that value. For ibuprofen, calibration curves using both selected ion chromatograms and total ion chromatograms yielded lower limits of quantitation around 10 parts per billion ( $\mu\text{g/L}$ ). This is several orders of magnitude higher than that observed in other studies where GC-MS was utilized for such analyses (13, 14). This in part reflects the effect of using only MS rather than MS-MS for quantitation, and the lack of sensitivity for the methyl esters of the compounds of interest. While negative ionization would also have resulted in lower limits of detection, this was unavailable.

**Table 2. Qualitative Results for NSAIDs Identified in River Raisin Water Samples**

<i>Location</i>	<i>ASA</i>	<i>IBU</i>	<i>NAP</i>
Onsted		x	
Brooklyn	x		
Sharon Hollow		x	
Manchester		x	
Clinton	x	x	
Tecumseh	x	x	
Adrian	x	x	x
Blissfield	x	x	
Petersburg	x	x	x
Dundee	x		
Raisinville Twp	x		
Monroe	x	x	x

## Conclusions from Research Project

Because all of the samples fell below the lower limit of quantitation, actual quantitation of the ibuprofen was not possible. A trend was observed in the peak area ratios (IBU:IS), showing increases in samples collected immediately downstream from population centers (Figure 1). Storm sewer overflows during heavy rains likely do affect the IBU content of water in the River Raisin. Further studies with higher sensitivity and lower backgrounds, preferably obtained with samples collected outside of the annual flooding of the River Raisin, should clarify the actual content of NSAIDs in this aquatic environment.

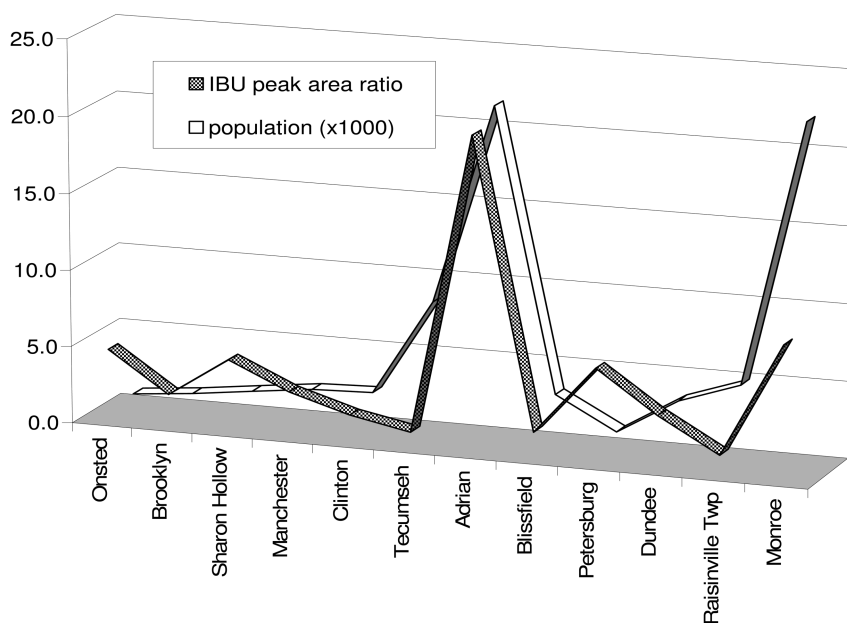


Figure 1. Graph showing correlation between IBU peak area ratio and population along the River Raisin.

## Outcomes and Assessment of CSIE Approach on Student Learning and Enthusiasm

Our guiding question in the analysis of the CSIE approach was “Do linking these courses result in a positive outcome for the students?” We were particularly interested in whether the completion of the course cluster resulted in an increased interest in conducting scientific (not specifically chemistry) research, if the linking of the courses resulted in students recognizing the content connections between them, and if the NSAIDs projects facilitated students in the integration of their knowledge.

Students in both the 2008 and the 2010 versions of the course were uniformly positive about conducting research after having completed the cluster. The primary motivating factor for them was that the lab projects they undertook in quant lab were authentic. The students felt as though they were doing something real, something important and that encouraged them to continue on in their training. Said one student, “I can actually see myself doing a career in chemistry now... after these courses, I can relate it to a career now and before that I couldn't.”

Although both sets of students developed an appreciation for research through completing the group projects, the students in the 2010 version of the CSIE cluster were much more aware of the connections between organic chemistry

and quantitative analysis. In the 2008 offering, a representative response from a student regarding the interconnectedness (or lack thereof) of the courses was “We learn about one thing in quant and then we would learn about something else in organic.” This comment is in stark contrast to a representative response to the same question from a student in the 2010 class: “Just coming in without really having any knowledge or experience with organic or analytical chemistry, they don’t seem like they are really intertwined beings. But you can definitely see that they are, that analytical has relevance to organic chemistry and obviously organic chemistry has relevance to analytical techniques and methods. I’ve definitely been able to see that there is a lot of interconnectedness.”

The primary difference in the structure of the 2008 and 2010 clusters was the culminating project. Part of the appeal of the NSAIDs project was that the nature of the analysis required more integration of the organic and quant principles than did the DDT project from 2008. In addition to a written analysis of their results, the students also had to do an oral presentation for the class. Although the question and answer session with the professors was difficult for many of the students, they also appreciated it as an integral part of their training. “If you were giving a real world presentation, people are going to ask you questions about how it relates to their field and it really makes you have to think and more fully understand the material,” noted one of the students. The other benefit of the NSAIDs project was that the test materials were something that the students could more easily relate to their daily lives. We hoped that this improved relatability would increase their interest in and motivation for the project, which it seemed to do. As one student summarized, “I was happy to be doing something that had some meaning behind it. Not that the titrations didn’t teach us anything, but we were working with real samples and looking for real things that we buy off the shelves everyday. It related it more to our lives. It makes me think twice when I open the medicine cabinet!” When it comes to educating consumers and future scientists, what more could we hope for than that?

## Acknowledgments

The authors thank the Eastern Michigan University CSIE Program (NSF award #DUE0525514); the EMU Chemistry Department and Sellers Fund; and BASF Wyandotte (especially Liz Hugel) for their support, both financial and material. One of us (JB) was supported by an Undergraduate Research Stimulus Program Award from the EMU Provost’s Office. The CSIE Chem 281 class during Winter 2010 provided the preliminary results. We thank both Christina Phillips (CSIE graduate assistant) and Dr. Jeff Guthrie, for making the 2010 cluster possible. JB and RAA thank our friends and family who helped collect water samples: Ben Burrell, Meaghan Elliott, Daniel Fraser, and Bruce Armitage.



## References

1. Hewitt, N. M.; Seymore, E. *Talking about Leaving: Why Undergraduates Leave the Sciences*; Westview Press: Boulder, CO, 1997.
2. Andrade, M. S. *J. Coll. Stud. Retention* **2007**, *9*, 1–20.
3. Driscoll, W. D.; Galabert, M.; Richardson, N. *J. Chem. Educ.* **2010**, *87*, 49–53.
4. Laine, L. *Gastroenterology* **2001**, *120*, 594–606.
5. Jasim, S. Y.; Irabelli, A.; Yang, P.; Ahmed, S.; Schweitzer, L. *Ozone: Sci. Eng.* **2006**, *28*, 415–423.
6. Wade, M. City of Ann Arbor Leader in Testing for Pharmaceuticals in Drinking Water, 2008. [http://www.a2gov.org/government/publicservices/water\\_treatment/Documents/waterplant\\_pharmaceuticals\\_2008\\_03\\_12.pdf](http://www.a2gov.org/government/publicservices/water_treatment/Documents/waterplant_pharmaceuticals_2008_03_12.pdf) (accessed June 12, 2010).
7. River Raisin Watershed Council. <http://riverraisin.org> (accessed May 17, 2010).
8. Combined Sewer Overflow (CSO), Sanitary Sewer Overflow (SSO), and Retention Treatment Basin (RTB) Discharge 2008 Annual Report. Michigan Department of Environmental Quality. [http://www.michigan.gov/documents/deq/deq-wbcsooreport08\\_299566\\_7.pdf](http://www.michigan.gov/documents/deq/deq-wbcsooreport08_299566_7.pdf) (accessed May 18, 2011).
9. Michigan Department of Natural Resources and Environment. Combined Sewer Overflow (CSO), Sanitary Sewer Overflow (SSO) and Retention Treatment Basin (RTB) Discharge 2009 Annual Report. [http://cdm15148.contentdm.oclc.org/cdm4/item\\_viewer.php?CISOROOT=/p9006coll4&CISOPTR=98836](http://cdm15148.contentdm.oclc.org/cdm4/item_viewer.php?CISOROOT=/p9006coll4&CISOPTR=98836) (accessed May 18, 2011).
10. U.S. Census, 2000. <http://factfinder.census.gov> (accessed May 17, 2010).
11. USGS WaterWatch Streamflow Data for River Raisin. [http://waterwatch.usgs.gov/new/index.php?r=mi=real=w\\_\\_table\\_flow](http://waterwatch.usgs.gov/new/index.php?r=mi=real=w__table_flow) (accessed June 12, 2010).
12. Frazier, S. W.; Nowack, K. O.; Goins, K. M.; Cannon, F. S.; Kaplan, L. A.; Hatcher, P. G. *J. Anal. App. Pyrolysis* **2003**, *70* (1), 99.
13. Samaras, V. G.; Thomaidis, N. S.; Stasinakis, A. S.; Gatidou, G.; Lekkas, T. D. *Int. J. Environ. Anal. Chem.* **2010**, *90* (3–6), 219–229.
14. Helenkar, A.; Sebok, A.; Zaray, G.; Molnar-Perl, I.; Vasanits-Zsigrai, A. *Talanta* **2010**, *82*, 600–607.

## Chapter 5

# The Relationship between Free and Bound Hydrophobic Organic Pollutants and Dissolved Organic Matter in Drinking Water

Meng-Horng (Chris) Hsu and I. H. (Mel) Suffet\*

Environmental Science and Engineering Program,  
University of California at Los Angeles, School of Public Health,  
Room 61-295, CHS, Charles E. Young Drive South,  
Los Angeles, California, 90095, U.S.A.

\*Phone: (310) 206-8230. Fax: (310) 206-3358. E-mail: msuffet@ucla.edu.

Hydrophobic organic pollutants (HOPs), such as polyaromatic hydrocarbons primarily from automobile exhausts and dissolved organic matter (DOM) are ubiquitous in the aquatic environment. The interaction between DOM and HOPs minimizes the bioavailability of HOPs and their potential health effects. In addition, DOM is also the precursor of disinfection by-products.

It is very important to understand the relationship between free and bound HOPs and DOM in drinking water. This chapter will explore the binding phenomenon between HOPs and DOM in raw and treated water from water treatment plants. This chapter introduces the analytical methodologies for characterizing DOM and the hazardous potential of HOPs and thus understanding their relationship. Initial studies have been completed and showed that monitoring both the free and bound forms of HOPs as well as disinfection by-products (such as trihalomethanes) and their relationship to DOM during drinking water treatment processes is necessary to better understand drinking water quality.

## Introduction

Dissolved organic matter (DOM) is a heterogeneous mixture of hundreds of aromatic and aliphatic organic compounds containing nitrogen, oxygen, and sulfur functional groups from decomposing natural organic matter by microorganisms in natural waters (1–3). DOM components include humic acids, fulvic acids, humin, amino acids, proteins, sugars, and polysaccharides (2–4). DOM transformation is a very important issue in water treatment processes because DOM is one of the main components to cause disinfection by-product formation (3–7) and membrane fouling (8–10) that can negatively affect drinking water quality.

DOM also has the ability to associate with hydrophobic organic pollutants (HOPs), such as polycyclic aromatic hydrocarbons (PAHs), chlorinated pesticides, and polychlorinated biphenyls in natural waters and during drinking water, reclaimed water, and wastewater treatment processes (11–13). The interaction between HOPs and DOM affects the bioavailability of pollutants and their resulting toxicity. Therefore, the interaction of HOPs and DOM during water treatment processes can affect the toxicity of hydrophobic organic contaminants, such as PAHs. Simultaneously as this occurs, DOM can form disinfection by-products such as trihalomethanes which are potentially carcinogenic. What fraction of DOM affects the bioavailability of HOPs and what fraction of DOM affects the formation of disinfection by-products is not understood.

## Hydrophobic Organic Pollutants (HOPs)

HOPs are defined as those compounds with a log octanol-water partition coefficient over five. PAHs are a group of representative HOPs that include over 100 different chemicals. PAHs are primarily generated from incomplete fossil fuel burning, oil spills, and other industrial processes (14). The U.S. Environmental Protection Agency (U.S. EPA) has listed 16 PAHs as priority pollutants in the aquatic environment due to toxicity and potential carcinogenicity (15). Of these PAHs, the U.S. EPA has set drinking water standards of 200 ng/L for benzo(a)pyrene (16). The European Union Directive 98/83/EC sets the maximum total concentration of four PAHs (benzo(b)fluoranthene, benzo(k)fluoranthene, benzo(ghi)perylene, and indeno(1,2,3-cd)pyrene) at 100 ng/L in drinking water, and at 10 ng/L for benzo(a)pyrene (17).

Several researchers began to find that HOPs can bind with DOM during the 1970 to 1980s (18–21). This phenomenon significantly affects the fate and transport of HOPs in the aquatic environment. In 1982, Carter and Suffet were the first to show quantitative data for binding behavior between DOM and one of the HOPs, namely DDT. In addition, Carter and Suffet proposed the idea for understanding the free and bound portions in the aquatic environment according to the partition coefficient,  $K_{\text{DOM}}$  (11). Equation 1 describes the binding behavior between DOM and HOPs via  $K_{\text{DOM}}$ .

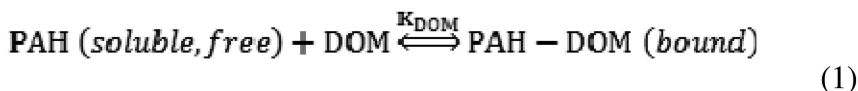


Figure 1 showed an example that illustrates that some parts of the PAHs present were dissolved in the water solution and some parts of PAHs were bound to the black materials which represents DOM in the water. When free PAHs bind with DOM to form the DOM-PAHs bound together, they are not bioavailable and thus not toxic. Thus, free PAHs are the bioavailable hazardous form. The partition coefficient between DOM and HOPs,  $K_{DOM}$ , describes the relative amount of free HOPs (See Equation 1).

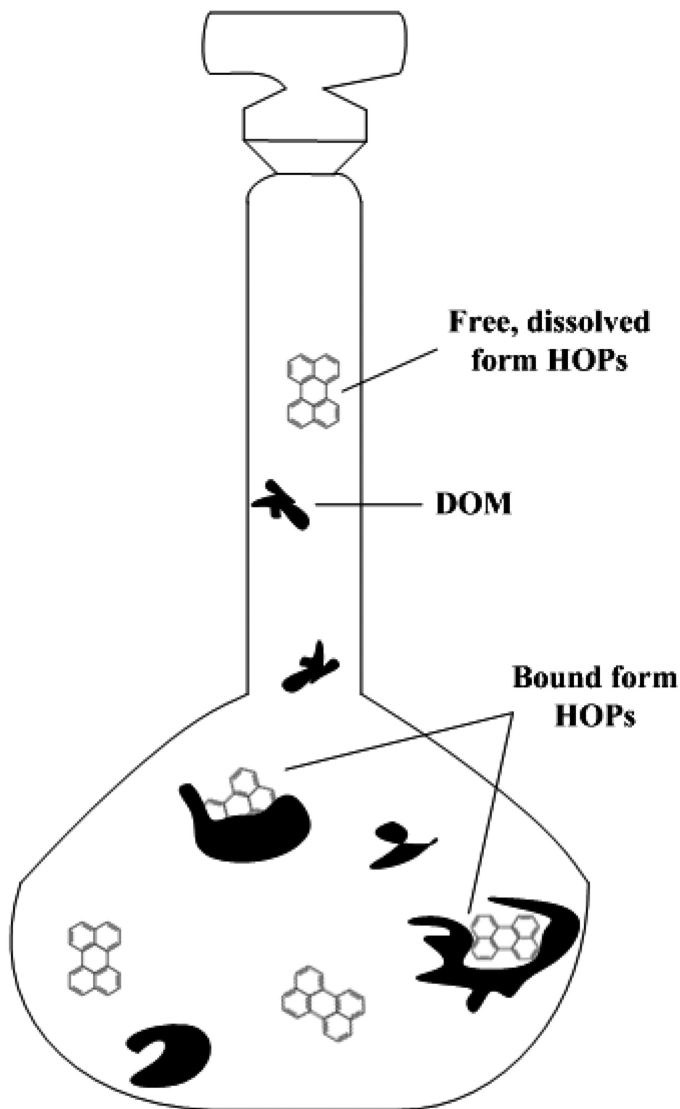


Figure 1. The illustration of binding behavior between DOM and HOPs. (Carter and Suffet, 1995 (11); Mackenzie et al., 2002 (37)).

The natural organic matter that forms DOM in a natural water is uniquely defined by the source of organic matter and its microbial breakdown. Therefore, each natural water will have unique DOM mixture of organic molecules of different sizes and polarities and thus also a unique interaction with HOPs that can be measured as the  $K_{\text{DOM}}$ . Thus, there will be different toxicity level of HOPs in each raw, treated and finished drinking waters. Since it is not possible to predict  $K_{\text{DOM}}$ , it is necessary to have a simple, quick, accurate, reliable, and consistent experimental methods to obtain the  $K_{\text{DOM}}$  information from the water of interest.

DOM interacts with HOPs through hydrophobic binding and forms humic-solute mixtures in the aqueous phase. This interaction can change due to DOM oxidation (e.g. chlorination or ozonation), DOM coagulation, and DOM sorption (e.g., activated carbon adsorption or sorption to suspended solids). The binding increases the overall solubility of HOPs in water by facilitating their sorption to DOM, and therefore, potentially enhancing their transport (11–13). However, sorption to DOM can potentially also serve as an environmentally friendly decontamination agent (22–25). Moreover, interaction with DOM can decrease the toxicity and bioavailability of HOPs, such as PAHs (26–28). Furthermore, the relationship between specific characteristics of DOM and trihalomethane formation potential and interaction of DOM with HOPs need to be disentangled.

## Analytical Methods for Measuring the Potential Formation of Free HOPs in Drinking Water

Due to the limitation of experimental techniques at ng/L levels and the variability of DOM at different locations, the interaction between HOPs and DOM are not well defined in drinking waters. This is especially needed for the freely dissolved form of HOPs, which are hazardous and bioavailable. Thus, it is necessary to monitor and measure free HOPs from the source waters, through the drinking water treatment process and in the drinking water supply.

Several researchers studied detection methods for free and bound portion of HOPs in surface waters and sediment pore water. The most popular methods used for these kind of experiments are solid phase microextraction (SPME) combined with GC/MS (29–35) and fluorescence quenching (26–28). Both SPME and fluorescence quenching methods have the advantage of analysis without changing the original water quality conditions. As a result, these methods do not change the equilibrium of the partition between DOM and HOPs.

In addition, fluorescence quenching is also a sensitive and precise method. SPME is a quick extraction method without any solvent which is environmentally friendly. On the other hand, each of these two methods also has their own disadvantages. For the fluorescence quenching method, several assumptions need to be evaluated. For SPME, during the extraction process, DOM might attach on the SPME fiber for a long extraction time and affect the final equilibrium results. Due to these problems, it is important to understand the relationship between these two analytical methods. Doll et al. (1999) and Mackenzie et al. (2002) used

phenanthrene and pyrene, respectively, to compare these two methods and found that  $K_{DOM}$  derived by fluorescence quenching was larger than the SPME method (36, 37). In addition, when measuring higher and lower  $K_{DOM}$  range of samples,  $K_{DOM}$  values obtained by the SPME method had larger errors.

Holbrook et al. (38) also applied the fluorescence techniques including fluorescence excitation-emission matrix (EEM), fluorescence regional integration and fluorescence quenching to understand the impacts of reclaimed wastewater on the surface water. Their results found that wastewater treatment facilities, including advanced treatment facilities from reclaimed wastewater to supplemental drinking water sources, can affect the components of organic matter in the receiving water body and thus change the behavior between organic matter and other HOPs.

Different components and characteristics (e.g. size, polarity, chemical components, etc.) of DOM affect the ability of PAHs to bind with DOM. Therefore, different water sources, treatment processes, and samples taken at different times can have different  $K_{DOM}$  values. Considering the complexity to measure  $K_{DOM}$  (39) and the importance to get this information at waters of interest, a consistent method is needed to measure  $K_{DOM}$ . Perylene, a less hazardous PAH, was chosen as a probe to determine  $K_{DOM}$  in different waters.

The first objective of this study was to develop methodology to monitor the potential formation of free HOPs during water treatment. In short, DOM can decrease HOPs toxicity by binding with HOPs. On the other hand, DOM is the precursor of disinfection by-products generating e.g. trihalomethanes. Therefore, the second objective of this paper is to begin to understand the changes of DOM characteristics and its effect on the association HOPs with DOM and trihalomethane formation potential before and after water treatment. This should enable better optimization of water treatment processes by decreasing trihalomethanes and simultaneously keeping water safer to drink by keeping a lower hazard potential of HOPs.

## Experimental

### Sample Preparation

Water samples were filtered through 0.7  $\mu\text{m}$  glass fiber membranes prior to any analysis procedure to remove filterable organic matter and microorganisms which may consume DOM. Before using, membranes were baked for 24 hours at 100  $^{\circ}\text{C}$  to reduce leaching of organics during filtration. This step is to ensure that the study is targeting on the dissolved form of natural organic matter. In this chapter, samples of influent and effluent water of two drinking water treatment plants in southern California from Castaic Lake Water Agency (CLWA) in Santa Clarita and Long Beach Water Department (LBWP) were tested. The effluent grab samples were taken 2-4 hours earlier than the influent samples.

## Comparison of KDOM Analysis Methods

A comparison of  $K_{\text{DOM}}$  values of the two methods, SPME and fluorescence quenching (29–35, 40, 41), was completed with perylene under a set of standard conditions to enable direct comparisons of the effect of DOM on free HOPs. All measurements of fluorescence intensities are obtained with a fluorescence spectrophotometer (Varian, R3896) at an excitation-emission wavelength pair of 434 and 467 nm respectively. Absorbance values at 434 and 467 nm were corrected for inner filtering effects which are usually below 1.2 using UV-Vis spectrophotometer (Shimadzu UV-1700) (42). The SPME used 1-cm long SPME fibers coated with 100  $\mu\text{m}$  of polydimethylsiloxane (PDMS) from Supelco (Bellefonte, PA). New fibers were conditioned in the GC injector at 250 °C for 0.5 hour. Forty ml water samples were loaded into 40-ml amber bottles with PTFE/silicone septum to prevent photodegradation of PAHs. All samples were run at 20 °C. The SPME fiber was immersed into the sample solution 1 cm from the surface and the solution was stirred with a PTFE-coated magnetic bar (10 mm  $\times$  6 mm o.d.) at 1000 rpm. The extraction time was 60 min. The analyte was then desorbed from the SPME fiber by injection into the GC splitless inlet at 275 °C for 4 minutes with a column temperature of 200 °C.

## Ultrafiltration To Measure Size Fraction of DOM

DOM size can be fractionated by ultrafiltration through different molecular weight cut off (MWCO) membranes, such as 10,000 (10kDa), 5,000 (5kDa), and 1,000 (1kDa) MWCO membranes (43). Membranes are soaked in deionized water and in 5% NaCl solution over night to reduce leaching of dissolved organic carbon (DOC). Ultrafiltration is performed in Millipore solvent-resistant stirred cells. The final step is to rinse the membranes with deionized water immediately before filtration. Nitrogen gas is used to pass fixed volumes of water samples through different MWCO membranes. Different size fractions after ultrafiltration are analyzed by a Total Organic Carbon Analyzer and UV-Vis spectrophotometry at 254 nm.

## Polarity Rapid Assessment Method (PRAM)

DOM polarity is identified by the polar rapid assessment method under ambient water quality conditions without any pretreatment (44, 45). Analysis takes into account the effect of pH and ionic strength on the structure of DOM under ambient conditions. Solid phase extraction (SPE) cartridges are cleaned by passing Milli-Q water to remove UV absorbing impurities. Parallel SPE cartridges with different sorbent polarities are used to adsorb DOM. The SPE cartridges include C18 (non-polar, hydrophobic), Diol (polar, hydrophilic), and  $\text{NH}_2$  (weak anion exchanger, negative charge). The retention coefficient (RC) is defined as  $1 - (C_{\text{max}}/C_0)$  in percentages describing the specific polarity characteristics (polar, non-polar, and negative charges) retained on the cartridges, where  $C_{\text{max}}$  is the maximum UV absorbance at 254 nm of the samples after breakthrough and  $C_0$  is the UV absorbance at 254 nm of the original sample.

## Fluorescence Spectroscopy

Fluorescence spectroscopy, a highly sensitive and rapid method for the identification of DOM characteristics, is used to obtain the EEM spectra (46). The five regions represent aromatic proteinaceous compounds I and II, fulvic acids, microbial by-products, and humic acids (I). EEM spectroscopy is measured with a fluorescence spectrophotometer using parameters modified from Holbrook, et al. (38). Excitation wavelengths span from 220 to 470 nm in 5 nm increments, and the emission wavelengths span from 280 to 580 nm in 4 nm increments using an integration time of 0.1 s and a bandwidth of 10 nm. The fluorescence intensities of spectra are normalized by Raman peak, which is measured daily at pair excitation-emission wavelengths of 350 and 397 nm in deionized water (Milli-Q water) and described in intensity units. All data are obtained by Matlab program to exclude the water-scattering peaks from Raleigh and Raman scattering (47). Adjusted EEMs are quantified by the fluorescence regional integration method to quantify and analyze fluorescence EEM spectra based on the integration of the total surface and subsequent divisions of the surface into five regions (I). Table I lists the regions and their associated excitation and emission wavelengths.

**Table I. Characterization of DOM and location of fluorescence regional integration regions**

<i>Region</i>	<i>Characterization of DOM</i>	<i>Excitation Range (nm)</i>	<i>Emission Range (nm)</i>
I	Aromatic proteins I	220-250	280-332
II	Aromatic proteins II	220-250	332-380
III	Fulvic acids	220-250	380-580
IV	Microbial by-products	250-470	280-380
V	Humic acids	250-470	380-580

## Trihalomethanes

Trihalomethanes are measured as a formation potential in this study. All samples are chlorinated according to Standard Method 5710 B (Trihalomethane Formation Potential, THMFP) under  $25 \pm 2$  °C for 7 days. Chlorine residuals in samples are quenched by sodium sulfite ( $\text{Na}_2\text{SO}_3$ ) before trihalomethane analysis.

## Results

### HOP Determination

Figure 2 is the relationship of  $K_{\text{DOM}}$  values derived by FQ and SPME combined with GC/MS methods for seven different water samples. The result of Figure 2 shows that the  $K_{\text{DOM}}$  values were not significantly different between fluorescence quenching and SPME methods within log  $K_{\text{DOM}}$  values from 4 to 6



at 95% confidence level. The reason might be due to the fluorescence life time of perylene which is only 5.5 ns, therefore, using perylene as a probe could possibly prevent other quenchers (e.g.  $O_2$ ) to inflate  $K_{DOM}$  values (28). This study uses perylene (fluorescence life time = 5.5 ns) as a PAH probe to obtain the relationship  $K_{FQ} \approx K_{SPME}$ . Other studies using phenanthrene (fluorescence life time = 60 ns) and pyrene (fluorescence life time = 200 ns) obtained the same relationships  $K_{FQ} \approx 2 \times K_{SPME}$  (36, 37).

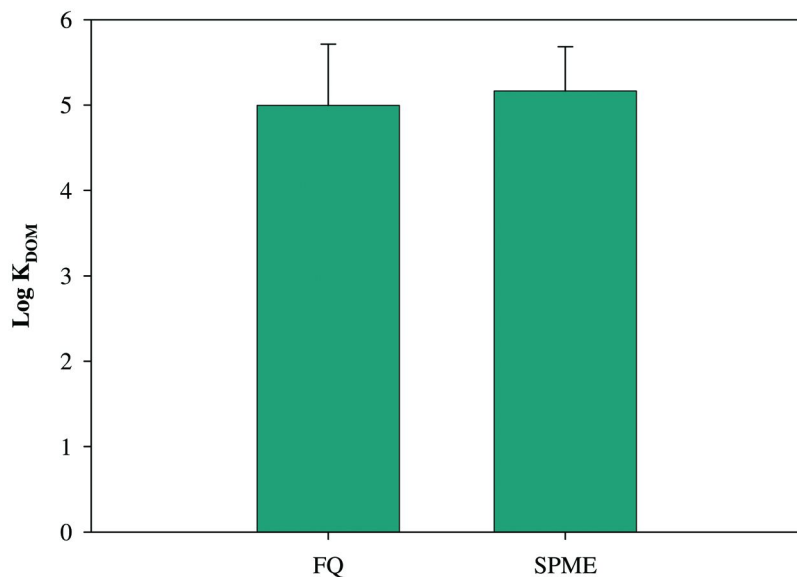


Figure 2. The comparison of  $K_{DOM}$  values derived by fluorescence quenching (FQ) and SPME-GC/MS methods (The values represent average  $\pm$  standard deviation,  $n=7$ ).

Fluorescence quenching was used to determine the free and associated fraction of PAH with DOM in an aquatic system. Perylene was used for all experiments because it is easy to measure the fluorescence and less hazardous in a laboratory setting. The fluorescence quenching method determines the  $K_{DOM}$  for perylene accurately and without separating the DOM from the water sample. Appendix A presents the specific fluorescence quenching method used.

### Understanding the Changes of DOM Characteristics, $K_{DOM}$ , and Trihalomethane Formation Potential

The second objective is to understand the changes of DOM characteristics and its effect on  $K_{DOM}$  and trihalomethane formation potential before and after water treatment. This should enable better optimization of water treatment processes by decreasing trihalomethanes and simultaneously keeping water safer to drink by keeping a lower hazard potential of free HOPs.

The  $K_{DOM}$  values shown in Table II were determined by the fluorescence quenching method with the probe- perylene. The higher  $K_{DOM}$  values of water samples represent the PAHs in the water are potentially less hazardous because more PAHs are bound to DOM. A regulated PAH, benzo(a)pyrene (BaP) has the drinking water standard at 200 ng/L in the United States is shown as a free portion in Table II in order to understand the degree of potential hazard caused by HOPs. The data were transformed according to the different degree of hydrophobicity of the PAH probe perylene and BaP. The free BaP concentrations were derived by % free portions and obtained by assuming 200 ng/L as reference concentration for all samples.

Table II presents different free fractions (hazardous fractions) of BaP for influent and effluent water of CLWA and LBWD. It is obvious that following the treatment processes of both CLWA and LBWD, the hazardous fractions of BaP was higher as a result of decreasing of  $K_{DOM}$  values. In CLWA, the DOC remains constant, however the free fraction of BaP increased from 86% to 98% after water treatment. In LBWD, the DOC decreases from 2.6 to 2.0 mg C/L, however the free fraction of BaP increased from 52% to 94% after the treatment processes. Therefore, if the PAHs are not removed by the treatment processes, the drinking water would be more hazardous than the influent water. Water treatment appears to eliminate or change the DOM that can bind to PAHs and increased the potential hazards of PAHs that exist. However this is on the basis that PAHs are not being removed by water treatment.

**Table II. Free fractions (hazardous fractions) of BaP and trihalomethanes (THMs) analysis before and after drinking water treatment processes for CLWA and LBWD**

<i>Water Sample</i>	<i>DOC (mg C L<sup>-1</sup>)</i>	<i>Log K<sub>DOM</sub></i>	<i>Free BaP (ng L<sup>-1</sup>)</i>	<i>Free BaP (%)</i>	<i>THMs (µg L<sup>-1</sup>)</i>
CLWA					
Raw	2.2	5.0	172	86	160
Treated	2.3	4.1	196	98	110
LBWD					
Raw	2.6	5.8	104	52	180
Treated	2.0	4.6	188	94	100

Table II includes trihalomethanes analysis in raw and treated waters for CLWA and LBWD treatment plants. For process water in CLWA and LBWD, following the treatment processes, THMs decreased 31% and 44% for CLWA and LBWD, respectively. This is apparently caused by removing DOM and differences in the overall DOM characteristics of the raw and treated drinking waters.

The characterization of DOM by ultrafiltration, polarity rapid assessment method and fluorescence regional integration analyses were applied in order to understand which parameters of DOM affect  $K_{\text{DOM}}$  and trihalomethane formation. Figure 3 shows the results from the ultrafiltration analysis of CLWA and LBWD process waters. The x-axis represents different size fractions of DOM and y-axis represents the DOM concentration with the fraction in terms of total organic carbon (mg C/L). For CLWA process waters, the main fraction of DOM in raw water was the 10 - 5 kDa fraction. After treatment processes, the 10 - 5 kDa fraction decreased and the lower molecular weight fractions- 5 - 1 kDa and < 1 kDa, increased. Thus, CLWA treatment processes mainly removed 10 - 5 kDa fraction of DOM and increased 5 - 1 kDa fraction. For LBWD process waters, the raw water DOM was dominated by > 10 kDa fraction and 5 - 1 kDa and the < 1 kDa fractions were less than 20%. The result indicates that most > 10 kDa DOM fraction decreased to smaller fractions in LBWD water after treatment processes. Figure 3 also shows that different water sources and water treatment processes would have different DOM size fraction distributions.

Figure 4 shows the results from the polarity rapid assessment method analysis of CLWA and LBWD process waters for both CLWA and LBWD process waters. The retention coefficient (RC) is defined as  $1-(C_{\text{max}}/C_0)$  in percentages describing the specific polarity characteristics (polar, non-polar, and negative charges) retained on the SPE cartridges, where  $C_{\text{max}}$  is the maximum UV absorbance at 254 nm of the samples after breakthrough and  $C_0$  is the UV absorbance at 254 nm of the original sample. The negative charge of the DOM measured by the  $\text{NH}_2$  anion exchange, SPE cartridge decreased following the treatment processes indicating some removal of DOM through the process. For both CLWA and LBWD treatment processes, overall  $\text{NH}_2$  negative charge decreased about 30%. In CLWA water samples, the treatment processes significantly decreased both C18 and Diol retention of DOM that represent non-polar and polar fractions of DOM, respectively. For LBWD water samples, the raw water sample which was from groundwater had a relative high  $\text{NH}_2$  negative charge of 96%. The non-polar components of DOM remained approximate 10% throughout the treatment process. However, the polar fraction increased after treatment.

Figure 5 shows fluorescence regional integration results of CLWA and LBWD fluorescent analysis. For both CLWA and LBWD, fulvic acids and humic acids were still the main components of DOM before and after the treatment processes. In addition, the chemical components of DOM identified by fluorescence also showed that the DOM compositions changed during the treatment processes.

All these parameters changed for both plants before and after the treatment processes and so does the HOPs free fraction distribution and trihalomethane formations. These DOM parameters might be correlated to  $K_{\text{DOM}}$  and trihalomethanes and dominate the water quality and significantly affect the efficiency of treatment processes. This requires further study.

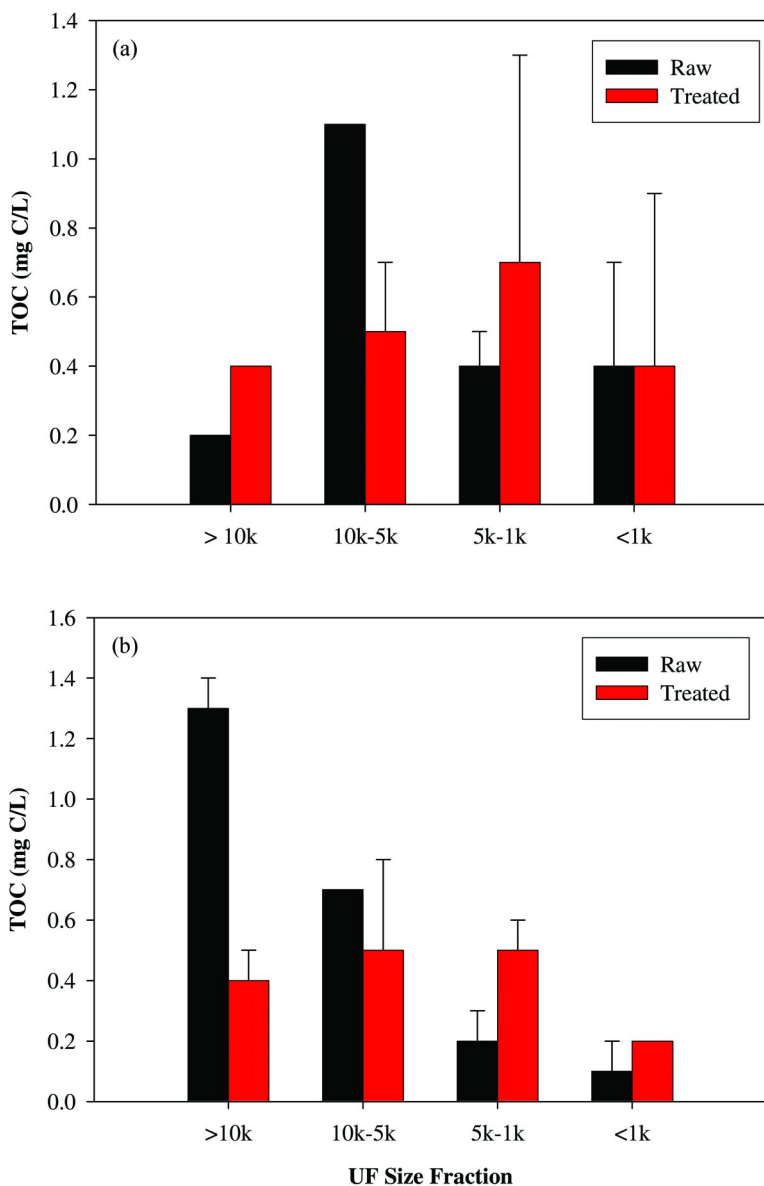


Figure 3. Ultrafiltration (UF) analysis of (a) CLWA and (b) LBWD. (The values represent average  $\pm$  standard deviation,  $n=2$ ).

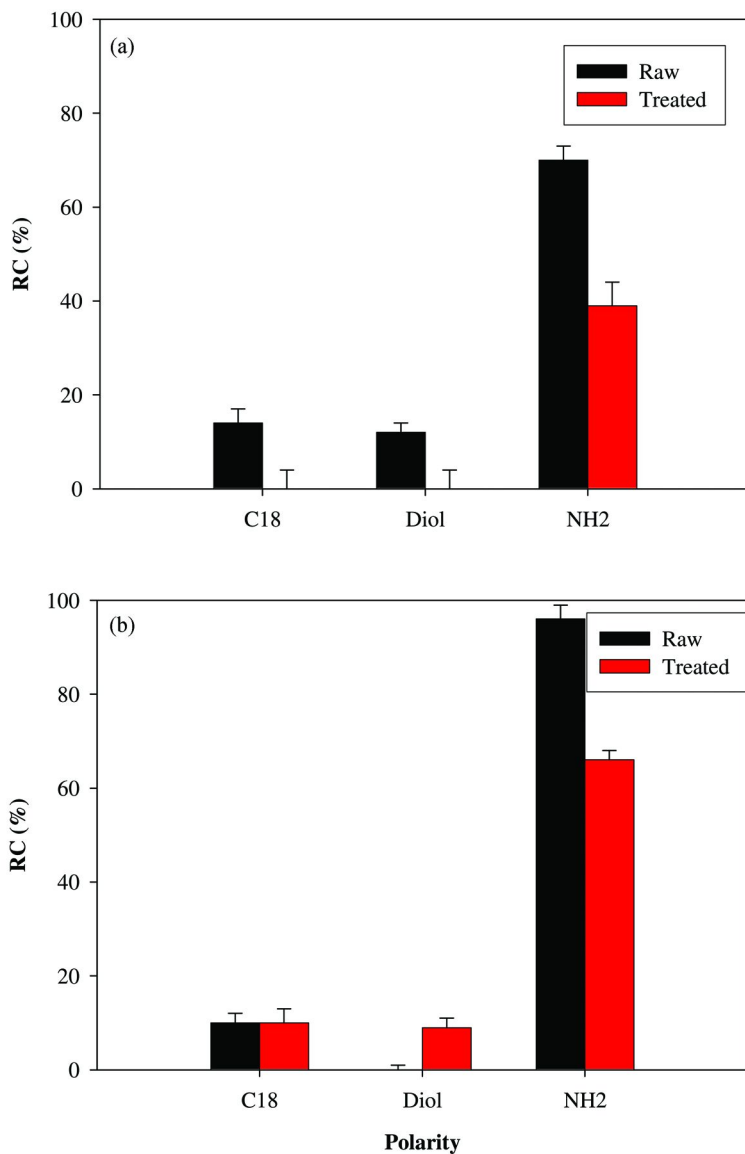


Figure 4. Polarity rapid assessment method analysis of (a) CLWA and (b) LBWD (The values represent average  $\pm$  standard deviation,  $n=3$ ).

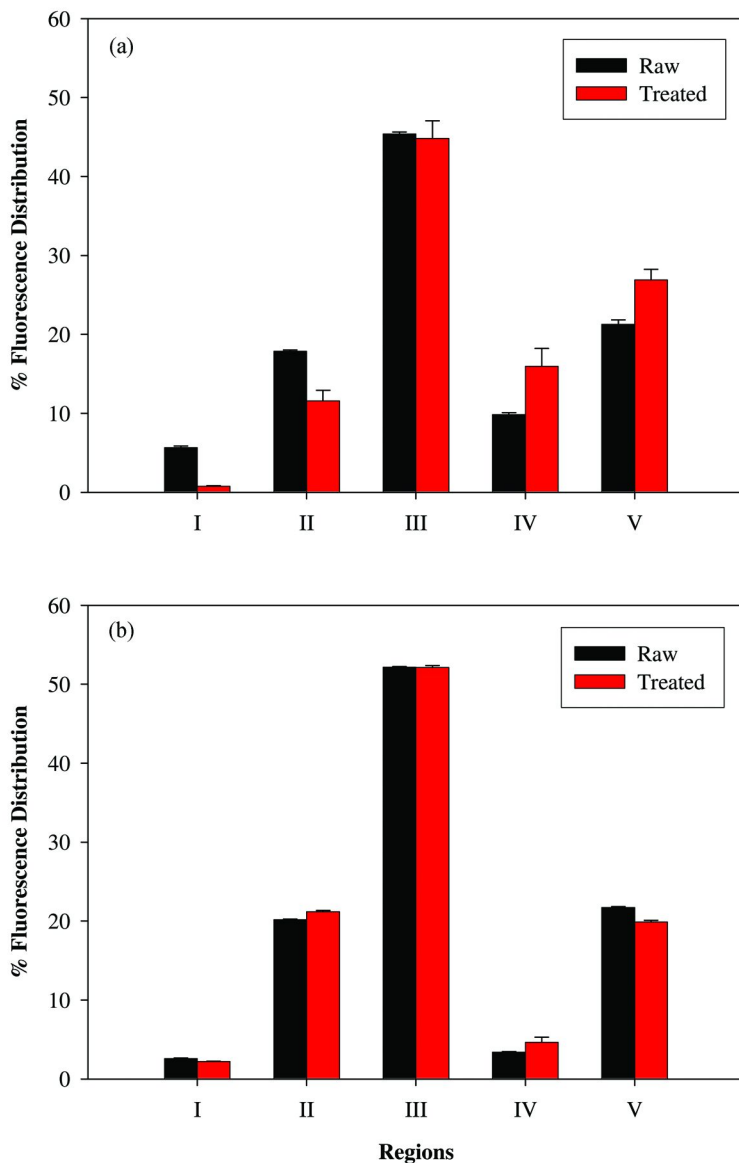


Figure 5. Fluorescence regional integration analysis of (a) CLWA and (b) LBWD (The values represent average  $\pm$  standard deviation,  $n=2$ ).

## Discussion

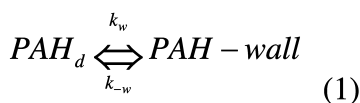
It is very important for water treatment agencies to treat water effectively and maintain the safest water quality. Higher  $K_{\text{DOM}}$  values can minimize any hazardous potential from HOPs such as accidental spill events. Lower trihalomethane formation values can minimize the formation of potentially harmful disinfection by-products. This study has shown that the removal and chlorination of DOM during drinking water treatment changes the source water DOM characteristics in the drinking water. The change of DOM character will affect the binding ability of DOM to HOPs. As a result, different free and bound portions of HOPs are observed in the source and treated water. Understanding the fate and transport of HOPs in drinking water sources and treatment processes should be better understood. At the same time, exploring the relationship between characteristics of DOM and trihalomethanes can offer valuable knowledge to guide water agencies towards optimization of water treatment processes and obtaining better water quality. The monitoring protocol and analysis methods of this chapter including ultrafiltration, polarity rapid assessment method, and fluorescence regional integration analysis should be applied to other unit operations and at other water treatment plants to continue to disentangle the complexities of the binding ability of DOM to HOPs and the effects of DOM on formation of disinfection by-product during drinking water treatment.

## Acknowledgments

The work was supported by the water research lab at the University of California, Los Angeles directed by Dr. Mel Suffet. We acknowledge UCLA undergraduates Christina Cheng, Jennifer Tsoi, Arthur Roh, Vincent Duong and Marcus Perry for assistance with lab work. Our thanks also to Dr. David Kimbrough from Castaic Lake Water Agency, Dr. Tai Tseng and Dr. Dian Tanuwidjaja from Long Beach Water Department for supplying water samples for the project.

## Appendix A: Fluorescence Quenching To Determine $K_{DOM}$

The sorption coefficient of DOM ( $K_{DOM}$ ) which describes the binding between DOM and perylene is determined by fluorescence quenching. Perylene is diluted in methanol to 4 mg/L perylene stock solution and stored in an amber bottle at 4°C. The stock solution is diluted to 0.3 µg/L perylene and added to DOM diluted samples to a final concentration three-fourths of the reported solubility 0.4 µg/L in water (48). To control for the loss of perylene from the cuvette system, the 12 measurements are made at defined time points (2 min intervals) to allow for extrapolation to initial conditions. Experiments are performed in a dimmed environment to prevent the photodegradation of perylene. Based on the assumption that partitioning of PAHs between water and DOM is fast compared to the adsorption of PAHs to the cuvette wall, sorption behavior can be modeled by:



where  $PAH_d$  is the dissolved portion of the total PAH concentration,  $PAH-wall$  is the portion adsorbed on the wall, and  $k_w$  and  $k_{-w}$  are first-order forward and backward rate constants for wall adsorption. Fluorescence intensity can be obtained by:

$$F = \frac{k_{-w}F_0'}{k_w + k_{-w}} + \frac{k_wF_0'}{k_w + k_{-w}} e^{-(k_w+k_{-w})t} \quad (2)$$

where  $F_0'$  is the free PAH intensity at time zero. Nonlinear curve-fitting program is used to get  $F_0'$ ,  $k_w$ , and  $k_{-w}$ .  $K_{DOM}$  values are determined by the Stern-Volmer equation which can be described as:

$$\frac{F_0}{F} = 1 + K_{DOM} [DOM] \quad (3)$$

where  $F_0$  and  $F$  are the fluorescence intensities in the absence and presence of DOM.  $[DOM]$  is the concentration of DOM measured as mg C/L (42). The percentage of bound PAH can be determined by equation 4 (49):

$$\%bound = \frac{K_{DOM} [DOM]}{1 + K_{DOM} [DOM]} \times 100 \quad (4)$$



## References

1. Chen, W.; Westerhoff, P.; Leenheer, J. A.; Booksh, K. *Environ. Sci. Technol.* **2003**, *37*, 5701–5710.
2. Stevenson, F. J. *Humus Chemistry: Genesis, Composition, Reactions*, 2nd ed.; John Wiley & Sons: New York, 1994.
3. Thurman, E. M. *Developments in Biochemistry: Organic Geochemistry of Natural Waters*; Nijhoff & Junk Publishers: Dordrecht, The Netherlands, 1985.
4. Krasner, S. W.; Croue, J. P.; Buffle, J.; Perdue, E. M. *J. Am. Water Works Assoc.* **1996**, *88* (6), 66–79.
5. Amy, G. L.; Thompson, J. M.; Tan, L.; Davis, M. K.; Krasner, S. W. *J. Am. Water Works Assoc.* **1990**, *82* (1), 57–64.
6. Zhang, X. G.; Minear, R. A. *Environ. Sci. Technol.* **2002**, *36* (19), 4033–4038.
7. Singer, P. C. *Water Sci. Technol.* **1999**, *40* (9), 25–30.
8. Lee, N.; Amy, G.; Croue, J.; Buisson, H. *Water Res.* **2004**, *38* (20), 4511–4523.
9. Taniguchi, M.; Kilduff, J. E.; Belfort, G. *Environ. Sci. Technol.* **2003**, *37* (8), 1676–1683.
10. Amy, G.; Cho, J. *Water Sci. Technol.* **1999**, *40* (9), 131–139.
11. Carter, C. W.; Suffet, I. H. *Environ. Sci. Technol.* **1982**, *16*, 735–740.
12. Chiou, C. T.; Malcolm, R. L.; Brinton, T. I.; Kile, D. E. *Environ. Sci. Technol.* **1986**, *20*, 502–508.
13. Rav-Acha, Ch.; Rebhun, M. *Water Res.* **1992**, *26*, 1645–1654.
14. Woodhead, R. J.; Law, R. J.; Matthiessen, P. *Mar. Pollut. Bull.* **1999**, *38*, 773–790.
15. Santos, F. J.; Galceran, M. T. *Trends Anal. Chem.* **2002**, *21*, 672–685.
16. Drinking Water Contaminants, National Primary Drinking Water Regulations. United States Environmental Protection Agency. <http://water.epa.gov/drink/contaminants/index.cfm#Organic> (accessed October 2011).
17. European Commission. Council Directive 98/83/EC. *Off. J. Eur. Communities* **1998**, *L330*, 32.
18. Hassett, J. P.; Anderson, M. A. *Environ. Sci. Technol.* **1979**.
19. Wershaw, R. L.; Burcar, P. J.; Goldberg, M. C. *Environ. Sci. Technol.* **1969**, *3*, 271–273.
20. Porrier, M. A.; Bordelon, B. R.; Laseter, J. L. *Environ. Sci. Technol.* **1972**, *6*, 1033–1035.
21. Boehm, P. D.; Quinn, J. G. *Geochim. Cosmochim. Acta* **1973**, *37* (11), 2459–2477.
22. van Stempvoort, D. R.; Lesage, S.; Novakowski, K. S.; Millar, K.; Brown, S.; Lawrence, J. R. *J. Contam. Hydrol.* **2002**, *54*, 249–276.
23. Molson, J. W.; Frind, E. O.; van Stempvoort, D. R.; Lesage, S. *J. Contam. Hydrol.* **2002**, *54*, 277–305.
24. Rebhun, M.; Desmedt, F.; Rwetabula, J. *Water Res.* **1996a**, *30*, 2027–2038.

25. Rebhun, M.; Rav-Acha, Ch.; Sabbah, I.; Rwetabula, J.; Desmedt, F. International Workshop on Soil and Aquifer Pollution, Haifa, May 13–15, 1996.
26. Backhus, D. A.; Gschwen, P. M. *Environ. Sci. Technol.* **1990**, *24*, 1214–1223.
27. Schlautman, M. A.; Morgan, J. J. *Environ. Sci. Technol.* **1993**, *27*, 961–969.
28. Backhus, D. A.; Golini, C.; Castellanos, E. *Environ. Sci. Technol.* **2003**, *37*, 4717–4723.
29. Ramos, E. U.; Meijer, S. N.; Vaes, W. H. J.; Verhaar, H. J. M.; Hermens, J. L. M. *Environ. Sci. Technol.* **1998**, *32*, 3430–3435.
30. Bondarenko, S.; Gan, J. *Environ. Sci. Technol.* **2009**, *43* (10), 3772–3777.
31. Xu, Y.; Spurlock, F.; Wang, Z.; Gan, J. *Environ. Sci. Technol.* **2007**, *41* (24), 8394–8399.
32. Porschmann, J.; Kopinke, F.-D.; Pawliszyn, J. *J. Chromatogr.* **1998**, *816* (2), 159–167.
33. van der Wal, L.; Hager, T.; Fleuren, R. H. L. J.; Barendregt, A.; Sinnige, T. L.; van Gestel, C. A. M.; Hermens, J. L. M. *Environ. Sci. Technol.* **2004**, *38* (18), 4842–4848.
34. Hawthorne, S.; Grabanski, C. B.; Miller, D. J.; Kreitinger, J. P. *Environ. Sci. Technol.* **2005**, *39* (81), 2795–2803.
35. Georgi, A.; Reichl, A.; Trommler, U.; Kopinke, F.-D. *Environ. Sci. Technol.* **2007**, *41* (20), 7003–7009.
36. Doll, T. E.; Frimmel, F. H.; Kumke, M. U.; Ohlenbusch, G. *J. Anal. Chem.* **1999**, *364*, 313–319.
37. Mackenzie, K.; Georgi, A.; Kumke, M.; Kopinke, F. D. *Environ. Sci. Technol.* **2002**, *36*, 4403–4409.
38. Holbrook, R. D.; Breidenich, J.; Derose, P. C. *Environ. Sci. Technol.* **2005**, *39*, 6453–6460.
39. Burkhard, L. P. *Environ. Sci. Technol.* **2000**, *34*, 4663–4668.
40. Lee, S.; Gan, J.; Liu, W. P.; Anderson, M. A. *Environ. Sci. Technol.* **2003**, *37*, 5597–5602.
41. van der Wal, L.; Jager, T.; Fleuren, R. H. L. J.; Barendregt, A.; Sinnige, T. L.; van Gestel, C. A. M.; Hermens, J. L. M. *Environ. Sci. Technol.* **2004**, *38*, 4842–4848.
42. Gauthier, T. D.; Shane, E. D.; Guerin, W. F.; Sitz, W. R.; Grant, C. L. *Environ. Sci. Technol.* **1986**, *20*, 1162–1166.
43. Revchuk, A. D.; Suffet, I. H. *Water Res.* **2009**, *43*, 3685–3692.
44. Rosario-Ortiz, F. L.; Snyder, S.; Suffet, I. H. *Water Res.* **2007**, *41*, 4115–4128.
45. Rosario-Ortiz, F. L.; Snyder, S.; Suffet, I. H. *Environ. Sci. Technol.* **2007**, *41* (14), 4895–4900.
46. Marhaba, T. F.; Van, D.; Lippincott, R. L. *Water Res.* **2000**, *34* (14), 3543–3550.
47. MacDonald, B. C.; Lvin, S. J.; Patterson, H. *Anal. Chem. Acta.* **1997**, *338*, 155–162.
48. Macay, D.; Shiu, W. Y. *J. Chem. Eng. Data* **1997**, *22*, 399.
49. Rubhun, M.; Meir, S.; Laor, Y. *Environ. Sci. Technol.* **1998**, *32*, 982–986.

## Chapter 6

# Photochemistry of Deepwater Horizon Oil

Sarah M. King, Peter A. Leaf, and Matthew A. Tarr\*

Department of Chemistry and Advanced Materials Research Institute,  
University of New Orleans, New Orleans, Louisiana 70148

\*E-mail: [mtarr@uno.edu](mailto:mtarr@uno.edu)

Oil from the Deepwater Horizon spill was collected from the surface of the Gulf of Mexico and subsequently exposed to simulated sunlight in order to observe its photochemical transformations. In line with previous studies, only small losses of alkanes were observed while substantial degradation of polycyclic aromatic hydrocarbons occurred. The toxicity of water exposed to the oil increased dramatically upon irradiation of the oil.

## Introduction

The oil spill from the destroyed Deepwater Horizon platform in the Gulf of Mexico represented an enormous disruption of the entire ecosystem. Both short and long term impacts of the spill are widespread. A wide range of challenges surrounded the effort to stop the spill, and consequently oil continued to contaminate the Gulf of Mexico for an extended period. Many of the impacts of this and other spills are poorly understood. Unfortunately, funding for oil spill response technology has declined in past years. Of the \$13 billion dollars in royalties collected annually by the U.S. Bureau of Ocean Energy Management, Regulation and Enforcement (formerly the Minerals Management Service), only \$7 million is spent each year on oil spill technology. Furthermore, US Coast Guard funding for oil spill technology had declined from \$5.6 million per year in 1993 to only \$500,000 per year for the four years ending in 2010. Numerous sources also indicate that oil spill technology has stagnated, and that many of the tools used today are the same tools that were used in response to the 1989 Exxon Valdez spill and even the 1979 Ixtoc I spill in the southern Gulf of Mexico.

Biodegradation and photodegradation are the two major pathways for crude oil transformations in marine systems. A wide range of literature is available on the biodegradation of crude oil and petroleum products. Many of these studies focus on soil systems, but studies in marine systems are also prevalent. The breadth of literature in this field is partially captured in a number of recent reviews (1–4) as well as publications on Deepwater Horizon biodegradation (5, 6). In contrast, relatively few research articles are available on the topic of crude oil photodegradation.

In April, 1979, the Ixtoc I exploratory well in the Bay of Campeche suffered a blowout. As a result, oil from the relatively shallow well was released from the sea floor for almost 10 months. The total release from the Ixtoc spill is estimated between 126 million and 210 million gallons of crude oil. This release occurred over a period of nearly 10 months, and the prevailing current pushed much of the oil offshore for an extended period before it impacted coastal areas. As a result, a large portion of the oil that reached shore was substantially weathered prior to landfall. A number of research projects undertaken in the 1979–1981 time period documented transformations and impacts of the oil near the spill site as well as at distant locations.

Bedinger and Nulton analyzed nearshore south Texas area water and sediment samples to determine levels of oil contamination from the Ixtoc spill. Seven months after this region was first contaminated, the researchers found little if any evidence of residual contamination (7). Coastal lagoons along the Bay of Campeche were partially impacted by the Ixtoc spill, and oysters were shown to be a useful indicator of oil contamination due to their effective bioaccumulation of these analytes (8). Studies on spot fish eggs exposed to crude oil equilibrated water revealed significant toxicity; more importantly, the level of toxicity was substantially higher when both dissolved oil and dispersant (Corexit 9527) were present (9). Red drum eggs were also found to be severely damaged by exposure to sea water with dissolved hydrocarbons from the Ixtoc spill (10). Floating oil from the Ixtoc spill was transformed into a mousse, an oil-water emulsion. Such emulsions were formed when oil was photooxidized to form polar products that acted as emulsifying agents (11). While dissolved hexadecane and naphthalene had expected biodegradation lifetimes of 1–10 days near the Ixtoc well, biodegradation of emulsions in the open Gulf of Mexico were very slow (on the order of 5% per year) (11). These very slow biodegradation rates for isolated mousse in the open Gulf were attributed to low levels of nutrients; furthermore, addition of nitrogen nutrients to these systems enhanced biodegradation rates by a factor of 20–300 fold (11). Despite the presence of elevated levels of oil degrading bacteria in areas with oil contamination, biodegradation was unable to proceed due to both nitrogen and phosphorous limitations as well as an unfavorable surface area to volume ratio (12). For biodegradation of crude oil, n-alkanes with 26 or fewer carbons are most readily utilized, while n-alkanes with greater numbers of carbons, branched alkanes, and aromatics with 3 or more rings are minimally degraded by bacteria (12). Lower molecular weight, more volatile components of crude oil are rapidly removed from surface oil and redistributed in the environment through evaporation or dissolution in sea water (13). These processes further limit the biodegradation process for surface oil as many of the

biodegradable materials are heavily depleted. Photochemistry can therefore play an important role in stimulating biodegradation through formation of bioavailable photoproducts.

Boehm and Fiest (14) reported the presence of an underwater plume of oil droplets emanating from the Ixtoc spill and extending 25 km away from the spill site. The Ixtoc spill occurred in water with a depth of 50 m. The Horizon spill emanated from a leak at a depth of 1500 m below the surface, so a much greater depth of the water column was available in which droplets or dissolved oil could exist and interact with the marine system. For the Ixtoc spill, Boehm, *et al.* clearly demonstrated that both the aliphatic and the aromatic fractions of the oil became depleted in lower molecular weight species as the oil aged (15). In their study, they developed models for oil fate based on evaporation, dissolution, and biodegradation. Similar to other reports, this study also indicated that biodegradation was minimal due to nutrient limitations. The report concluded that photochemistry became the major process for surface oil transformations at distances of more than 100 km from the spill site. Despite this conclusion, photochemistry was not incorporated into the modeling effort.

According to one study, the effectiveness of chemical dispersants is diminished as surface oil ages (16). This observation is likely due to the fact that the more easily dispersed compounds are lost as the spill ages. Dispersant applied to aged oil that no longer has the lower molecular weight compounds will therefore be less able to disperse the oil. These effects, however, seem to be dependent on the oil properties (e.g. viscosity, density, etc.) as well as the physical properties of the spill (e.g. film thickness) (17).

Photochemical transformation of intact crude oil has been studied to a limited extent over the last 40 years. In 1975, Hansen reported on the photodegradation of thin films of crude oil fractions on sea water (18). This study reported rates of degradation, and noted that the products were primarily aliphatic and aromatic acids as well as smaller amounts of alcohols and phenols. Tjessem and Aaberg also noted that photolysis of crude oil resulted in substantial changes in its chemical and physical properties (19), and additional studies noted photochemical formation of ketones (20). Photodegradation was deemed a major pathway for crude oil degradation in aquatic systems in a study that sampled oxidation products in natural water under an oil slick (21). Thominet and Verdu suggested that polycyclic aromatic hydrocarbons (PAHs) are important in radical propagation of chain reactions (22) and that phase separation can occur due to insoluble, high molecular weight species formed by cross-linking of aromatics (23). Other reports indicated the importance of photosensitized reactions involved in photochemical transformations of otherwise unreactive linear and branched alkanes (24, 25). In more recent work, a number of benzothiophene photooxidation products were identified (26), and other studies reported on the photodegradation of water soluble fractions of oil (27, 28). Evident in these and other studies is the fact that oil photodegradation is dependent on the source oil (29, 30). Many previous studies on oil photodegradation utilized mercury lamps instead of simulated sunlight. Reports on toxicity and biodegradation indicated that photodegradation of oil increases its toxicity but also enhances the extent of its biodegradation (28, 29). Major weaknesses in the applicability of the available literature to

understanding transformations of Deepwater Horizon surface oil include: 1) the photochemistry of oil is dependent on the source oil, so the behavior of oil from the Deepwater Horizon spill cannot be readily predicted from the current literature; 2) a number of earlier studies utilized mercury lamps that contain higher UV intensities and shorter wavelengths than present in sunlight; 3) only a few studies have identified photochemical products, and these were for oil other than that from the Gulf of Mexico; 4) very few studies have focused on mechanisms, so it is unclear what specific intermediates are involved in oil photochemistry; 5) the impact of dispersants on oil photochemistry is poorly documented.

Titanium dioxide has been extensively used as a photocatalyst (31–39). Although not covered in this study, a few applications to oil spills have been conducted. Several reports have discussed the use of TiO<sub>2</sub> for oil degradation (27, 28, 40–43), but due to the limited number of studies, the limited number of source oils, the use of mercury lamps, and the lack of mechanistic and product data, much remains poorly understood in these systems. Nevertheless, because of its low cost, low toxicity, and wide availability, this material is a good candidate for enhancing solar decomposition of oil on the surface of water. Additional studies utilizing photocatalysts would add to our understanding of oil transformation processes that could be applied to speed oil degradation.

## Experimental Materials and Methods

Crude oil and water samples were collected on May 26, 2010 from approximately 47 miles (28 48.316N, 89 07.949W) northwest of the Deepwater Horizon site (see Figure 1). Oil samples collected were thick and dark brown. The water samples were collected from a nearby area in the Gulf of Mexico that was not visibly contaminated with oil. After collection the water samples were filtered through 0.2 μm polycarbonate filters to sterilize the water and were subsequently stored at 4 °C.

Dichloromethane (DCM) and toluene were OmniSolv ultra high purity obtained from EMD Chemicals (Gibbstown, NJ). HPLC solvent grade pentane was obtained from J. T. Baker/Avantor (Center Valley, PA).

Prior to exposure to simulated sunlight, 100 mg of crude oil was weighed and dissolved in a mixture of pentane and toluene (20:1). The mixture was then sonicated to fully disperse the oil. The mixture was then poured onto the surface of 10 mL Gulf water in a 150 mL water-jacketed beaker (5 cm i.d.). The sample was kept uncovered for several minutes to allow the pentane and toluene to evaporate. The samples were then exposed to simulated sunlight (Atlas, Chicago, IL, Suntest CPS+ equipped with a 1500 W air cooled xenon arc lamp). The solar simulator was operated at full power, which corresponds to about 1.26 times AM1 sunlight intensity (1000 W/m<sup>2</sup>) as measured with a NIST calibrated photocell. Assuming that a full day of sunlight on a clear day is equivalent to approximately 6 hours of irradiation at 1000 W/m<sup>2</sup>, we estimated that 4.8 hours of irradiation in our simulator corresponded to one day of irradiation with no cloud cover. During irradiation, the samples were kept at 27°C by circulating water through the jacketed beakers. During exposure, each beaker was covered

with a piece of quartz, but there was not a complete seal between the top of the beaker and the quartz cover. A dark control was always used to compare to each irradiated sample. After irradiation the samples were either extracted with DCM for GC-FID and fluorescence analysis or the water was collected for toxicity screening. For GC-FID analysis, dodecane, which was not already present in the samples, was added to samples as an internal standard prior to injection.

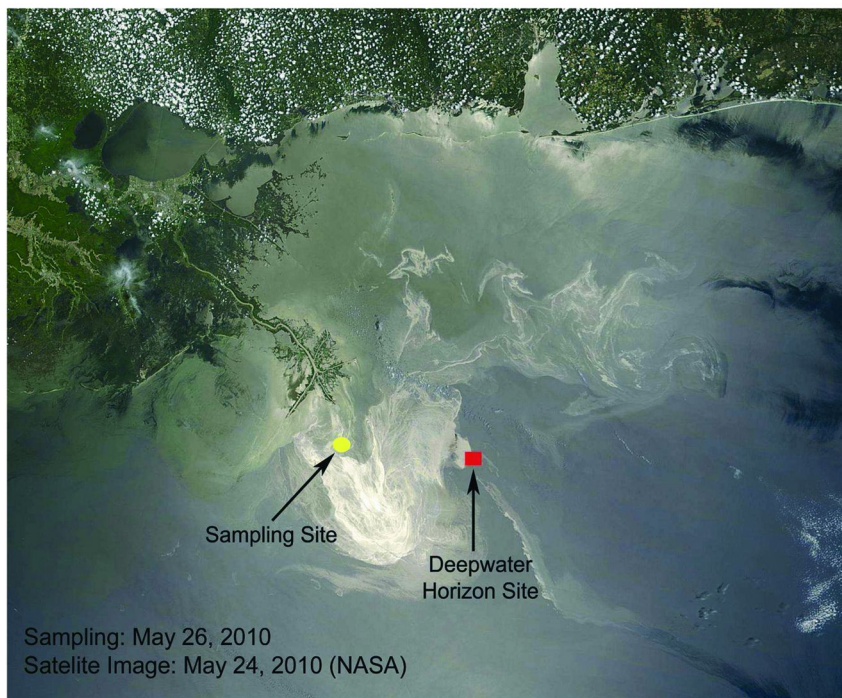


Figure 1. Sampling location (satellite image from NASA). (see color insert)

Oil extracts were analyzed on a Hewlett-Packard (now Agilent, Santa Clara, CA) 6890 GC coupled to an auto sampler with a flame ionization detector and a 30 m  $\times$  0.32 mm (i.d.) AT-1 capillary column. The injector and detector temperatures were set to 300 °C and 350 °C, respectively, and the temperature programming was as follows: 80 °C held for 1 minute, ramp at 15 °C/min until a final temperature of 320 °C which was held for 15 minutes. Peak areas from each gas chromatogram were normalized to dodecane that was added to each sample prior to analysis as an internal standard. The internal standard was used to correct for variations in injection volume or efficiency. For each compound, the normalized peak area for the irradiated sample was divided by the normalized peak area for the corresponding dark control in order to determine the percent of each compound remaining in the irradiated sample relative to the dark control.

Synchronous fluorescence scans were collected with a PerkinElmer (Waltham, MA) LS 55 luminescence spectrometer. Synchronous scans of the oil extracts (further diluted with DCM) were collected from 250 to 500 nm with a delta lambda of 25 nm and excitation and emission slits set to 2.5 and 5.0 nm, respectively. These parameters were similar to those used in previous reports that utilized synchronous fluorescence scans to characterize polycyclic aromatic hydrocarbons (PAHs) in oil samples (44–48). To determine changes in oil exposed to sunlight, the fluorescence intensity of each irradiated sample was divided by the intensity of the corresponding dark control. This approach eliminated any sample to sample variations since the dark controls were prepared and measured at the same time as the irradiated samples.

Microtox<sup>®</sup> analysis was performed using a Microtox<sup>®</sup> 500 Analyzer (SDIX, Newark, DE). In this approach, luminescent bacteria were exposed to samples and the decrease in luminescence was proportional to the toxicity of the sample. Microtox<sup>®</sup> diluent, osmotic adjusting solution, reconstitution solution, and acute reagent were obtained from SDIX. Crude oil was allowed to equilibrate with Gulf of Mexico water, then the aqueous fraction was analyzed using Microtox<sup>®</sup> screening. The protocol used to analyze the toxicity of the water exposed to the oil was the SDIX comparison test for marine and estuarine samples. For each day Microtox<sup>®</sup> was used, the basic test was run using phenol or zinc sulfate standards to ensure proper function of the Microtox<sup>®</sup> analyzer.

## Results and Discussion

Oil utilized in this study was collected from the surface of the Gulf of Mexico on May 26, 2010. The oil had been on the surface for an undetermined time period and had previously traveled through the entire water column from its source of release to the surface. As a result, the oil was depleted in compounds of greater water solubility and higher volatility. The process of rising through the water column acted as a multi-step extraction in which the more water soluble compounds were dissolved in the water and removed from the oil. Once on the surface, volatile compounds were free to escape into the atmosphere, resulting in loss of lower molecular weight species. Our gas chromatographic data indicate that the collected oil sample had no detectable levels of compounds smaller than C13 hydrocarbons. Synchronous fluorescence spectra were acquired in order to assess the PAH content of the oil samples (44–48). The fluorescence data suggest that the abundance of single ring aromatics were largely absent, and two ring polycyclic aromatic hydrocarbons (PAHs) were present in low abundance relative to other PAHs. The collected oil was dark brown in color with a small amount of orange coloration apparent when it was on the surface of the Gulf of Mexico. Figure 2 shows oil being collected from the surface of the Gulf of Mexico. Based on observation of the oil on the surface, it is estimated that the oil was several millimeters thick at the locations that were sampled.



Visible changes in oil appearance were observed during irradiation (see Figure 3). Initially, 100 mg of oil was dispersed as a thin film on top of Gulf of Mexico water in a jacketed beaker with an internal diameter of 5 cm. Based on the approximate density of the oil, and assuming a uniform film, we estimate the thickness of the film to be 60  $\mu\text{m}$ . However, considerable variability in the film thickness was evident (Figure 3a). Irradiation for 3 hours ( $\sim 0.63$  days of sunlight) did not cause a visible change in the appearance of the oil. After 6 hours irradiation ( $\sim 1.25$  days of sunlight), the oil film was cracked and somewhat leathery (Figure 3c). Additional irradiation for up to 48 hours ( $\sim 10$  days of sunlight) caused further changes to the oil film (Figure 3d-f).

In order to more quantitatively assess changes in the oil as a function of irradiation, we extracted the oil/water mixture with dichloromethane and analyzed the extract using gas chromatography and fluorescence spectroscopy.



*Figure 2. Surface oil being collected. Photo courtesy of Benjamin Lyons. (see color insert)*

Using GC analysis, we observed small losses of hydrocarbons as a function of irradiation time. In general, the observed concentration of hydrocarbons decreased with increasing irradiation. However, the extent of loss of hydrocarbons was not constant as a function of hydrocarbon size. Lower molecular weight compounds were depleted more rapidly than higher molecular weight species. Figure 4 illustrates the change in concentration of several hydrocarbons as a function of irradiation time. For each sample, exposures were done in jacketed beakers maintained at 27°C. During exposure, each beaker was covered with a piece of quartz, but there was not a complete seal between the top of the beaker and the quartz cover. Because our samples were kept in thermostated beakers and since the compounds present were of relatively low volatility, we do not believe that volatilization was a major factor in these experiments. Boiling points and vapor pressures for selected n-alkanes are provided in Table I.

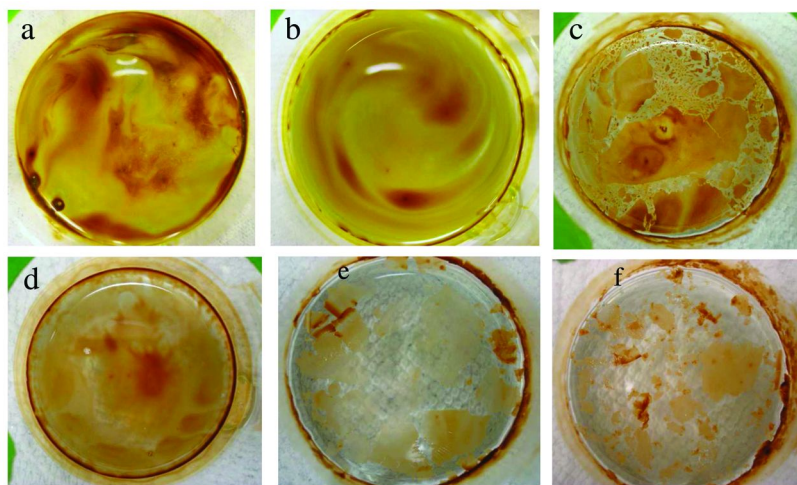


*Figure 3. Appearance of oil as a function of irradiation time: (a) before irradiation, and after (b) 3 h, (c) 6 h, (d) 12 h, (e) 24 h, and (f) 48 h of solar irradiation. Irradiation for 4.8 h in the solar simulator is approximately equal to one full day of sunlight. (see color insert)*

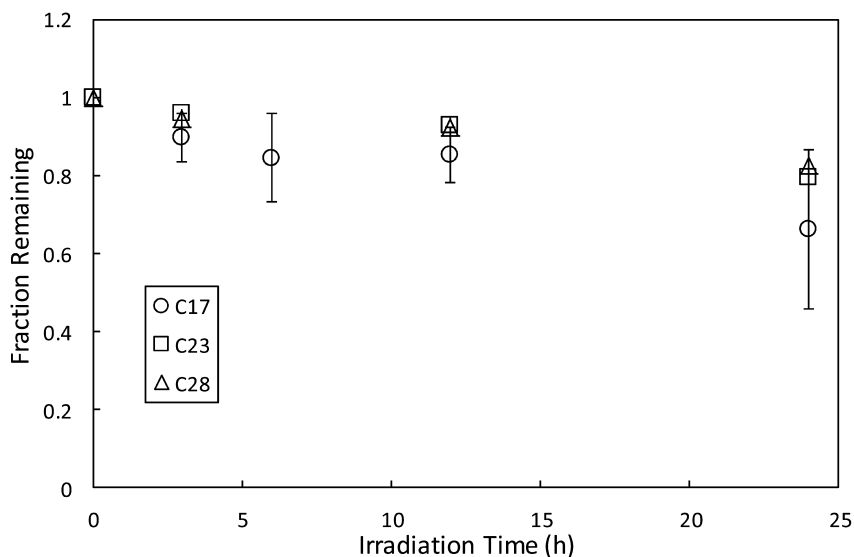


Figure 4. Fraction of selected hydrocarbons remaining after irradiation based on GC-FID analysis. Irradiation times are reported as hours of exposure in a solar simulator with 4.8 h approximately equivalent to one day of sunlight. Data points represent the mean of triplicate exposures. For clarity, error bars (one standard deviation) are only shown for C17, which had the largest error.

**Table I. Boiling point and vapor pressure for selected n-alkanes**

<i>Compound</i>	<i>Boiling Point (°C)</i>	<i>Vapor Pressure</i>
Tridecane	234	1 mmHg at 59°C
Tetradecane	253	1 mmHg at 76°C
Hexadecane	302	1 mmHg at 105°C
Heptadecane	287	1 mmHg at 115°C

Triplicate experiments yielded an average relative standard deviation (RSD) of 7.7% for C17-C28 hydrocarbons evaluated. For the higher molecular weight alkanes (e.g. C19, C20, C22, C23, C28), the decrease in their concentration was on average only 5% for a 3 hour irradiation (~0.63 day of sunlight) and 20% for a 48 hour irradiation (~10 days of sunlight). Dutta and Haryama (29) reported an increase in concentration of moderate molecular weight alkanes (C15-C19). They attributed this increase to cleavage of alkyl side chains from aromatics. We did not observe similar behavior in our study. Their study utilized a different source oil, irradiated with a mixture of lights that was similar to natural sunlight, and carried out irradiations for 4 weeks in an open container, considerably longer than the times used in our study. Furthermore, their use of a mercury vapor lamp may have resulted in higher levels of UV radiation than are normally present in sunlight. Other studies have reported minimal degradation of n-alkanes in irradiated oil samples (40, 49). However, it has also been demonstrated that photosensitized reactions can result in n-alkane degradation. Guiliano, et al. showed photosensitized decomposition of C12-C22 n-alkanes in seawater to which anthraquinone was added (50). Although PAHs present in petroleum are capable of acting as photosensitizers, degradation of the n-alkanes in the Deepwater Horizon oil was apparently slow (about 20% loss for the equivalent of 10 days of exposure).

In addition to GC studies, we probed transformations of aromatic compounds using fluorescence spectroscopy. We utilized synchronous scan fluorescence spectra since these data can differentiate between aromatics with varying numbers of rings (14, 47). Consequently, we report the synchronous scan fluorescence intensity for 1-2 ring (305 nm), 2-3 ring (326), and 3-5 ring (390) PAHs. In agreement with previous studies, the aromatic compounds were degraded very rapidly compared to the alkanes. Figure 5 illustrates the loss in fluorescence for each wavelength as a function of irradiation time. In general, the larger PAHs degraded more rapidly than the smaller PAHs. After 24 hours of irradiation (~5 days of sunlight), the fluorescence at 305 nm (1-2 rings) was only 23% of the original value. For emission at 326 nm (2-3 rings), 15% of the fluorescence remained, and at 390 (3-5 rings) only 13% of the fluorescence remained. Unlike for shorter irradiation times, the PAH concentrations did not change substantially between for longer times (up to 48 hours of irradiation). In fact, for all three wavelengths studied, loss of fluorescence slowed as exposure time increased. Figure 5b illustrates the deviation of these reactions from first order kinetics. The decrease in degradation rate with exposure time could reflect loss of sensitizers. If a sensitizer initially absorbs radiation and then results in decomposition of another compound, depletion of the sensitizer would result in a slower decomposition rate for the compound. Another possible explanation is the buildup of photodegradation products that can act as scavengers. As the parent compounds react, they produce products which can also react with sensitizers or other photochemical intermediates. Such reactions would compete with degradation of the parent compounds, resulting in a slower observed rate of decomposition with increasing exposure time. Previous studies have reported the formation of a wide range of degradation products, mostly oxygenated compounds (20, 21).

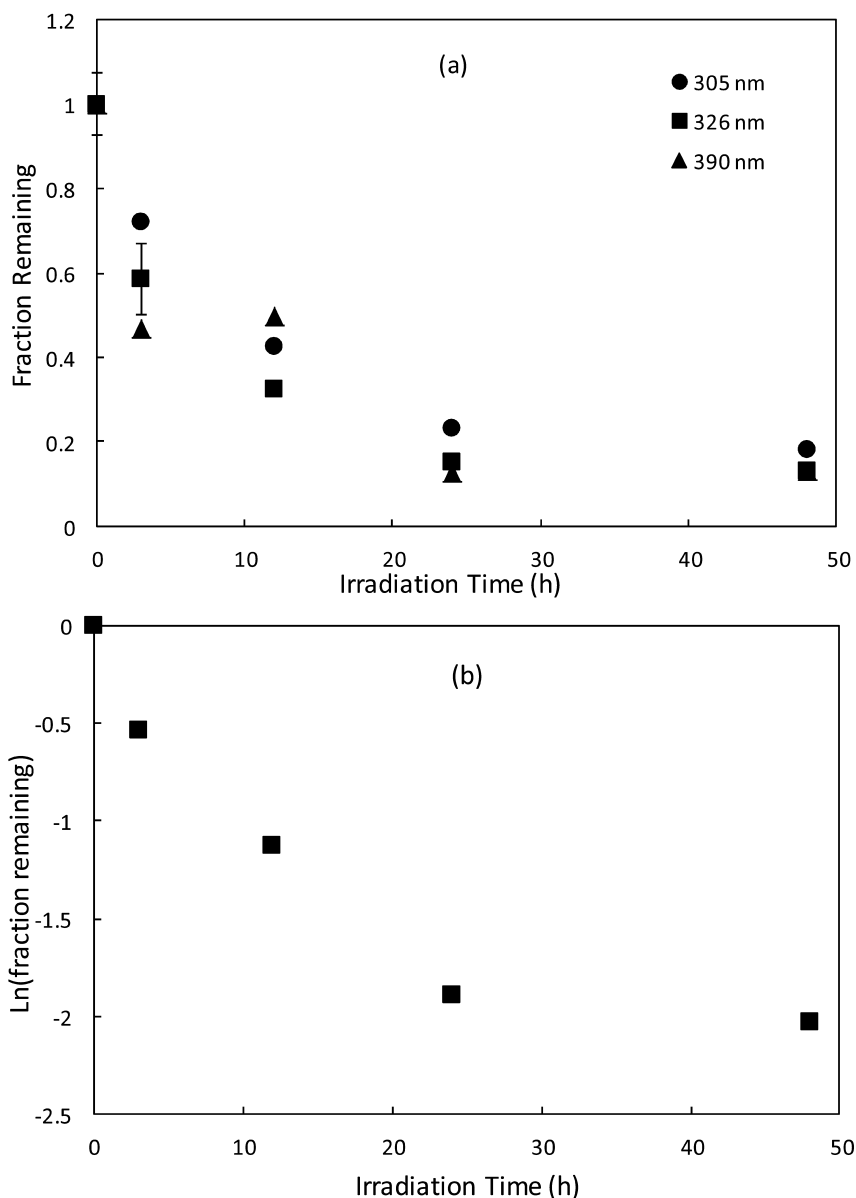


Figure 5. (a) Loss of fluorescence as a function of irradiation time for three wavelengths using synchronous scans. For clarity, error bars (one standard deviation) are included for 326 nm only. For most points, error bars are smaller than the symbol. (b) Logarithmic plot for data at 326 nm. Irradiation times are reported as hours of exposure in a solar simulator with 4.8 h approximately equivalent to one day of sunlight.

In order to assess the toxicity of the crude oil, we utilized Microtox<sup>®</sup> screening. In this approach, luminescent bacteria were exposed to samples and the decrease in luminescence was proportional to the toxicity of the sample. Crude oil was allowed to equilibrate with Gulf of Mexico water, then the aqueous fraction was analyzed using Microtox<sup>®</sup> screening. For samples that had not been exposed to simulated sunlight, no measurable toxicity of the aqueous phase was observed. This result is reasonable since the crude oil had already been depleted of water soluble compounds. Consequently, the remaining compounds were too insoluble in water to present substantial toxicity. However, upon exposure to simulated sunlight, the toxicity of the aqueous phase increased with increasing exposure time. These data are presented in Figure 6. The %Effect value represents the percentage of the bacteria killed by the exposure. For comparison, control experiments utilizing phenol showed an IC<sub>50</sub> of 18 ppm (equivalent to 50 %Effect). Previous studies have indicated an increase in toxicity upon irradiation. Such effects are most likely due to the formation of oxygenated products that have higher water solubility than the parent compounds. Once formed, these compounds are more bioavailable than the parent compounds, and consequently an increase in toxicity is observed. Despite these toxicity effects, research has shown that photodegradation stimulates biodegradation of crude oil (28, 29).

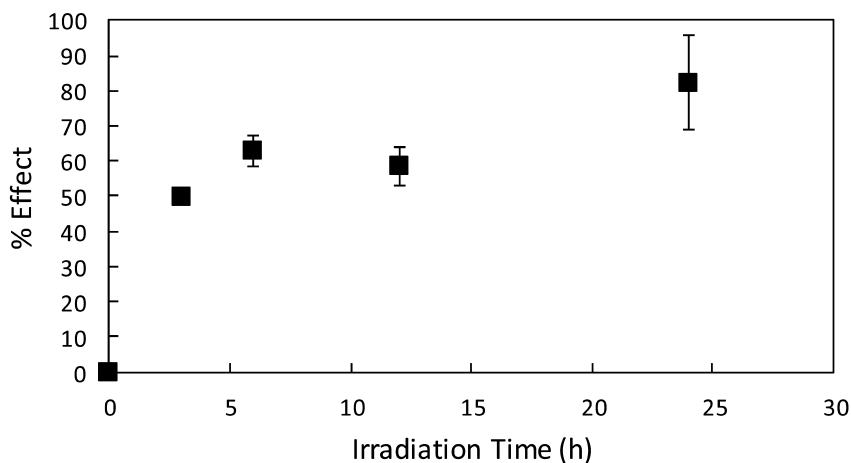


Figure 6. Observed changes in toxicity of water exposed to oil after irradiation for various times. Irradiation times are reported as hours of exposure in a solar simulator with 4.8 h approximately equivalent to one day of sunlight. Error bars represent one standard deviation for triplicate samples.

## Conclusions

Photochemical behavior of oil from the Deepwater Horizon spill behaved similarly to oil from previous studies. In thin films of oil, PAHs degraded fairly rapidly, showing about 80% loss of PAHs with the equivalent of 5 days of exposure to sunlight. Alkanes showed only small losses over 10 days of irradiation, indicating that sensitized photodegradation of these compounds was not a significant pathway. Toxicity of the oil increased dramatically on exposure to sunlight, presumably due to the formation of bioavailable compounds. The observed behavior of this oil was certainly impacted by its previous weathering, which depleted the oil of low molecular weight, water soluble, and bioavailable compounds.

## Acknowledgments

This research was supported by the National Science Foundation (CHE-0611902), by BP via the Gulf of Mexico Research Initiative and the Northern Gulf Institute (10-BP\_GRI-UNO-01), and by the University of New Orleans College of Sciences. Undergraduate students Aisa Carter and Anastasia Whitney and high school student Elizabeth Balga contributed to this study. Elizabeth Balga was supported by the Army Research Office via a subgrant from the Academy of Applied Science (W911NF-04-1-0226). We thank SDIX for loaning us a Microtox<sup>®</sup> 500 analyzer.

## References

1. Brooijmans, R. J. W.; Pastink, M. I.; Slezén, R. J. *Microb. Biotechnol.* **2009**, *2*, 587–594.
2. Cameotra, S. S.; Makkar, R. S. *Pure Appl. Chem.* **2010**, *82*, 97–116.
3. Rojo, F. *Environ. Microbiol.* **2009**, *11*, 2477–2490.
4. Yemashova, N. A.; Murygina, V. P.; Zhukov, D. V.; Zakharyantz, A. A.; Gladchenko, M. A.; Appanna, V.; Kalyuzhnyi, S. V. *Rev. Environ. Sci. Bio/Technol.* **2007**, *6*, 315–337.
5. Hazen, T. C.; Dubinsky, E. A.; De, S. T. Z.; Andersen, G. L.; Piceno, Y. M.; Singh, N.; Jansson, J. K.; Probst, A.; Borglin, S. E.; Fortney, J. L.; Stringfellow, W. T.; Bill, M.; Conrad, M. E.; Tom, L. M.; Chavarria, K. L.; Alusi, T. R.; Lamendella, R.; Joyner, D. C.; Spier, C.; Baelum, J.; Auer, M.; Zemla, M. L.; Chakraborty, R.; Sonnenthal, E. L.; D'Haeseleer, P.; Holman, H.-Y. N.; Osman, S.; Lu, Z.; Van, N. J. D.; Deng, Y.; Zhou, J.; Mason, O. U. *Science* **2010**, *330*, 204–208.
6. Valentine, D. L.; Kessler, J. D.; Redmond, M. C.; Mendes, S. D.; Heintz, M. B.; Farwell, C.; Hu, L.; Kinnaman, F. S.; Yvon-Lewis, S.; Du, M.; Chan, E. W.; Tigreros, F. G.; Villanueva, C. J. *Science* **2010**, *330*, 208–211.
7. Bedinger, C. A., Jr.; Nulton, C. P. *Bull. Environ. Contam. Toxicol.* **1982**, *28*, 166–171.
8. Botello, A. V.; Goni, J. A.; Castro, S. A. *Bull. Environ. Contam. Toxicol.* **1983**, *31*, 271–277.

9. Slade, G. J. *Bull. Environ. Contam. Toxicol.* **1982**, *29*, 525–530.
10. Rabalais, S. C.; Arnold, C. R.; Wohlschlag, N. S. *Tex. J. Sci.* **1981**, *33*, 33–38.
11. Atwood, D. K.; Ferguson, R. L. *Bull. Mar. Sci.* **1982**, *32*, 1–13.
12. Atlas, R. M. *Environ. Int.* **1981**, *5*, 33–38.
13. Brooks, J. M.; Wiesenburg, D. A.; Burke, R. A., Jr.; Kennicutt, M. C. *Environ. Sci. Technol.* **1981**, *15*, 951–959.
14. Boehm, P. D.; Fiest, D. L. *Environ. Sci. Technol.* **1982**, *16*, 67–74.
15. Boehm, P. D.; Fiest, D. L.; Mackay, D.; Paterson, S. *Environ. Sci. Technol.* **1982**, *16*, 498–505.
16. McAuliffe, C. D.; Johnson, J. C.; Greene, S. H.; Canevari, G. P.; Searl, T. D. *Environ. Sci. Technol.* **1980**, *14*, 1509–1518.
17. Linton, T. L.; Koons, C. B. *Oil Petrochem. Pollut.* **1983**, *1*, 183–188.
18. Hansen, H. P. *Mar. Chem.* **1975**, *3*, 183–195.
19. Tjessem, K.; Aaberg, A. *Chemosphere* **1983**, *12*, 1373–1394.
20. Jacquot, F.; Guiliano, M.; Doumenq, P.; Munoz, D.; Mille, G. *Chemosphere* **1996**, *33*, 671–681.
21. Barth, T. *Chemosphere* **1984**, *13*, 67–86.
22. ThomINETTE, F.; Verdu, J. *Mar. Chem.* **1984**, *15*, 91–104.
23. ThomINETTE, F.; Verdu, J. *Mar. Chem.* **1984**, *15*, 105–115.
24. Rontani, J. F.; Giral, P. J. P. *Int. J. Environ. Anal. Chem.* **1990**, *42*, 61–68.
25. Ehrhardt, M. G.; Burns, K. A.; Bicego, M. C. *Mar. Chem.* **1992**, *37*, 53–64.
26. Bobinger, S.; Andersson, J. T. *Environ. Sci. Technol.* **2009**, *43*, 8119–8125.
27. Ziolli, R. L.; Jardim, W. F. J. *Photochem. Photobiol., A* **2003**, *155*, 243–252.
28. Ziolli, R. L.; Jardim, W. F. J. *Photochem. Photobiol., A* **2002**, *147*, 205–212.
29. Dutta, T. K.; Harayama, S. *Environ. Sci. Technol.* **2000**, *34*, 1500–1505.
30. Dutta, T. K.; Harayama, S. *Environ. Sci. Technol.* **2001**, *35*, 102–107.
31. Uzunova-Bujnova, M.; Kralchevska, R.; Milanova, M.; Todorovska, R.; Hristov, D.; Todorovsky, D. *Catal. Today*, *151*, 14–20.
32. Akpan, U. G.; Hameed, B. H. *Appl. Catal., A*, *375*, 1–11.
33. Nie, X.; Zhuo, S.; Maeng, G.; Sohlberg, K. *Int. J. Photoenergy* 2009No pp. given.
34. Akpan, U. G.; Hameed, B. H. *J. Hazard. Mater.* **2009**, *170*, 520–529.
35. Tada, H.; Kiyonaga, T.; Naya, S.-I. *Chem. Soc. Rev.* **2009**, *38*, 1849–1858.
36. Taga, Y. *Thin Solid Films* **2009**, *517*, 3167–3172.
37. Gaya, U. I.; Abdullah, A. H. J. *Photochem. Photobiol., C* **2008**, *9*, 1–12.
38. Aprile, C.; Corma, A.; Garcia, H. *Phys. Chem. Chem. Phys.* **2008**, *10*, 769–783.
39. Pichat, P. *Water Sci. Technol.* **2007**, *55*, 167–173.
40. D'Auria, M.; Emanuele, L.; Racioppi, R.; Velluzzi, V. *J. Hazard. Mater.* **2009**, *164*, 32–38.
41. Yue, X.; Zhang, R.; Wang, W.; Wang, L.; Yang, Y. *Mater. Lett.* **2008**, *62*, 1919–1922.
42. Berry, R. J.; Mueller, M. R. *Microchem. J.* **1994**, *50*, 28–32.
43. Nair, M.; Luo, Z.; Heller, A. *Ind. Eng. Chem. Res.* **1993**, *32*, 2318–2323.
44. Apicella, B.; Ciajolo, A.; Tregrossi, A. *Anal. Chem.* **2004**, *76*, 2138–2143.
45. Berruoco, C.; Venditti, S.; Morgan, T. J.; Alvarez, P.; Millan, M.; Herod, A. A.; Kandiyoti, R. *Energy Fuels* **2008**, *22*, 3265–3274.



46. Devos, O.; Fanget, B.; Saber, A. I.; Paturel, L.; Naffrechoux, E.; Jarosz, J. *Anal. Chem.* **2002**, *74*, 678–683.
47. Kister, J.; Pieri, N.; Alvarez, R.; Diez, M. A.; Pis, J. J. *Energy Fuels* **1996**, *10*, 948–957.
48. Li, S. P.; Shen, B. X.; Tang, F.; Zhang, B. L.; Yang, J. Y.; Xu, X. R. *Pet. Sci. Technol.* **2008**, *26*, 1510–1521.
49. Garcia-Martinez, M. J.; Da, R. I.; Canoira, L.; Llamas, J. F.; Alcantara, R.; Gallego, J. L. R. *Appl. Catal., B* **2006**, *67*, 279–289.
50. Guiliano, M.; El, A.-L. F.; Doumenq, P.; Mille, G.; Rontani, J. F. *J. Photochem. Photobiol., A* **1997**, *102*, 127–132.

## Chapter 7

# Developing Antifouling Marine Coatings Using Protein-Resistant Betaine-Based Polymers

Zheng Zhang\* and Christopher Loose

Semprus BioSciences, Cambridge, Maine 02139, U.S.A.

\*E-mail: [jonathan.zhang@semprusbio.com](mailto:jonathan.zhang@semprusbio.com)

Polymers with high protein resistance have been designed for marine coatings to resist attachment of marine organisms. Different methods and platforms, including self-assembled monolayers, polymer brushes and copolymers, have been applied in an attempt to create an effective antifouling surface. It has been found that betaine-based polymer brushes are among the most nonfouling surfaces to resist protein adsorption. Sulfobetaine polymer brushes were grafted on glass surfaces and show strong resistance to the attachment of green algae, diatoms, and barnacle cyprids. When grafted on a polyurethane substrate, their antifouling performance can be maintained after long-term exposure to complex media. Betaine polymers can be designed based on the main chains or the backbones of the polymers, the linking groups that connect betaine moieties to the backbones, and the spacer groups between the charged groups. Some betaine polymers can be tailored to integrate other antifouling designs, such as immobilizing active agents, self-polishing surfaces, releasing surfaces, and releasing active agents.

## 1. Introduction

Biofouling (growth on external surfaces by bacteria, algae, barnacles, mussels, and other marine organisms) occurs on ships, underwater constructions, and marine devices such as environmental sensors, causing mechanical wear and a reduction in performance. It is one of the most prominent issues affecting ships, and even a slime film imposes substantial drag with associated fuel penalties (*1*).

Biofouling on crucial components of marine and hydrokinetic (MHK) devices imposes substantial mass and hydrodynamic loading with associated efficiency and maintenance penalties (2). For ocean monitoring sensors, biofouling can disrupt the quality of the measurements in less than a week (3, 4). Most antifouling approaches rely on non-permanent coatings, which leach active ingredients such as copper and tributyltin (TBT) through an eroding or “self-polishing” process. Increasingly stringent regulation of biocides has led to interest in the development of non-biocidal technologies to control fouling (5). Non-toxic fouling-release coatings are developed based on silicones and fluoropolymers with low surface energy (6). These coatings “release” weakly attached accumulated fouling organisms, but they are generally only effective on vessels moving at speeds greater than 14 knots. Usually, these coatings do not resist biofouling on a static device and the foulants have to be removed on a floating platform or onshore by water jets. Other potential solutions to this problem, such as biocide-binding, self-polishing and degrading, quorum sensing-based solutions, and enzyme-based solutions, have been reviewed in many publications (7–9). These methods have shown promising efficacy in resisting some marine organisms, but none seems to be able to solve marine fouling universally due to the complex process included in biofouling.

In addition to the involvement of numerous fouling organisms, marine fouling challenges vary dramatically based on season, environment, and geography. The settlement and growth of marine organisms is a complex phenomenon that is still not fully understood (10)(11). Generally, the process of biological fouling is regarded as progressive process and can be divided into several stages. These stages include an initial accumulation of adsorbed organics, the settlement and growth of pioneering bacteria creating a biofilm matrix, and the subsequent succession of micro- and macro-organisms (7). These stages may not necessarily happen sequentially and a competitive process is very common. In all these stages, protein adsorption plays an important role in facilitating the settlement of marine organisms. Proteins adsorb on a surface immediately after the substrate is immersed in water, forming a conditional layer with other substances that can promote settlement of micro-organisms. Some proteins such as biofilm-associated proteins presenting on bacterial surfaces initiate both bacteria attachment and subsequent biofilm formation (12). It is also believed that many marine organisms, such as algal spores, barnacle cyprids, and mussels, can secrete proteinaceous adhesives to attach themselves onto a surface (13, 14). It is logical to expect that a material that resists protein adsorption should inhibit the attachment of various marine organisms. Recent progress on “nonfouling” materials that can highly resist protein adsorption makes it attractive to develop environmentally benign, effective, and durable antifouling marine coatings (15).

Some materials with “nonfouling” functional groups can highly resist protein adsorption. These materials, mainly hydrophilic polymers, can be divided into two classes, non-ionic polymers and ionic polymers. Non-ionic polymers include polyethylene glycol (PEG)-based polymers, poly(2-hydroxyethyl methacrylate) (polyHEMA), poly(*N*-vinyl pyrrolidone) (PVP), poly(2-methyl-2-oxazoline) (PMOXA), and some polysaccharides (16). Nonfouling ionic polymers include zwitterionic betaine polymers and some polyampholytes, such as

phosphorylcholine(PC)-based polymers, sulfobetaine (SB)-based polymers, and carboxybetaine (CB)-based polymers (17, 18). These materials are also finding application in medical devices, biosensors, and drug delivery carriers. While most of the research on these materials focuses on evaluating their clinical-related performance such as anti-thrombosis and antimicrobial efficacy, some have been tested for their resistance to marine organisms (Table 1) (19–28). These surfaces can be both non-ionic and ionic, and were prepared as self-assembled monolayers (SAMs), polymer brushes, and copolymers. Limiting biofouling in marine environments poses a great challenge because of the complexity of the environment, the variety of organisms, and the need for a long-life coating. A successful design may be based on understanding the best material and chemical structure that can broadly resist protein adsorption over a long duration, and incorporating other characteristics that are crucial for a marine coating such as stability, mechanical properties, and applicability.

**Table 1. Protein-resistant coatings that can reduce settlement of marine organisms**

<i>Protein-Resistant Components</i>	<i>Coatings</i>	<i>Marine Organisms</i>
Poly(2-hydroxyethyl methacrylate) (polyHEMA)	Cross-linked hydrogels (19)	Algal cells: <i>Enteromorpha intestinalis</i> and <i>Melosira nummuloides</i>
Poly( <i>N</i> -vinyl pyrrolidone) (PVP)	PVP/polyHEMA copolymers (19)	
Poly(ethylene glycol) (PEG)	PEG SAMs (20, 41)	Zoospores of macroalga <i>Ulva</i> and cells of diatom <i>Navicula</i>
	PEG brushes (21)	
	Branched polymers (22)	
	Amphiphilic copolymers (23, 24)	
	PEG-HEMA hydrogel (28)	
Poly(2-methacryloyloxyethyl phosphorylcholine) (polyMPC)	Random copolymers (25)	Diatom cells: <i>Nitzschia closterium</i>
Poly(sulfobetaine methacrylate) (polySBMA)	Polymer brushes (26)	Zoospores of macroalga <i>Ulva</i> and cells of diatom <i>Navicula</i> and <i>Craspedostaurus</i>

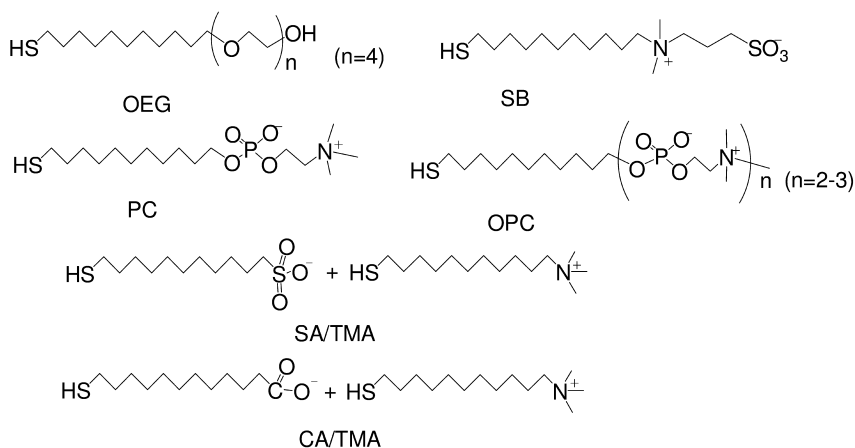
This chapter reviews the methods that prepare and evaluate protein-resistant materials. Using a highly protein-resistant betaine-based polymer, we show significant reduction of attachment of model marine organisms: a green algae, two diatom species, and a barnacle species. The stability of the SB-modified surface under long-term challenges was also evaluated. Furthermore, approaches

are described to design marine coatings by varying their chemical structures to developing an applicable coating and incorporating other antifouling mechanisms.

## 2. Preparing and Evaluating Antifouling Surfaces

### 2.1. Self-Assembled Monolayers

Self-assembled monolayers (SAMs) provide one of the most ideal surfaces for evaluating interfacial interaction of biomolecules and organisms. A typical SAM can be prepared by applying an alkanethiolate substituted with a head group on a gold substrate. The alkanethiol groups can be densely packed through thiol-gold interaction, exposing the head groups on the surface. By flowing a protein solution over the SAMs, protein adsorption can be detected using a highly sensitive detector such as surface plasmon resonance (SPR), or other surface-based sensors (29). Based on this method, SAMs with different head groups have been prepared and their level of protein adsorption was measured (30). The following functional groups are among the most protein-resistant moieties found by SAMs: (1) oligoethylene glycol (OEG) or PEG groups and their analogues (31), (2) zwitterionic betaine groups such as PC (32, 33), and SB (33), (3) mixed positively and negatively charged groups with balanced charges (33, 34), and (4) some sugar or sugar alcohol-based groups (35). Scheme 1 provides some examples of these structures. OEG-based SAMs are one of the most studied monolayer surfaces on which protein resistance as a function of terminal groups, repeat units, and packing density has been reported in previous literature (30, 31, 36, 37).

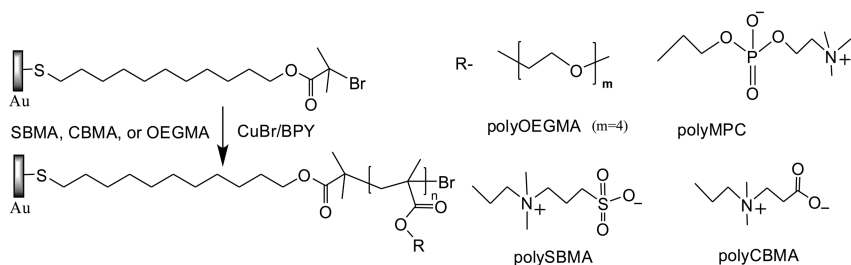


*Scheme 1. Alkanethiolates that can prepare protein-resistant SAMs on gold surfaces with headgroups of (1) oligoethylene glycol(OEG), (2) sulfobetaine (SB), (3) phosphorylcholine (PC), (4) oligophosphorylcholine (OPC), (5) mixed sulfonic acid (SA)/ trimethylammonium (TMA) with balanced charges, and (6) mixed carboxylic acid (CA)/TMA with balanced charges.*

SAMs have also been used to study the interaction of marine organisms and surfaces with different characteristics such as protein resistance, hydration, roughness, and surface energy (38–40). Using OEG- and PEG-based SAMs, the resistance of algal spores correlates well with protein (i.e., fibrinogen) resistance (41). Usually a highly protein-resistant OEG SAM can effectively reduce the settlement density and adhesion strength of algal spores. However, subtle differences have been observed in the response to the SAMs with different terminal groups, a different number of repeat units of ethylene glycol groups, and different packing densities (20, 41). It should be noted that while OEG SAMs on gold can be applied to investigate marine organism interaction, the surfaces are not applicable for long-term applications due to the low stability of OEG and thiol-gold bond, which are known to be susceptible to oxidation.

## 2.2. Polymer Brushes

Polymer brushes are molecular chains with one end attached to a solid surface and the rest of the chain stretched away from the interface. A surface-initiated polymerization can generate a highly packed brush-like structure. The brushes can be composed of polymers with protein-resistant moieties. These include polymers with OEG side chains such as poly(oligo(ethylene glycol) methyl ether methacrylate) (polyOEGMA) (42), zwitterionic polybetaines such as poly(2-methacryloyloxyethyl phosphorylcholine) (polyMPC) (43), poly(sulfobetaine methacrylate) (polySBMA) (44, 45), and poly(carboxybetaine methacrylate) (polyCBMA) (45–47). Scheme 2 demonstrates the preparation of these polymer brushes. Briefly, an alkylthiolate,  $\omega$ -mercaptoundecyl bromoisobutyrate, was applied on a gold substrate, and forms a SAM with head groups as initiators for an atom transfer radical polymerization (ATRP) (48). Then the ATRP was performed to graft monomer from the initiator SAMs (one of the “graft-from” methods). As a living polymerization, ATRP can control the chain length, density, and add a second monomer to create either random polymer brushes or block copolymer brushes. The density, composition, and thickness can be controlled by using this surface-initiated polymerization method (49–51). Like SAMs on gold surfaces, protein adsorption can be detected by SPR, and compared with SAMs and other polymer brushes. Polymer brushes can also be grafted from surfaces other than gold utilizing different chemistries (52–54). In addition to the “graft-from” method via surface-initiated polymerization, polymer brushes can be prepared using a “graft to” method by assembling branched polymers, block copolymers, or polymers with adhesive functional groups on solid substrates (37, 55). Both OEG- and betaine-based polymers have been applied for this method and show high protein resistance (22, 56, 57). However, most polymer brushes from “graft-to” methods generally do not reach the high density of those from “graft-from” methods. Usually less protein resistance was found compared with “graft-from” chemistries.



Scheme 2. Preparation of nonfouling polymer brushes on gold surfaces: polyOEGMA, polyMPC, polySBMA, and polyCBMA.

### 2.3. Copolymers

To apply a protein-resistant polymer on a substrate, one readily achieved way is to combine the polymer with other functional groups. Since protein-resistant polymers are mostly hydrophilic polymers, the additional groups usually are hydrophobic groups and/or crosslinkable groups. These copolymers, when dissolved in a solution, can be easily applied on many substrates. Due to the amphiphilic nature of these copolymers, a phase separation usually happens on the surface during drying. A further curing process may be needed with crosslinkable groups. For PEG-based polymers, random copolymers, block copolymers, and crosslinkable formulations have been prepared to show resistance to some marine organisms (23, 27, 28, 58).

For betaine polymers, copolymers with PC (59, 60), SB (57, 61, 62), and carboxybetaine (63) have been applied on various of surfaces by spin coating or dip coating. A typical example of an applicable betaine coating is a random copolymer with hydrophobic groups and crosslinkable groups (59–61). As shown in Scheme 1, the hydrophobic moieties include a laurel methacrylate, which provides mechanical strength and flexibility. The crosslinkable moiety is 3-(trimethoxysilyl)propyl methacrylate (60, 61), which is likely to have similar reactivity to the other methacrylate monomers in the system. The copolymer can be simply dissolved in organic solvents and applied on many substrates such as metals, glass, and plastics. An optimized formulation with reduction of protein adsorption and bacteria/cell attachment comprise a betaine concentration of ca. 23 mol. %. The PC-based coatings have been tested against a marine organism and demonstrate the reduction of diatom attachment (25).

### 2.4. Comparison of Antifouling Platforms

#### SAMs vs. Polymer Brushes

Both SAMs and polymer brushes can be used as platforms for evaluating nonfouling performance on surfaces. However, polymer brushes usually provide a better protein-resistant performance than SAMs, especially in complex media and in a broad range of pHs and ionic strengths. Five SAMs from Scheme 1

and three polymer brushes from Scheme 2 were tested for their resistance to both fibrinogen adsorption and 100 % plasma adsorption using SPR (Table 2). For fibrinogen adsorption from a 1 mg/mL fibrinogen solution, all five SAMs and three polymer brushes presented high protein resistance. Compared with an adsorption on a unmodified gold (ca. 250 ng/cm<sup>2</sup>), the adsorption on these eight surfaces were extremely low: fibrinogen adsorption was ca. 3.8 ng/cm<sup>2</sup> on PC SAMs, and was lower than 0.3 ng/cm<sup>2</sup> on the other surfaces (0.3 ng/cm<sup>2</sup> is the detection limit of SPR). It was confirmed that surfaces with OEG groups, betaine moieties, or balanced charges can highly resist adsorption from the diluted fibrinogen solution. However, when all these surfaces were challenged with 100 % plasma solution, protein adsorption on all five SAMs significantly increased. Protein adsorption on mixed sulfonic acid (SA)/ (trimethylammonium) TMA SAMs was ca. 251 ng/cm<sup>2</sup>, and on the remaining four SAMs was more than 300 ng/cm<sup>2</sup>. However, the surfaces with polySBMA, polyOEGMA, and polyCBMA brushes had protein adsorption levels from plasma of ca. 9.1 ng/cm<sup>2</sup>, ca. 9.2 ng/cm<sup>2</sup>, and ca. 0.4 ng/cm<sup>2</sup>, respectively. These demonstrate high resistance to protein adsorption for these polymer brushes even from 100% blood plasma (18).

**Table 2. Fibrinogen adsorption from buffer solution and protein adsorption from plasma on five SAMs and three surfaces grafted with polymer brushes as measured with SPR (18)**

Adsorption* (ng/cm <sup>2</sup> )	SAMs					Polymer Brushes		
	OEG	PC	OPC	SA/TMA	CA/TMA	SBMA	CBMA	OEGMA
Fibrinogen	<0.3	3.8±1.9	≤0.3	<0.3	<0.3	<0.3	<0.3	<0.3
Plasma	>300	>300	>300	251.3±12.9	>300	9.1±0.6	0.4±0.9	9.2 ± 6.5

\* Adsorption measured from 1 mg/mL human fibrinogen in PBS buffer (0.15 M and pH 7.4) or from 100% human plasma.

This evidence suggests that two mechanisms may be simultaneously involved to explain the protein-resistant property of these surfaces: water structuring ability and chain conformational entropy. All the molecular units explored in this work have the ability to tightly bind structured water. The tightly bound surface water may be responsible for the reduced protein adsorption at low protein solution concentrations. At high protein concentration, the protein solution may serve as a water structure breaking solvent. Thus, the water structure at the surface of these films is interrupted and only surface layers that would lose chain conformational entropy will continue to resist protein adsorption. These results indicate polymer brushes retain strong protein resistance in a complex medium.



Another advantage of betaine polymer brushes over betaine SAMs is that their protein adsorption is very low in a wide range of ionic strengths. The protein adsorption behavior of betaine polymer brushes is different from that of SB or PC SAMs, which have a much higher protein adsorption at low ionic strengths. It was reported that fibrinogen adsorption on SB-based SAMs and PC-based SAMs is about 88 ML% (percentage of the monolayer covered by the adsorbed proteins) and 48 ML% at an ionic strength of 10 mM, respectively (33), which is much higher than 4.3 ML% on polyCBMA-grafted surfaces (47). For zwitterionic SB or PC SAMs, high protein adsorption at low ionic strengths is attributed to the dipole vectors, which have a perpendicular component to the surface and correspond to a net electric field associated with the dipoles at the SAM surfaces (33, 64). At higher ionic strengths, the net electric field can be reduced due to electrostatic screening effects. Furthermore, polymer brushes provide a much thicker zwitterionic layer and a better chain flexibility than those of SAMs (55). Unlike rigid zwitterionic SAMs, the dipole vectors on polymer pendant groups can be oriented in different directions and the net electric field is reduced. Because of all these factors, protein adsorption on betaine polymer brushes is much lower than that on zwitterionic SAMs at low ionic strengths.

### *Polymer Brushes vs. Random Copolymers*

Protein resistance of polymer brushes and copolymers were also compared (45). Grafting polySBMA brushes on a glass slide has been reported and characterized (Figure 1). Glass substrates were silanized with an ethanol solution containing a silane initiator (BrTMOS). PolySBMA was grafted on the glass slides via ATRP as described previously with a dry thickness of about 10-15 nm (45). In Figure 2, a polySBMA-based copolymer contains SB moieties and hydrophobic and crosslinkable functional groups (Scheme 3). The SB composition for the copolymer used in this study is ca. 23 mol %. Copolymers with higher SB compositions are hard to apply on a glass surface since they tend to gel in the bulk. The polymer was dip-coated on the glass surface with a thickness of ca. 1-2  $\mu\text{m}$ . Figure 1 shows that protein adsorption is reduced to a certain degree ( $40 \pm 13\%$ ) as compared with uncoated surfaces. However, protein adsorption on the polySBMA-based copolymer is still much higher than that on the surface grafted with pure polySB ( $3 \pm 3\%$ ) or polyCB ( $4 \pm 3\%$ ). These results indicate that well-packed betaine brushes can provide a highly protein-resistant surface compared with copolymers, on which the protein resistance is reduced by the hydrophobic moieties.

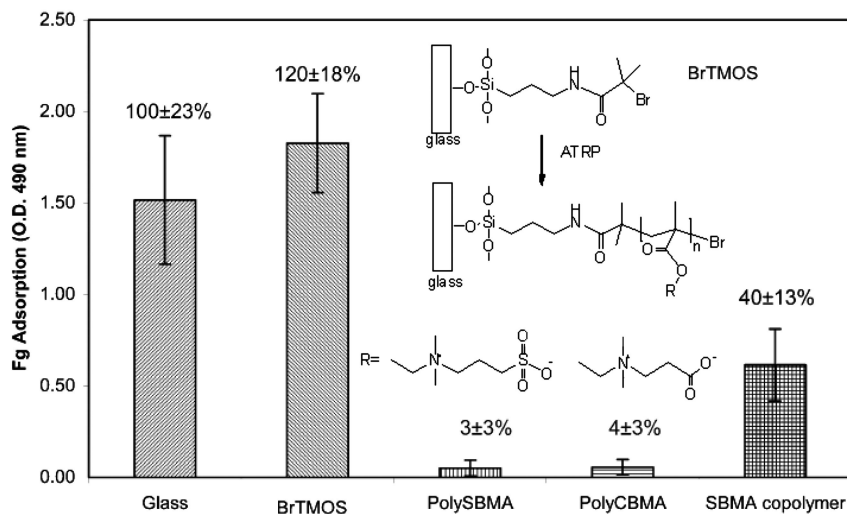
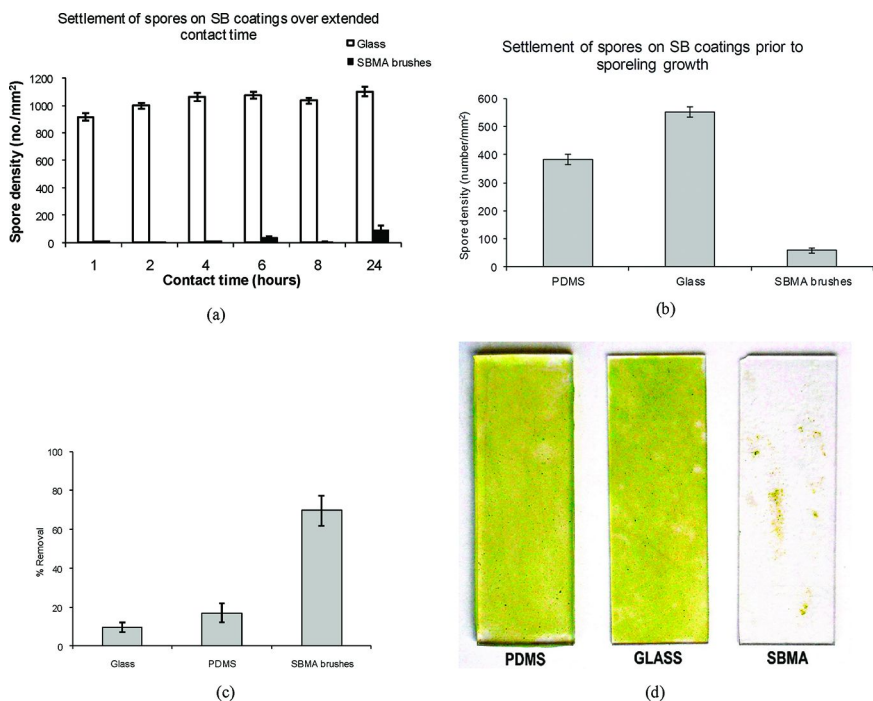
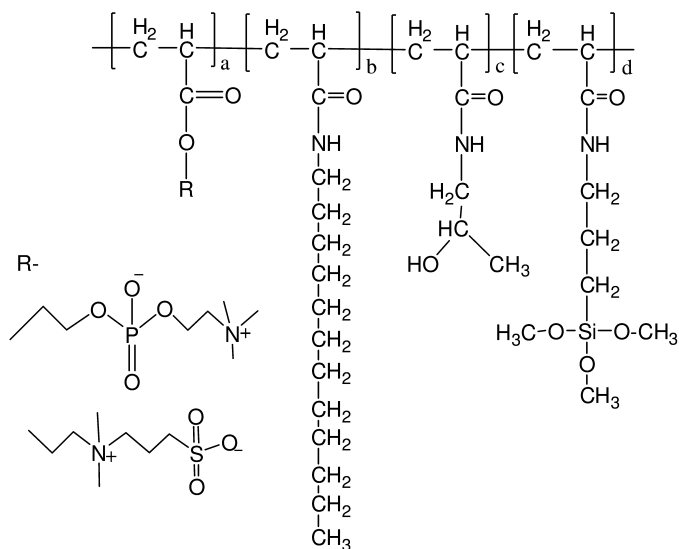


Figure 1. Amounts of adsorbed human fibrinogen (Fg) measured from ELISA. The data on the top of the columns are relative adsorption values (mean  $\pm$ SD %). Glass, BrTMOS silanized glass, glass grafted with polySBMA or polyCBMA via ATRP, and glass dip-coated with a polySBMA-based random copolymer (23 mol % sulfobetaine) were exposed to 1 mg/mL Fg at 37 °C for 90 min ( $n = 4-7$ ). As a reference, the adsorption of Fg on a glass coverslip surface is about 36 ng/cm<sup>2</sup>, and relative Fg adsorption on a PEG-like surface was 4-8% (radiolabeled method) (90).

Table 3 summarizes the three above methods in protein-resistant performance, as a model to evaluate protein resistance, and in applicability at industrial scale. SAMs are a model surface for evaluation of protein resistance, but their protein resistance can decrease in complex media. Copolymers are an applicable as a coating that can be applied to many surfaces. However, the integrated hydrophobic groups will compromise the protein resistance. Polymer brushes provide the best protein resistance in a complex medium and solutions with a broad range of ionic strength. Their long-term performance in resisting marine organisms, stability, and applicability as a coating still need to be further investigated.



**Figure 2.** (a) The settlement of *Ulva* spores on SBMA coatings over a range of contact times. Bars show 95% confidence limits from 90 counts on 3 replicate slides. The density of spores settled after 1, 2, 4, and 8 h contact times was extremely low between 1 and 10/mm<sup>2</sup>. (b) Settlement of spores on PDMS-coated slides, bare glass slides, and polySBMA-grafted slides before growth and transformation into sporelings. (c) The removal of *Ulva* spores from SBMA coatings after a contact time of 6 hours. Settled spores were subjected to a water jet creating a surface pressure of 63 kPa. Bars show 95% confidence limits derived from arcsine transformed data from 90 counts from 3 replicate slides. (d) Biomass of sporelings on different surfaces after a 6-day growth. From left: a PDMS-coated slide, a bare glass slide, and a polySBMA-grafted glass slide (26).



Scheme 3. A typical betaine-based copolymer formulation ( $a=0.23$ ,  $b=0.47$ ,  $c=0.25$ ,  $d=0.05$ ). (61)

**Table 3. Comparison of three model protein-resistant surfaces**

	<i>Performance of protein resistance</i>	<i>As a model to evaluate protein resistance</i>	<i>Applicable at industrial scale</i>
SAMs	++	++	+
Polymer Brushes	+++	+++	++
Copolymers	+	+	+++

### 3. Performance of Sulfobetaine-Based Polymers in Resisting Marine Fouling

When grafted under controlled conditions, SB-based polymer brushes have imparted superior protein resistance to existing antifouling surfaces on various substrates and in complex media (18, 44, 45, 65). The nonfouling properties of SB-grafted surfaces are attributed to an engineered surface polymer structure that provides, amongst other things, a high degree of hydration. Because of their superior nonfouling properties, the SB-modified surfaces can also highly resist bacteria attachment and biofilm formation (66). PolySB brushes present protein resistance within a broad range of pH and ionic strengths. Additionally,

the SB-based modifications are significantly more stable than other reported fouling-resistant coatings, including some PC- and PEG-based polymers that could be hydrolyzed and/or auto-oxidized. Altogether, these advantages rank polySB brushes among the most promising candidates for providing resistance to marine organisms and stability.

### 3.1. SB-Based Polymers Highly Resist the Growth of *Ulva* Sporelings and Reduce Strength of Sporeling Attachment

The settlement of green algal (*Ulva linza*) zoospores, growth of spores and sporelings, and attachment strength of spores were evaluated as described previously (26, 67). Spore settlement was evaluated on bare glass slides and polySBMA-grafted slides (45). Figure 2a shows that the density of attached spores recorded on the polySBMA-grafted surfaces was extremely low (between 1 and 33 /mm<sup>2</sup>) over 1-8 hours of contact time. At 24 hours the settlement density had increased to 88 /mm<sup>2</sup>, still less than 10% of the settlement density on glass (i.e., close to 1000 /mm<sup>2</sup>). The spore settlement densities for glass slides, polydimethylsiloxane (PDMS)-coated slides and polySBMA-grafted slides are shown in Figure 2b. PDMS is used as a model surface for “fouling release” coatings. The data show the densities of the precursors of the sporelings, which are much lower on polySBMA-grafted surfaces than those on glass or PDMS coatings. The strength of the attachment of those spores was examined for the 6-hour contact time sample and is shown in Figure 2c. Bare glass and PDMS were used as references. Although the settlement density of spores on polySBMA-grafted surfaces was very low, the removal efficacy was very high. The removal at 63 kPa was approximately 66% from the SBMA coating, while at the same pressure it was less than 20% from PDMS.

Biomass of sporelings was compared on different surfaces including PDMS-coated slides, bare glass slides, and polySBMA-grafted glass slides after a 6-day growth (Figure 2d). As shown in Figure 2d, the growth of sporelings on the SBMA coatings was low due to the extremely low spore attachment and high spore removal. Since disturbing the coating caused the sporelings to detach, the amount of biomass could not be quantified. However, it was evident that biomass was much lower on polySBMA-grafted surfaces than on glass or PDMS coatings. It was found that any movement of the dishes caused sporelings to be detached from the SBMA coatings. The attachment of the plants was extremely weak and detachment would almost certainly have been 100% at the lowest pressure attainable using the water jet (ca. 20 kPa).

Durable spore attachment involves the transition from a free-swimming spore to an adhered non-motile spore. During this process a polydisperse glycoprotein is secreted from the free-swimming spore, which is crosslinkable and capable of strongly adhering. A surface highly resistant to protein adhesion is thought to also resist the attachment of algal spores. However, it has been reported that the adhesive spreads more on hydrophilic surfaces (38, 39). The adhesion strength of the settled spores, as measured by resistance to detachment in a turbulent flow cell, was greatest on a hydrophilic surface (67–69). Not like other hydrophilic

surfaces, polySBMA exhibits both low spore attachment and high spore removal. The mechanism of the phenomenon is still in the process of study (26).

### 3.2. SB-Based Polymers Highly Resist Settlement of Diatom Cells

Diatom cells of *Navicula perminuta* were cultured in F/2 medium contained in 250 mL conical flasks as described (68). Such diatom cells are not motile in the water column and cannot “choose” where to settle. In the laboratory assays they reach the surface by way of gravity. Most cells land on their sides with their girdles adjacent to the substratum, before pulling themselves up so that the raphe(s), through which extracellular polymeric substances (EPS) are secreted, are firmly attached to the substratum. This process and subsequent gliding motility involves an adhesion complex, which provides a connection between the extracellular adhesive strands of EPS and the actin-myosin system in the cell (70).

The number of diatom cells associated with the polySBMA surface after gentle water washing was low (15%) compared to the density on glass (Fig 3a). As reported for spores of *Ulva*, a slight disturbance of the assay dish caused cells to detach from the surface of the polySBMA coating. The detached cells formed clumps due to cell-cell adhesion. Coatings on which cells were cultured for 8 days showed a dense covering of cells on the surface of both glass and polySBMA when observed *in situ*. On glass, the biofilm was undisturbed by placement of the dish on the microscope stage, compared to the extensive clumping of cells seen on polySBMA.

*In situ* observations of cells of a larger species of diatom, *Craspedostaurus australis*, up to one hour after the addition of cells onto the test surfaces indicated that the cells on polySBMA could not adjust their position or move as freely as they could on glass or PDMS. On the polySBMA surface, a smaller proportion of cells were able to physically orientate themselves and move into a position in which the raphe contacted the surface. Out of observations made of one hundred individual cells, only 18 were able to move on the polySBMA surface compared to 65 on glass and 63 on a polydimethylsiloxane elastomer. Of the 18 cells showing movement on the polySBMA, only 6 were able to glide in a normal manner, the rest were restricted to a shunting action resulting in a slower rate of progression than on glass (26).

### 3.3. SB-Based Polymers Highly Resist Settlement of Barnacle Cyprids

Barnacle cyprids (*Balanus amphitrite*) were batch cultured and tracked by video to measure pre-settlement behavior in cyprids (71, 72). Cyprids were introduced to polystyrene Petri dishes containing artificial seawater (ASW) and SB-modified glass discs. The results of settlement assays are presented in Figure 3b. All surfaces with SBMA polymer brushes had zero settlement after 48 hours with all cyprids remaining visually healthy and exhibiting normal behavior. By comparison, the glass control surfaces had 16% settlement of cyprids after 48 hours and the 24-well plate 20% settlement. This control settlement is not high; around 30–40% settlement would be expected and the overall low settlement in this assay can be attributed to batch variation in the cyprid culture. Although

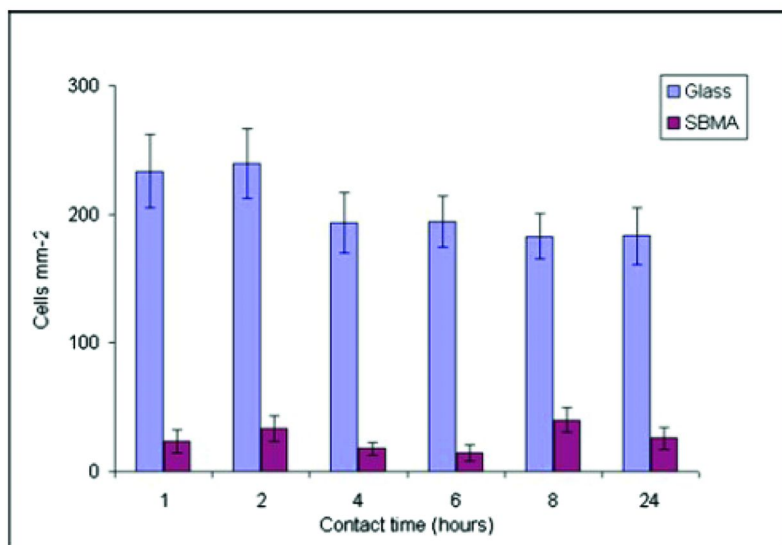
statistics could not be used to compare mean settlement values when one of the values is zero (which rarely happens with cyprid assays), it seems that the SB-modified surfaces effectively prevent settlement over 48 hours in the laboratory, without invoking any detectable toxic/narcotic effect.

The pre-settlement behavior in cyprids was tracked with video tracking (data not shown). Two parameters, meander (sinuosity of the track) and distance moved, were significantly different between surfaces, with mean turn angle also being close to significance. No other parameters including mean velocity and angular velocity approached significance at the 95% confidence level. With a higher total distance moved and lower meander, the data suggested that cyprids spent significantly more time swimming and engaging in non-exploratory behavior on the modified samples. The lower mean turn angle on SBMA surfaces reinforced this hypothesis suggesting that cyprid movement was predominantly unidirectional with little or no exploratory behavior. These data could be interpreted as suggesting that polySBMA treatment of a glass surface significantly reduces exploration by cyprids on that surface.

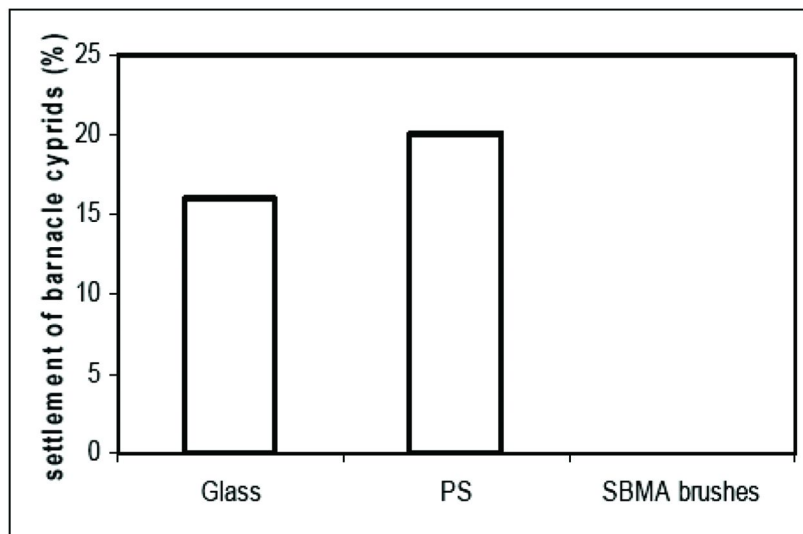
### 3.4. Stability of SB-Based Polymers and Their Antifouling Performance in Complex Media

The stability on a polySBMA-grafted polyurethane substrate was evaluated. The sample was incubated with PBS (150 mN, pH 7.4), 50% fetal bovine serum (FBS), or 100% citrated human plasma (CHP) for periods of up to 90 days, and the resistance of protein adsorption and bacterial attachment/biofilm formation were evaluated. Protein adsorption was measured using a radiolabeling method. The sample was exposed to 300  $\mu$ L of a 70  $\mu$ g/ml unlabeled fibrinogen solution containing 1.4  $\mu$ g/mL I-125 radiolabeled fibrinogen. Reduction in microbial adherence was measured using a modified CDC biofilm reactor. Following pre-incubation, samples were adjusted to ensure equal exposure to bacterial suspension. The samples were incubated in the solution at 37 °C for 2 hours under stirring. Then samples were removed to a new reactor, followed by surface growth at a flow rate of 8 mL/min at 37 °C for 22 hours. Accumulated bacteria (*Escherichia coli*) on materials were numbered through dilution plating.

The results exhibited the stability of SB modifications in both protein resistance after PBS storage for 100 days (Figure 4a) and anti-colonization activity after PBS storage for 112 days (Figure 4b). Antimicrobial assay showed ca. 99% reduction in colonization after 50% FBS serum exposure from one to 90 days of 50% FBS (Figure 4c). These results demonstrated a surface modification capable of significantly reducing bacterial biofilm after long-term (90 day) exposure to complex media, indicating a long-term stability and antifouling performance of the SB-based polymers.



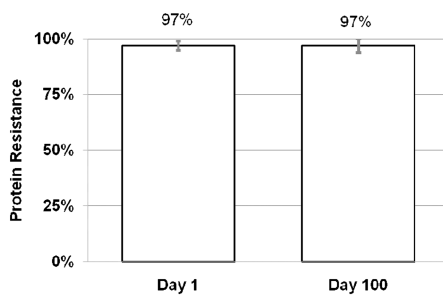
(a)



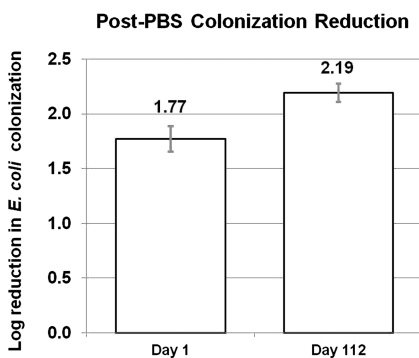
(b)

Figure 3. (a) The number of cells of the diatom *Navicula* attached to the polySBMA coating and glass over a range of contact times. Bars show 95% confidence limits from 30 counts on single slides (26). (b) Settlement of barnacle cyprids on glass, polystyrene (PS), and polySBMA-grafted glass after 48 hours.

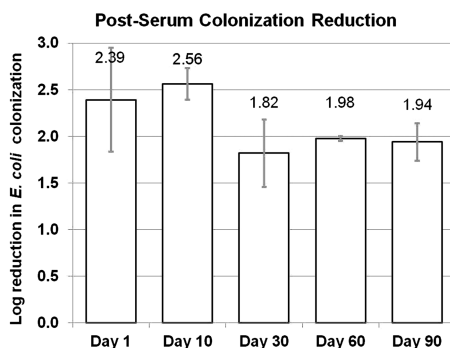




(a)



(b)



(c)

Figure 4. (a) Constant protein resistance after PBS storage for 100 days, (b) constant anti-colonization activity after PBS storage for 112 days, and (c) antimicrobial assay shows ca. 99% reduction in colonization after 50% FBS serum exposure from one to 90 days.

### 3.5. SB-Based Polymers Are Non-Toxic to Marine Organisms and Mammalian Cells

SB-modified glass substrates had not exhibited any toxicity to green alga, diatom, and barnacle cyprid in previous experiments. In addition, linear SBMA polymers with different molecular weights were synthesized (73). Three linear SBMA polymers with different molecular weights were prepared as described above. A toxicity assay was performed on three polySBMA polymers with molecular weights of 20.9, 169, and 203 kDa to establish whether the low number of spores and sporelings associated with the polySBMA brushes was due to loss of viability. Spores germinated and grew normally in all three concentrations (50, 500, and 5000 mg L<sup>-1</sup>) of the polySBMA polymers, and the amount of biomass after 4 days was not significantly different than that in the seawater control wells (data not shown), indicating the SBMA polymers at concentrations up to 5000 mg/L had no biocidal effect (26).

SB-based hydrogels were prepared per our previous publications (46, 73). For example, a typical transparent SBMA hydrogel was prepared by polymerizing SBMA monomer with tetraethylene glycol dimethacrylate (TEGDMA) through free radical polymerization initiated by sodium metabisulfite and ammonium persulfate. All compositions in the indicated studies were tested for their cytotoxicity and endotoxin level. All hydrogels prepared were found to be non-cytotoxic and contain less than 0.06 units (EU)/mL of endotoxin using a Limulus Amebocyte Lysate (LAL) endotoxin assay kit. Thus, these zwitterionic hydrogels were nontoxic to mammalian cells and acceptable for *in vivo* implantation (74). The SB-based polymers were also blood compatible and showed no sign of negative effect to blood clotting time, hemolysis, and complement activation.

## 4. Structural Design of Betaine Polymers as Antifouling Marine Coatings

For betaine polymers to be applied as a marine coating, more material characteristics need to be considered, such as chemical/physical stabilities, mechanical properties, coating applicability, and performance under different environmental factors (e.g., salinity, temperature, mineral deposition, and pH). A rational design is needed to choose the proper betaine moieties, linking groups, main chains, and spacer groups. Moreover, some betaine polymers can be tailored to incorporate other antifouling designs, which include immobilizing antifouling agents, self-polishing surfaces by degradation/hydrolysis, releasing fouling substance through shear force, and releasing antifouling agents. The designed betaine polymers and their derivatives are expected to enhance antifouling performance through a synergetic effect.

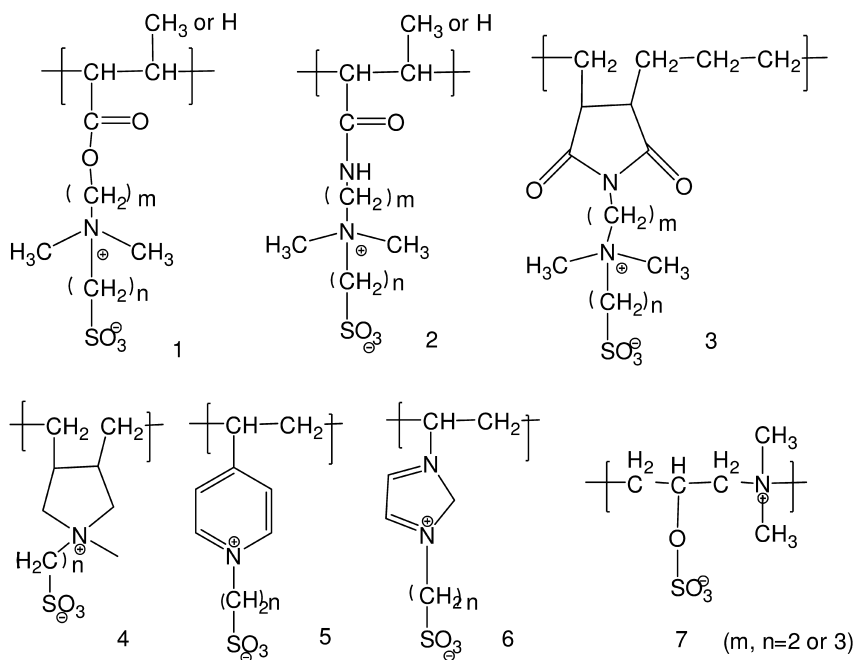
As shown in previous sections, highly protein-resistant betaine polymers include SB-, CB-, and PC-based polymers. All of them have exhibited resistance to attachment of marine organisms or biofilm formation. The SB-based polymers have activity in a broad range of pH, stability in complex media and long-term

efficacy. PolyCB, with its functionalizable pendant groups, can be designed for a coating immobilized with active agents. PC-based polymers with hydrolyzable phosphate esters may find some application in agent release coatings.

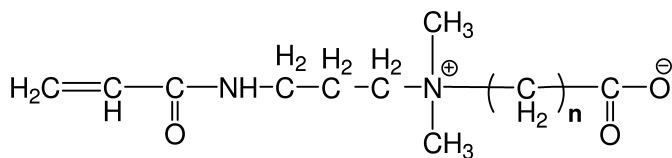
#### 4.1. Design Backbones, Linking Groups, and Spacer Groups of Betaine Polymers

The backbones of betaine polymers and the linking groups that connect the betaine groups determine the physical and mechanical properties, hydrolytic and chemical stability, and protein resistance. SB-based polymers, for example, can be designed with various linkage groups and backbones. Scheme 4 demonstrates some examples of different SB-based polymers including poly(meth)acrylates (1), poly(meth)acrylamides (2), derivatives from maleic anhydride copolymers (3), polypyrrolidiniums (4), polyvinylpyridiums (5), polyvinylimidazoliums (6), and zwitterionic polyionenes (7). It was reported that some of these polymers with different structures present different solution properties (viscosity and hydration ability) and bulk properties (thermal and physical properties) (75–78). Based on these observations, polymers with desired properties can be designed. For example, acrylamide was regarded to be more hydrolytically stable than polymethacrylate, and changing from methacrylate to acrylamide will have little effect on protein resistance (47, 79). A more hydrolytically stable coating can be designed based on acrylamides. For mechanical properties, many betaine hydrogels are fragile. It was shown that introduction of a vinylimidazole backbone improves tensile and compressive properties of the SB-based hydrogel by an order of magnitude over the same properties of a methacrylate hydrogel. The presence of the imidazole groups does not compromise the nonfouling properties attributed to the zwitterionic SB groups (80).

For a betaine moiety, there is a spacer group between the positive and the negative charges. By varying the spacer group, the hydrophobicity, pKa, and the reactivity of the betaine group can be changed. These are related to protein resistance, mechanical properties, and the response to ionic strength and pH. It was reported that the properties of CB groups depend on their spacer groups between the positive quaternary amine groups and the negative carboxyl groups. In this work, four polyCB acrylamides (polyCBAAAs) with different spacer groups were synthesized (Scheme 5,  $n=1, 2, 3, 5$ ). Although protein adsorption tended to increase at low ionic strength and low pH value, it was still very low for polyCBs with a methylene, an ethylene, or a propylene spacer group, but more pronounced for polyCBAA with a longer spacer group (i.e., a pentene group). The response to ionic strengths and pH values can be attributed to the antipolyelectrolyte (or “salt-in”) behavior and protonation/deprotonation of polyCBs, respectively. Both of these properties are related to the spacer groups of CBs (47).



*Scheme 4. Examples of sulfobetaine-based polymers with different pendant groups and main chains including (1) poly(meth)acrylates, (2) poly(meth)acrylamides, (3) derivatives from maleic anhydride copolymers, (4) polypyrrolidiniums, (5) polyvinylpyridiums, (6) polyvinylimidazoliums, and (7) zwitterionic polyionenes.*



*Scheme 5. Monomer of poly(carboxybetaine acrylamide) (polyCBAA). Protein resistance, pKa, and hydrophobicity changes when n were changed from 1 to 5. The carboxylic groups can be functionalized on polyCBAA using NHS/EDC chemistry to bind active agents.*

## 4.2. Functionalizable Betaine Polymers

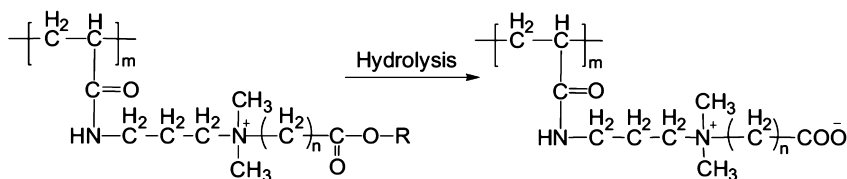
It was reported that some active agents and groups can be covalently bound on a surface and resist the settlement of biofilm and marine organisms. These active agents include compounds with biocidal groups, antifouling enzymes and peptides, and anti-colonization agents (9, 81, 82). A nonfouling background may be needed to keep constant bioactivity by resisting nonspecific adsorption. Protein-

resistant polymers, such as PEG and polyMPC, must add some functional groups to immobilize ligands, and these extra groups can increase protein adsorption.

Carboxybetaine polymers not only highly resist protein adsorption/cell adhesion, but also have abundant functional groups (carboxylic groups) convenient for the immobilization of various ligands. This treatment was first demonstrated on a CB-based polymer brush and a crosslinked CB-based hydrogel (46). Using a bioconjugate chemistry, such as ethyl(dimethylaminopropyl) carbodiimide /*N*-hydroxysuccinimide (EDC/NHS) chemistry, the unfunctionalized groups could be returned back to a nonfouling CB group. Various ligands, such as proteins and antibodies, were immobilized on the surfaces with controlled concentrations and coverage (83, 84). The surface grafted with polyCB prevented the nonspecific adsorption of proteins, even in 100% plasma, and still showed strong function of immobilized antibodies and proteins. Zwitterionic CB-based surface has unique “dual functionality” for ligand immobilization on a nonfouling background and is promising for designing marine coatings with active agents.

### 4.3. Hydrolyzable Betaine Polymers

A novel derivative of CB-based polymer, polycarboxybetaine ester, was designed as a convertible coating from a biocidal surface to a nonfouling surface by releasing the foulants from the surface (85). The antimicrobial poly(carboxybetaine ester) can be converted to a nontoxic and nonfouling zwitterionic polymer upon its hydrolysis (Scheme 6). In the first proof-of concept research, three positively charged polyacrylamides, of which the pedant groups bear carboxybetaine ester groups, were synthesized. These three polymers have different spacer groups between the quaternary ammonium and the ester groups. Their interactions with biomolecules and micro-organisms before and after hydrolysis were demonstrated by protein adsorption/resistance and antimicrobial properties. The poly(carboxybetaine ester) with a pentene spacer exhibited evident antimicrobial properties when it is incubated with one of Gram negative bacteria (*Escherichia coli*). After hydrolysis, the surfaces became nonfouling (85). Based on this design, more surfaces have been developed and the hydrolysis rates can be controlled by employing different ester groups (86).



*Scheme 6. Hydrolysis of cationic poly(carboxybetaine ester) to zwitterionic polycarboxybetaine. The antimicrobial poly(carboxybetaine ester) can be converted to a nontoxic and nonfouling zwitterionic polymer upon its hydrolysis (85).*

Unlike hydrophilic polyCBs, the poly(carboxybetaine ester) can be a hydrophobic polymer, which means that the polymer can be applied as a normal coating dissolved in organic solution given appropriate mechanical properties (85). The cationic polymers can turn into nonfouling polyCBs after hydrolysis, leaving no toxic residues in the environment or dead microbes on the surface. This work demonstrates that the biological properties of the cationic polycarboxybetaine esters can be dramatically changed by controlling their hydrolysis, making them a promising candidate for antifouling and antimicrobial coatings.

#### 4.4. Releasing Incorporated Active Agents from Betaine Polymers

Environmentally benign antifouling active agents can be formulated within a coating and released by diffusing from the surface into the water. These compounds include organic biocides, enzymes, and some natural marine products (87). While there has been little study of releasing active agents from a betaine-based marine coatings, some coatings used as medical device or drug delivery carriers have applied betaine-based polymers as reservoirs for active agents. Extensive experience with PC-coated medical devices supports its biocompatibility, protein/cell resistance, and stability in complex media. These characteristics, together with its ability to load and release a variety of active agents, provide the ability of both antifouling and drug release capabilities (88). Unlike other hydrophilic polymers, polybetaines have an anti-polyelectrolyte behavior, or “salt-in” behavior, which means the polymers tend to keep salts within their molecular structures. Due to this unique saltphilic property of the zwitterionic betaine, polybetaine can also be used to entrap salt-based agents and release them in the presence of ions. It was reported that a polySB copolymer was investigated as a sustained drug release matrix, and the release of the active agent could be controlled by copolymer composition and environmental ionic strength (89). All the previous experience in medical device coatings showed that it is reasonable to add antifouling reagents in betaine-based marine formulations.

## 5. Conclusions

Marine biofouling can be reduced by applying a protein-resistant modification on a surface to perform underwater. Protein resistance was analyzed by comparing surfaces modified with various functional groups and polymers. The protein-resistant surfaces were prepared based on SAMs, polymer brushes, and copolymers, of which surfaces grafted with polybetaine brushes were among the most protein resistance surfaces, especially in complex environments. SB-based polymer brushes were grafted on glass surfaces and showed strong resistance to the attachment of green algae, diatoms, and barnacle cyprids. The surfaces also presented long-term performance in saline and complex protein media and demonstrated biocompatibility to marine organisms and mammalian cells.

As a marine coating, the polymer structure and formulation must meet requirements for mechanical and chemical stability, applicability, and antifouling

performance during the full life service of the coating. Betaine-based polymers can be structurally designed to improve their properties based on backbones, linking groups, and spacer groups. To enhance the antifouling performance, betaine polymers can be tailored to integrate other antifouling designs, such as active agent immobilization, self-polishing foulant release, and active agent release.

## Acknowledgments

We acknowledge the financial support provided by the Department of Energy, USA (DE-EE0004566). The authors wish to thank Rahul Bose for his help in the writing of this chapter.

## References

1. Schultz, M. P. *Biofouling* **2007**, *23*, 331–341.
2. Miller, V. B.; Schaefer, L. A. *J. Fluids Eng.* **2010**, *132*.
3. Delauney, L.; Compere, C.; Lehaitre, M. *Ocean Sci.* **2010**, *6*, 503–511.
4. Kerr, A.; Cowling, M. J.; Beveridge, C. M.; Smith, M. J.; Parr, A. C. S.; Head, R. M.; Davenport, J.; Hodgkiess, T. *Environ. Int.* **1998**, *24*, 331–343.
5. Kiil, S.; Weinell, C. E.; Pedersen, M. S.; Dam-Johansen, K. *Ind. Eng. Chem. Res.* **2001**, *40*, 3906–3920.
6. Evans, L. V.; Clarkson, N. *J. Appl. Bacteriol.* **1993**, *74*, S119–S124.
7. Chambers, L. D.; Stokes, K. R.; Walsh, F. C.; Wood, R. J. K. *Surf. Coat. Technol.* **2006**, *201*, 3642–3652.
8. Banerjee, I.; Pangule, R. C.; Kane, R. S. *Adv. Mater.* **2011**, *23*, 690–718.
9. Dobretsov, S.; Teplitski, M.; Paul, V. *Biofouling* **2009**, *25*, 413–427.
10. Clare, A. S. *J. Mar. Biotechnol.* **1998**, *6*, 3–6.
11. Abelson, A.; Denny, M. *Annu. Rev. Ecol. Syst.* **1997**, *28*, 317–339.
12. Lasa, I.; Penades, J. R. *Res. Microbiol.* **2006**, *157*, 99–107.
13. Callow, J. A.; Callow, M. E. In *Biological Adhesives*; Smith, A. M., Callow, J. A., Eds.; Springer: Berlin, 2006; pp 63–78.
14. Clare, A. S.; Freet, R. K.; McClary, M. *J. Mar. Biol. Assoc. U. K.* **1994**, *74*, 243–250.
15. Callow, J. A.; Callow, M. E. *Nature Commun.* **2011**, *2*.
16. Otsuka, H.; Nagasaki, Y.; Kataoka, K. *Adv. Drug Delivery Rev.* **2003**, *55*, 403–419.
17. Ishihara, K.; Oshida, H.; Endo, Y.; Ueda, T.; Watanabe, A.; Nakabayashi, N. *J. Biomed. Mater. Res.* **1992**, *26*, 1543–52.
18. Zhang, Z.; Zhang, M.; Chen, S. F.; Horbett, T. A.; Ratner, B. D.; Jiang, S. Y. *Biomaterials* **2008**, *29*, 4285–4291.
19. Cowling, M. J.; Hodgkiess, T.; Parr, A. C. S.; Smith, M. J.; Marrs, S. J. *Science Total Environ.* **2000**, *258*, 129–137.
20. Schilp, S.; Kueller, A.; Rosenhahn, A.; Grunze, M.; Pettitt, M. E.; Callow, M. E.; Callow, J. A. *Biointerphases* **2007**, *2*, 143–150.

21. Statz, A.; Finlay, J.; Dalsin, J.; Callow, M.; Callow, J. A.; Messersmith, P. B. *Biofouling* **2006**, *22*, 391–399.
22. Krishnan, S.; Ayothi, R.; Hexemer, A.; Finlay, J. A.; Sohn, K. E.; Perry, R.; Ober, C. K.; Kramer, E. J.; Callow, M. E.; Callow, J. A.; Fischer, D. A. *Langmuir* **2006**, *22*, 5075–5086.
23. Krishnan, S.; Wang, N.; Ober, C. K.; Finlay, J. A.; Callow, M. E.; Callow, J. A.; Hexemer, A.; Sohn, K. E.; Kramer, E. J.; Fischer, D. A. *Biomacromolecules* **2006**, *7*, 1449–1462.
24. Weinman, C. J.; Finlay, J. A.; Park, D.; Paik, M. Y.; Krishnan, S.; Sundaram, H. S.; Dimitriou, M.; Sohn, K. E.; Callow, M. E.; Callow, J. A.; Handlin, D. L.; Willis, C. L.; Kramer, E. J.; Ober, C. K. *Langmuir* **2009**, *25*, 12266–12274.
25. Li, Y.; Liu, C. M.; Yang, J. Y.; Gao, Y. H.; Li, X. S.; Que, G. H.; Lu, J. R. *Colloids Surf., B* **2011**, *85*, 125–130.
26. Zhang, Z.; Finlay, J. A.; Wang, L.; Gao, Y.; Callow, J. A.; Callow, M. E.; Jiang, S. *Langmuir* **2009**, *25*, 13516–13521.
27. Rosenhahn, A.; Schilp, S.; Kreuzer, H. J.; Grunze, M. *Phys. Chem. Chem. Phys.* **2010**, *12*, 4275–4286.
28. Ekblad, T.; Bergstroem, G.; Ederth, T.; Conlan, S. L.; Mutton, R.; Clare, A. S.; Wang, S.; Liu, Y. L.; Zhao, Q.; D'Souza, F.; Donnelly, G. T.; Willemsen, P. R.; Pettitt, M. E.; Callow, M. E.; Callow, J. A.; Liedberg, B. *Biomacromolecules* **2008**, *9*, 2775–2783.
29. Chapman, R. G.; Ostuni, E.; Takayama, S.; Holmlin, R. E.; Yan, L.; Whitesides, G. M. *J. Am. Chem. Soc.* **2000**, *122*, 8303–8304.
30. Ostuni, E.; Chapman, R. G.; Holmlin, R. E.; Takayama, S.; Whitesides, G. M. *Langmuir* **2001**, *17*, 5605–5620.
31. Prime, K. L.; Whitesides, G. M. *J. Am. Chem. Soc.* **1993**, *115*, 10714–10721.
32. Tegoulia, V. A.; Rao, W. S.; Kalambur, A. T.; Rabolt, J. R.; Cooper, S. L. *Langmuir* **2001**, *17*, 4396–4404.
33. Holmlin, R. E.; Chen, X. X.; Chapman, R. G.; Takayama, S.; Whitesides, G. M. *Langmuir* **2001**, *17*, 2841–2850.
34. Chen, S. F.; Yu, F. C.; Yu, Q. M.; He, Y.; Jiang, S. Y. *Langmuir* **2006**, *22*, 8186–8191.
35. Luk, Y.-Y.; Kato, M.; Mrksich, M. *Langmuir* **2000**, *16*, 9604–9608.
36. Li, L.; Chen, S.; Zheng, J.; Ratner, B. D.; Jiang, S. *J. Phys. Chem. B* **2005**, *109*, 2934–2941.
37. Michel, R.; Pasche, S.; Textor, M.; Castner, D. G. *Langmuir* **2005**, *21*, 12327–12332.
38. Callow, M. E.; Callow, J. A.; Ista, L. K.; Coleman, S. E.; Nolasco, A. C.; Lopez, G. P. *Appl. Environ. Microbiol.* **2000**, *66*, 3249–3254.
39. Ista, L. K.; Callow, M. E.; Finlay, J. A.; Coleman, S. E.; Nolasco, A. C.; Simons, R. H.; Callow, J. A.; Lopez, G. P. *Appl. Environ. Microbiol.* **2004**, *70*, 4151–4157.
40. Ederth, T.; Pettitt, M. E.; Nygren, P.; Du, C. X.; Ekblad, T.; Zhou, Y.; Falk, M.; Callow, M. E.; Callow, J. A.; Liedberg, B. *Langmuir* **2009**, *25*, 9375–9383.



41. Schilp, S.; Rosenhahn, A.; Pettitt, M. E.; Bowen, J.; Callow, M. E.; Callow, J. A.; Grunze, M. *Langmuir* **2009**, *25*, 10077–10082.
42. Ma, H.; Hyun, J.; Stiller, P.; Chilkoti, A. *Adv. Mater.* **2004**, *16*, 338–341.
43. Feng, W.; Brash, J.; Zhu, S. *J. Polym. Sci., Part A: Polym. Chem.* **2004**, *42*, 2931–2942.
44. Zhang, Z.; Chen, S.; Chang, Y.; Jiang, S. *J. Phys. Chem. B* **2006**, *110*, 10799–10804.
45. Zhang, Z.; Chao, T.; Chen, S.; Jiang, S. *Langmuir* **2006**, *22*, 10072–10077.
46. Zhang, Z.; Chen, S. F.; Jiang, S. Y. *Biomacromolecules* **2006**, *7*, 3311–3315.
47. Zhang, Z.; Vaisocherova, H.; Cheng, G.; Yang, W.; Xue, H.; Jiang, S. *Biomacromolecules* **2008**.
48. Jones, D. M.; Huck, W. T. S. *Adv. Mater.* **2001**, *13*, 1256–1259.
49. Matyjaszewski, K.; Miller, P. J.; Shukla, N.; Immaraporn, B.; Gelman, A.; Luokala, B. B.; Siclovan, T. M.; Kickelbick, G.; Vallant, T.; Hoffmann, H.; Pakula, T. *Macromolecules* **1999**, *32*, 8716–8724.
50. Jones, D. M.; Brown, A. A.; Huck, W. T. S. *Langmuir* **2002**, *18*, 1265–1269.
51. Bernards, M. T.; Cheng, G.; Zhang, Z.; Chen, S.; Jiang, S. *Macromolecules* **2008**, *41*, 4216–4219.
52. Xu, J.; Yuan, Y.; Shan, B.; Shen, J.; Lin, S. *Colloids Surf., B* **2004**, *35*, 259.
53. Zhang, J.; Yuan, Y.; Wu, K.; Shen, J.; Lin, S. *Colloids Surf., B* **2003**, *28*, 1–9.
54. Yuan, J.; Chen, L.; Jiang, X.; Shen, J.; Lin, S. *Colloids Surf., B* **2004**, *39*, 87–94.
55. Milner, S. T. *Science* **1991**, *251*, 905–914.
56. Bergstroem, K.; Holmberg, K.; Safran, A.; Hoffman, A. S.; Edgell, M. J.; Kozlowski, A.; Hovanes, B. A.; Harris, J. M. *J. Biomed. Mater. Res.* **1992**, *26*, 779–90.
57. Chang, Y.; Chen, S. F.; Zhang, Z.; Jiang, S. Y. *Langmuir* **2006**, *22*, 2222–2226.
58. Gudipati, C. S.; Finlay, J. A.; Callow, J. A.; Callow, M. E.; Wooley, K. L. *Langmuir* **2005**, *21*, 3044–3053.
59. Lewis, A. L. *Colloids Surf., B* **2000**, *18*, 261–275.
60. Lewis, A. L.; Cumming, Z. L.; Goreish, H. H.; Kirkwood, L. C.; Tolhurst, L. A.; Stratford, P. W. *Biomaterials* **2001**, *22*, 99–111.
61. West, S. L.; Salvage, J. P.; Lobb, E. J.; Armes, S. P.; Billingham, N. C.; Lewis, A. L.; Hanlon, G. W.; Lloyd, A. W. *Biomaterials* **2003**, *25*, 1195–1204.
62. Lowe, A. B.; Vamvakaki, M.; Wassall, M. A.; Wong, L.; Billingham, N. C.; Armes, S. P.; Lloyd, A. W. *J. Biomed. Mater. Res.* **2000**, *52*, 88–94.
63. Kitano, H.; Tada, S.; Mori, T.; Takaha, K.; Gemmei-Ide, M.; Tanaka, M.; Fukuda, M.; Yokoyama, Y. *Langmuir* **2005**, *21*, 11932–11940.
64. Chen, S. F.; Zheng, J.; Li, L. Y.; Jiang, S. Y. *J. Am. Chem. Soc.* **2005**, *127*, 14473–14478.
65. Ladd, J.; Zhang, Z.; Chen, S.; Hower, J. C.; Jiang, S. *Biomacromolecules* **2008**, *9*, 1357–1361.
66. Cheng, G.; Zhang, Z.; Chen, S.; Bryers, J. D.; Jiang, S. *Biomaterials* **2007**, *28*, 4192–4199.

67. Callow, J. A.; Callow, M. E.; Ista, L. K.; Lopez, G.; Chaudhury, M. K. *J. R. Soc., Interface* **2005**, *2*, 319–325.
68. Casse, F.; Stafslie, S. J.; Bahr, J. A.; Daniels, J.; Finlay, J. A.; Callow, J. A.; Callow, M. E. *Biofouling* **2007**, *23*, 121–130.
69. Finlay, J. A.; Callow, M. E.; Ista, L. K.; Lopez, G. P.; Callow, J. A. *Integr. Comp. Biol.* **2002**, *42*, 1116–1122.
70. Molino, P. J.; Wetherbee, R. *Biofouling* **2008**, *24*, 365–379.
71. Hellio, C.; Marechal, J.-P.; Veron, B.; Bremer, G.; Clare, A. S.; Le Gal, Y. *Mar. Biotechnol.* **2004**, *6*, 67–82.
72. Marechal, J.-P.; Hellio, C.; Sebire, M.; Clare Anthony, S. *Biofouling* **2004**, *20*, 211–7.
73. Zhang, Z.; Chao, T.; Jiang, S. *J. Phys. Chem. B* **2008**, *112*, 5327–5332.
74. Zhang, Z.; Chao, T.; Cheng, G.; Ratner, B. D.; Jiang, S. *J. Biomater. Sci., Polym. Ed.* **2009**, *20* (13), 1845–1859.
75. Kudaibergenov, S.; Jaeger, W.; Laschewsky, A. In *Supramolecular Polymers Polymeric Betains Oligomers*; Springer-Verlag Berlin: Berlin, 2006; Vol. 201, pp 157–224.
76. Wielema, T. A.; Engberts, J. *Eur. Polym. J.* **1987**, *23*, 947–950.
77. Wielema, T. A.; Engberts, J. *Eur. Polym. J.* **1990**, *26*, 415–421.
78. Wielema, T. A.; Engberts, J. *Eur. Polym. J.* **1990**, *26*, 639–642.
79. Nishiyama, N.; Suzuki, K.; Yoshida, H.; Teshima, H.; Nemoto, K. *Biomaterials* **2004**, *25*, 965–969.
80. Carr, L.; Cheng, G.; Xue, H.; Jiang, S. Y. *Langmuir* **2010**, *26*, 14793–14798.
81. Olsen, S. M.; Pedersen, L. T.; Laursen, M. H.; Kiil, S.; Dam-Johansen, K. *Biofouling* **2007**, *23*, 369–383.
82. Fusetani, N. *Nat. Prod. Rep.* **2011**, *28*, 400–410.
83. Vaisocherova, H.; Zhang, Z.; Yang, W.; Cao, Z. Q.; Cheng, G.; Taylor, A. D.; Piliarik, M.; Homola, J.; Jiang, S. Y. *Biosens. Bioelectron.* **2009**, *24*, 1924–1930.
84. Vaisocherova, H.; Yang, W.; Zhang, Z.; Cao, Z. Q.; Cheng, G.; Piliarik, M.; Homola, J.; Jiang, S. Y. *Anal. Chem.* **2008**, *80*, 7894–7901.
85. Zhang, Z.; Cheng, G.; Carr, L. R.; Vaisocherova, H.; Chen, S. F.; Jiang, S. Y. *Biomaterials* **2008**, *29*, 4719–4725.
86. Cheng, G.; Xite, H.; Zhang, Z.; Chen, S. F.; Jiang, S. Y. *Angew. Chem., Int. Ed.* **2008**, *47*, 8831–8834.
87. Handa, P.; Fant, C.; Nyden, M. *Prog. Org. Coat.* **2006**, *57*, 376–382.
88. Lewis, A. L.; Willis, S. L.; Small, S. A.; Hunt, S. R.; O’Byrne, V.; Stratford, P. W. *Bio-Med. Mater. Eng.* **2004**, *14*, 355–370.
89. Kamenska, E.; Kostova, B.; Ivanov, I.; Rachev, D.; Georgiev, G. *J. Biomater. Sci., Polym. Ed.* **2009**, *20*, 181–197.
90. Johnston, E. E.; Bryers, J. D.; Ratner, B. D. *Langmuir* **2005**, *21*, 870–881.

## Chapter 8

# Elemental Analysis of a Variety of Dried, Powdered, Kelp Food Supplements for the Presence of Heavy Metals via Energy-Dispersive X-ray Fluorescence Spectrometry

Danielle M. Garshott,\* Elizabeth A. MacDonald,  
Meghann N. Murray, Mark A. Benvenuto,  
and Elizabeth S. Roberts-Kirchhoff

Department of Chemistry & Biochemistry, University of Detroit Mercy,  
Detroit, Michigan 48221

\*E-mail: garshodm@udmercy.edu

Seventeen samples of kelp supplement powders and capsules presumed to contain significant trace amounts of heavy metals were analyzed via energy dispersive x-ray fluorescence spectrometry and examined for the following elements: arsenic, mercury and lead. In order for the XRF to determine accurate percent compositions, a method was built from a set of standards produced for each of the three heavy metals in question. The methodology for developing the standards is discussed. Of the seventeen samples studied none were found to contain any significant amounts of lead or mercury. Detectable levels of arsenic that exceeded both the EPA's and AHPA's suggested reference doses were present in every sample, ranging from 10.5 ppm to 43.2 ppm.

## Introduction

Kelp generally refers to a species of large, brown algae (class Phaeophyceae) that grows on the clear, rocky, shallow ocean shorelines predominantly in the Pacific; although also in the Atlantic. Kelp grows abundantly in underwater kelp forests. There are roughly 30 different kinds of kelp growing in oceanic waters. The four primary kelp species found in kelp supplements, all of which

were included in this study, are *Laminaria digitata* (oarweed), *Fucus vesiculosus* (Bladderwrack), *Laminaria japonica* (Hoku Kombu) and *Ascophyllum nodosum* (Norwegian kelp). Unlike a traditional plant, kelp does not have true roots. Instead the algae attaches to rocks on the ocean floor by way of small fingerlike projections called holdfasts. Kelp flourishes in temperate and arctic waters (below 20 °C), and is capable of growing up to a half a meter a day. Over the years, kelp has been used in large amounts for the production of soaps and glass (1). In Scotland in the 1800s kelp was burned as the industry's primary source for sodium carbonate (1). Alginate is a carbohydrate derived from kelp. It has been used as a thickening agent in many household products including ice cream, jelly, and toothpaste (2). For many years the Japanese have been a frequent consumer of kelp; as it is an important ingredient in their cuisine (3). China became the largest producer of *Laminaria*, from 1950s to 1980s, when their kelp production increased exponentially from 60 to over 250,000 dry weight metric tons annually. The eastern world was the first to introduce the use of kelp as an added dietary supplement. The trend soon spread across the world as people have become more health conscious.

Kelp was originally harvested directly from its natural aquatic forest habitats. In the 1940s Japanese experts, working with Chinese connoisseurs, began experimenting with kelp farming (4). Kelp farming was not established on a large scale until the 1950s, once natural landscape interferences were overcome (4). Due to the increased demand for kelp supplements, kelp farms have become common along coastal shore lines.

Farming of kelp begins with seedling production in a kelp hatchery. Seawater temperatures are controlled and maintained at 20 °C. Fertilizers of nitrates and phosphates are added, and other species of algae are removed. When water temperatures decline further, the seedlings, attached to a substrate, are transplanted to the surface of a rope that is anchored to the ocean floor (no more than 10 m deep) in a containment area known as a kelp farm (4). Note that these kelp farms are not isolated from the rest of the ocean and its natural currents. Once the kelp has matured, it is harvested from the ropes and dried in the sun. It is later ground into a fine powdery substance to be packaged and sold as a supplement (4).

Kelp that is sold for medicinal use as a dietary supplement is claimed to be a good source of iodine and vitamins, and rich in nutrients. Many people consume kelp as a non-prescription treatment for thyroid malfunction, and to maintain healthy metabolism and glandular function. Kelp has been used to treat rheumatic pain, and strengthen the immune system. The sodium alginate ( $\text{NaC}_6\text{H}_7\text{O}_6$ ) found in the cellular walls of brown algae can chelate from the body harmful chemicals and heavy metal pollutants (5). It should be noted as well that sodium alginate is an effective chelator for removing radioactive toxins from the body; such would include iodine-131 and strontium-90 (5). Unproven claims regarding kelp's ability to chelate all heavy metal induce major criticism about how safe the end products are, whether they are being properly manufactured, the potential for toxicity of heavy metals because of kelp's nature to extract such from the ocean waters, and safe regulation by the FDA.

The FDAs regulation of dietary supplements is as follows: “FDA regulates dietary supplements under a different set of regulations than those covering “conventional” foods and drug products (prescription and over-the-counter). Under the Dietary Supplement Health and Education Act of 1994 (DSHEA), the dietary supplement manufacturer is responsible for ensuring that a dietary supplement is safe before it is marketed. FDA is responsible for taking action against any unsafe dietary supplement product after it reaches the market. Generally, manufacturers do not need to register their products with FDA nor get FDA approval before producing or selling dietary supplements. Manufacturers must make sure that product label information is truthful and not misleading (6).”

Heavy metals are defined as any chemical element that has a specific gravity five times that of water. This subset of elements exhibit metallic properties, and are toxic at low concentrations. Many heavy metals are found naturally in our environment, while others appear as a result of human pollution (7). Organisms, including humans, require certain quantities of heavy metals to survive, such as iron, cobalt, copper, and manganese. This is not the case for all heavy metals, and some of them are dangerous to the body, even at low concentrations. These toxic elements include arsenic, mercury, and lead. Humans are exposed to a number of heavy metals on a daily basis through consumption and inhalation (7). Constant exposure to these metals can lead to a buildup in the body, ultimately resulting in toxicity or even death. This study looks primarily at the presence of arsenic, lead and mercury in kelp supplements.

Lead and mercury accumulate in the soft tissues of the body, with eventual toxicity occurring. Lead accumulates in tissues such as bone, the brain, kidneys, blood and thyroid gland. Mercury builds up in the kidneys and the brain (7). Toxicity occurs if ingested amounts of these heavy metals are greater than the background concentrations that are found in nature.

Broadly, there are two types of arsenic that exist, organic and inorganic. Little is known about the effects of organic arsenic on the human body, through government agencies such as the Department of Health and Human Services (DHHS), the International Agency for Research on Cancer (IARC) and the Environmental Protection Agency (EPA) have classified inorganic arsenic as a known human carcinogen (8, 9). Inorganic arsenic can exist as one of two valencies, either arsenite or arsenate (Figure 1). Arsenite is a chemical compound that contains an arsenic oxoanion, with arsenic having a valency of 3, As(III). Arsenite is considered to be mobile and is most commonly found in waters with high levels of methane or sulfide (10). Arsenate, sometimes referred to as pentavalent arsenic, As(V), is a salt or ester of arsenic acid. Arsenate is a stable compound, commonly found in aerobic water (10). Arsenate poisoning, in particular, is of concern. “Arsenate can replace inorganic phosphate in the step of glycolysis that produces 1,3-bisphosphoglycerate, yielding 1-arseno-3-phosphoglycerate instead. This molecule is unstable and quickly hydrolyzes, forming the next intermediate in the pathway, 3-phosphoglycerate. Therefore glycolysis proceeds, but the ATP molecule that would be generated from 1,3-bisphosphoglycerate is lost - arsenate is an un-coupler of glycolysis, explaining its toxicity (11).”

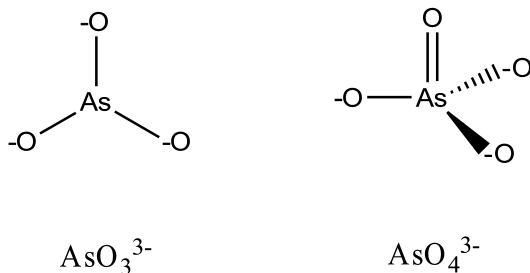


Figure 1. Inorganic forms of arsenic. Arsenite ion, As (III) [left]; and arsenate ion, As (V) [right] (10).

Nine over-the-counter herbal kelp products were studied by UC Davis public health personnel. The findings concluded that medicinal use of herbal kelp supplements may inadvertently cause arsenic poisoning (12, 13). This study was the result of a case study of a 54 year-old woman seen at UC Davis Occupational Medicine Clinic with symptoms of arsenic poisoning: worsening alopecia, fatigue and memory loss (two year history) (12, 13). It was documented that the woman was taking a variety of herbal therapies, but over the course of her illness, the kelp supplement was the only one taken regularly. Over the course of several months, the woman experienced a severe impairment of her short- and long-term memory. At one point, she could no longer recall her home address (12, 13). Other symptoms included rash, nausea and vomiting (12, 13). When the woman's physician could not determine a diagnosis, she increased her dosage of kelp from two to four pills a day (12, 13). Laboratory tests determined, the presence of arsenic in the woman's blood and urine (83.6  $\mu\text{g/g}$  creatinine; normal < 50  $\mu\text{g/g}$ ) (13). The woman immediately discontinued the use of the kelp supplements. In a matter of weeks, her symptoms were gone, and within a few months the arsenic was no longer detectable in her urine; arsenic levels in the blood also dropped significantly (12, 13). "It's unfortunate that a therapy that's advertised as contributing to 'vital living and well being' would contain potentially unsafe levels of arsenic," said Marc Schenker, a professor of Public Health Sciences and a leading authority on occupational and environmental diseases and respiratory illness (12). Of the nine kelp supplements originally studied, eight of them were found to contain detectable amounts of arsenic that were higher than the FDA tolerance level of 0.5-2 ppm (specified food products) (12).

## Experimental Methods

A set of pure standards, each varying in concentration but measured in parts per million, was developed for arsenic, lead and mercury. Each group consisted of seven standards with the following concentrations: 5.0, 20.0, 50.0, 100.0, 250.0, 500.0 and 1000.0 ppm. The solid reference samples did not yield reproducible results, and were therefore replaced by liquid reference samples. Three certified AA standard solutions were used: arsenic trioxide (1000.0 ppm), lead (1000.0 ppm) and mercuric oxide (1000.0 ppm). Eight standards were prepared for each metal at varying concentrations: 5.0, 20.0, 50.0, 100.0, 250.0, 500.0, 750.0 and 1000.0 ppm. A 30-mL sample of each concentration was prepared by dilution with distilled water. Each standard was stirred vigorously for 15 minutes to ensure a homogenous dilution. A 5-mL aliquot of each standard was transferred into a XRF sample container. The calibration parameters were set as follows: linear analysis, generation of conditions, concentrations, uncertainty, peak intensities, and background intensities. The conditions most suitable for each analyte were determined. The sample excitation conditions were: 28 kV, 0.14 mA, 100 sec count,  $L_{\alpha\beta}$ , Pd thick filter, Mid Z conditions for lead and mercury; and 48 kV, 0.24 mA, 100 sec count,  $K_{\alpha}$ , Pd thick filter, High Zb condition for arsenic.

Most of the samples studied were purchased in capsule form. Only samples that contained kelp and no other fillers or additives were used. Before any of the samples could be analyzed via EDXRF, the capsules were opened and the kelp transferred into light sensitive amber vials. The kelp powder from each capsule was individually mixed in a coffee grinder to ensure homogeneity. Five 800-mg samples were transferred into five XRF sample containers for analysis. The five samples were taken at random from the bulk sample of a given product. The concentration was reported as the average of the five different trials. Note that of the seventeen products studied, there were two sets from the same manufacturer: K4.1, K4.2 and K7.1, K7.2 (shown in Table I). By studying samples from the same manufacturer, but of different batch numbers, we were able to examine variations in heavy metal composition between batches.

**Table I. Details of the kelp supplements**

<i>Sample ID</i>	<i>Product Name</i>	<i>Manufacturer</i>	<i>Species of Kelp</i>	<i>Country of Origin</i>
K 1.1	Kelp Powder	Marine Coast Sea Vegetables	<i>Laminaria digitata</i>	North Atlantic
K 2.1	Kelp	Nature's Way	<i>Ascophyllum nodosum</i>	unknown
K 3.1	Sea Kelp	Nature's Herbs	<i>Fucus vesiculosus</i>	unknown
K 4.1	Kelp Plant	Christopher's Original Formulas	<i>Ascophyllum nodosum</i>	unknown
K 4.2	Kelp Plant	Christopher's Original Formulas	<i>Ascophyllum nodosum</i>	unknown
K 5.1	Kelp Powder	Now Foods	<i>Laminaria digitata and Ascophyllum nodosum</i>	unknown
K 6.1	Atlantic Kelp	StarWest Botanicals	<i>Ascophyllum nodosum</i>	unknown
K 7.1	Kelp	Herbal Extract Plus	unknown	unknown
K 7.2	Kelp	Herbal Extract Plus	unknown	unknown
K 9.1	Kelp Caps	Now Foods	<i>Laminaria digitata and Ascophyllum nodosum</i>	unknown
K 10.1	Kelp	Bulk Herb Store	unknown	unknown
K 11.1	Organic Kelp Powder	Sharp Labs	<i>Ascophyllum nodosum</i>	Iceland
K 12.1	Bladderwrack Powder	Marine Coast Sea Vegetables	<i>Fucus vesiculosus</i>	North Atlantic
K 13.1	Kelp Powder Organic	StarWest Botanicals	<i>Ascophyllum nodosum</i>	Canada
K 14.1	Pure Brown Seaweed Extract	Modifilan	<i>Laminaria japonica</i>	Northern Pacific
K 15.1	Kelp Powder	Health Herbs	<i>Ascophyllum nodosum</i>	France
K 16.1	Kelp Powder	Plum Flower	<i>Laminaria japonica</i>	unknown



## Results and Discussion

For lead, the daily ingestion was compared to the US Pharmacopeia (USP) specifications for the maximum allowable lead content (4.5- $\mu\text{g}$ ) in a 1500-mg dose of calcium carbonate (14). For mercury and arsenic, the daily ingestion was compared to their respective Environmental Protection Agency established reference doses (RfDs) for oral chronic exposure (0.3  $\mu\text{g}/\text{kg}$  per day for both mercuric chloride and arsenic) (15). The daily ingestion of lead, mercury and arsenic was also compared to the American Herbal Product Association's (AHPA) recently suggested limits of arsenic (10  $\mu\text{g}/\text{day}$ ), lead (10  $\mu\text{g}/\text{day}$ ) and mercury (2.0  $\mu\text{g}/\text{day}$ ) (16).

Seventeen kelp supplement products were analyzed for the presence of heavy metals arsenic, lead and mercury. Of these seventeen samples, none of them contained detectable amounts of lead or mercury. They did however all contain detectable amounts of arsenic, which supports the findings of previous studies and case reports of potential arsenic poisoning secondary to kelp supplement ingestion (17–25). The calculated average concentrations of arsenic found in each of the seventeen samples are listed in Tables II and III. The arsenic levels detected range from 10.5 to 43.2 ppm. For ten of the seventeen samples the approximate daily amount of arsenic (in micrograms) that would result from following the manufactures recommended daily dose revealed all exceeded the AHPA's suggested limits. Of the ten, only two manufacturer samples fell just outside of these limitations (17.3 and 13.6  $\mu\text{g}/\text{day}$ ). The remaining samples revealed the daily ingestion of arsenic to range from 25.9 to 129.7 ppm; exponentially higher than the AHPA's suggested limits.

Figure 2 shows that the concentration of arsenic in products from the same manufacturer can vary both slightly and significantly (i.e., K 4.1, K 4.2 and K7.1, K7.2). Therefore, just because a specific product has a certain concentration of arsenic in one batch, does not mean it can be extrapolated to the next; every batch will be unique.

Being that all seventeen samples contained detectable amounts of arsenic far exceeding suggested reference doses, the EDXRF spectra files were studied extensively to make sure the instrument software was not misinterpreting data. In energy dispersive x-ray fluorescence spectrometry, the x-ray emitted as a result of the collapsing outer electron orbitals is unique to an element at a particular energy level (keV). It is however plausible, due to the limitations of the instrument, that two element's alpha and beta lines (K or L) can overlap thus resulting in software data misinterpretation. An example of such a case would be the  $K_{\alpha}$  line of arsenic (10.532 keV) and the  $L_{\alpha}$  line of lead (10.549 keV). Often the software will read the spectrum line as lead instead of arsenic. Another way to clarifying the presence of a particular element is to study the spectra for the occurrence of both  $K_{\alpha}/K_{\beta}$  or  $L_{\alpha}/L_{\beta}$  lines. Two findings were evidence that the instrument was reading arsenic and not lead. The first being there was no  $L_{\beta}$  line present for lead, but both  $K_{\alpha}$  and  $K_{\beta}$  lines were present for arsenic. Secondly, the average concentration of arsenic across all samples was significantly higher than the instruments lower limit of detection (2 ppm). With these clarifications there is no reason to believe these findings were artificially extrapolated in any way.

**Table II. Concentration of arsenic in the kelp supplements for which packaging did not provide a manufacturer recommended daily dosage or usage instructions**

<i>Sample ID</i>	<i>Average ppm*</i>	<i>Serving Size</i>	<i>Total As (μg) Per Package</i>
K 1.1	37.4 ± 2.3	Net Wt. 454.0 g	16,965.5
K 10.1	29.5 ± 1.6	Net Wt. 227.0 g	6,704.9
K 11.1	26.2 ± 2.5	Net Wt. 454.0 g	11,881.6
K 12.1	28.2 ± 1.7	Net Wt. 454.0 g	12,808.7
K 13.1	24.8 ± 1.5	Net Wt. 454.0 g	11,277.4
K 15.1	25.3 ± 1.7	Net Wt. 113.5 g	2,868.9
K 16.1	25.2 ± 1.5	Net Wt. 100.0 g	2,523.4

\* Average Concentration in an 800-mg sample.

**Table III. Concentration of arsenic found in the kelp supplements for which packaging provided a manufacturer recommended daily dosage or usage instructions**

<i>Sample ID</i>	<i>Average ppm*</i>	<i>Serving Size</i>	<i>As (μg) Per day</i>	<i>Total As (μg) Per Package</i>
K 2.1	39.3 ± 3.9	1 capsule/day (660.0 mg)	25.9	4,673.9
K 3.1	42.4 ± 3.6	3 capsules/day (1.92 g)	81.5	2,716.4
K 4.1	26.3 ± 2.2	6 capsules/day (3.45 g)	90.7	1,511.4
K 4.2	26.7 ± 1.9	6 capsules/day (3.45 g)	92.1	1,535.5
K 5.1	43.2 ± 2.9	2 scoops/day (400.0 mg)	17.3	9,810.5
K 6.1	28.5 ± 2.3	3 capsules/day (1.5 g)	42.7	1,424.8
K 7.1	10.5 ± 1.5	6 capsules/day (3.6 g)	37.9	379.2
K 7.2	19.4 ± 1.9	6 capsules/day (3.6 g)	69.9	698.5
K 9.1	27.1 ± 1.6	1 capsule/day (500.0 mg)	13.6	3,393.5
K 14.1	43.2 ± 1.6	6 capsules/day (3.0 g)	129.7	1,946.2

\* Average Concentration in an 800-mg sample.

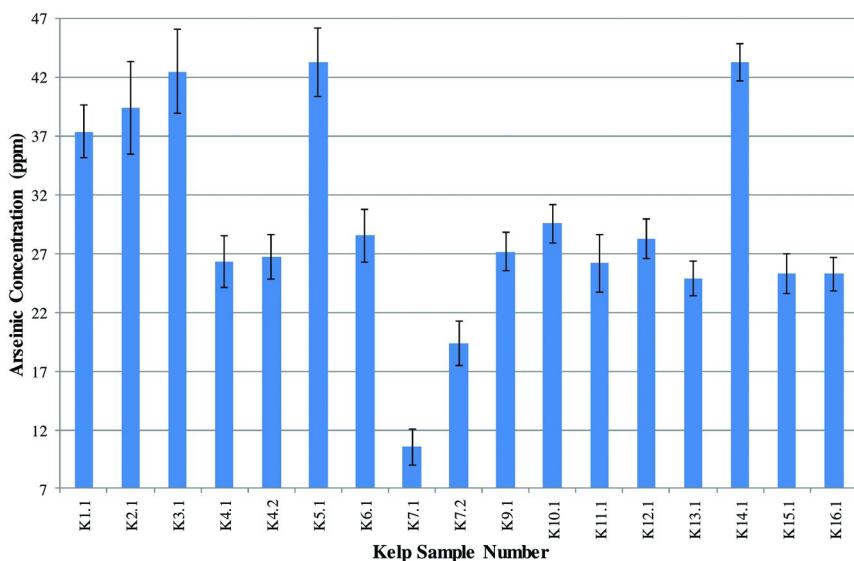


Figure 2. The average arsenic concentration found in the kelp supplements studied (samples K4.1 and K4.2 were the same product, from the same manufacturer, but different lot numbers, as are samples K7.1 and K7.2).

## Conclusions

Arsenic concentrations in the dietary supplements, at the manufacturer's recommended daily dosage, were found to be exponentially higher than the AHPA's arsenic reference dose of 10  $\mu\text{g}$  per day. The problem often arises, as was the case with the 54-year-old woman, when consumers do not adhere to the manufacturer's recommended daily dose. The misconception amongst most consumers is that kelp supplements, along with many other dietary supplements, are natural herbs and therefore 'the more I take the better the results will be'. There are two problems with this logic. First, just because something is found in nature does not mean that it does not contain trace amounts of substances that can be harmful to the body. Arsenic is found both naturally occurring, but also as a result of pollution. Kelp naturally chelates heavy metals out of the ocean water; this is one of the original purposes for growing it. Thus, the kelp being consumed has heavy metals chemically bound within its composition. The arsenic found in the kelp is from either natural sources or polluted waste by-products from industries located along the coastlines. The second problem is, the more the kelp supplement consumed (any dietary supplement for that matter), the faster the concentrations of those trace substances could potentially build up in the body. Initially the likelihood of arsenic toxicity actually occurring within the consumer's lifetime was very slim, but now due to over consumption of the product; there is an increased risk of toxicity in a reduced amount of time. It should be noted that the concentrations of arsenic presented here do not indicate amounts of organic

versus inorganic arsenic. The organic arsenic is rather nonhazardous to the human body, while inorganic arsenic is dangerous if allowed to accumulate within the tissues.

## Acknowledgments

Technical and analytical support by Bill Jambard and Randy Cohn at Thermo Fischer Scientific, as well as Gabe Kelly and Dr. Guy Wicker at Capital Assay Inc. was greatly appreciated. This research would not have been possible without the financial support of the University of Detroit Mercy.

## References

1. Clow, A.; Clow, N. *The Chemical Revolution: A Contribution to Social Technology*; Batchworth Press: London, 1952; pp 65–90.
2. Powers, J.; Ronald, S.; Robert, G. *Craig's Restorative Dental Materials*, 12th ed.; Powers, J., Ronald, S., Eds.; Mosby Elsevier: Kansas City, MO, 2006; p 270.
3. Kazuko, E. *Japanese Cooking: The Tradition, Techniques, Ingredients and Recipes*; Hermes House: London, 2002; p 78.
4. Chen, J. Cultured Aquatic Species Information Programme, *Laminaria japonica*, 2009. FAO Fisheries and Aquaculture Department. [http://www.fao.org/fishery/culturedspecies/Laminaria\\_japonica/en](http://www.fao.org/fishery/culturedspecies/Laminaria_japonica/en) (accessed December 1, 2009).
5. Sutton, A.; Harrison, G.; Carr, T.; Barltrop, D. Reduction in the absorption of dietary strontium in children by an alginate derivative. *J. Radiol.* **1971**, *44*, 567.
6. Dietary Supplements, 2009. U.S Department of Health and Human Services, FDA US Food and Drug Administration. <http://www.fda.gov/food/DietarySupplements/default.htm> (accessed December 9, 2009).
7. Heavy Metals, 2009. Physicians for Social Responsibility. <http://www.psr.org/environment-and-health/confronting-toxics/heavy-metals> (accessed June 2010).
8. Inorganic Arsenic: Toxicity and Exposure Assessment for Children's Health Chemical Summary. U.S. Environmental Protection Agency. [http://www.epa.gov/teach/chem\\_sum/Arsenic\\_summary.pdf](http://www.epa.gov/teach/chem_sum/Arsenic_summary.pdf) (accessed June 14, 2011).
9. Occupational Safety and Health Guideline for Arsenic. United States Department of Labor. <http://www.osha.gov/SLTC/healthguidelines/arsenic/recognition.html> (accessed June 14, 2011).
10. Lytle, D.; Sorg, T.; Frietch, C. Accumulation of arsenic in drinking water distribution systems. *Environ. Sci. Technol.* **2004**, *38*, 5365–5372.
11. Case Studies in Environmental Medicine. Arsenic Toxicity, 2009. Agency for Toxic Substances and Disease Registry. <http://www.atsdr.cdc.gov/csem/arsenic/docs/arsenic.pdf> (accessed April 28, 2011).

12. Amster, E.; Tiwary, A.; Schenker, M. Case report: Potential arsenic toxicosis secondary to herbal kelp supplement. *Environ. Health Perspect.* **2007**, *115*, 606–608.
13. Washam, C. Peril of the shallows? Elevated arsenic in kelp supplements. *Environ. Health Perspect.* **2007**, *115*, 212.
14. *USP 27 NF 22-2004 United States Pharmacopeia: National Formulary*; United States Pharmacopeial: Rockville, MD, 2003.
15. Integrated Risk Information System. US Environmental Protection Agency. <http://www.epa.gov/iris> (accessed March 17, 2009).
16. AHPA Adopts New Trade Recommendation; Guidance on Heavy Metal, Microbiological Limits, 2008. American Herbal Products Association. <http://www.ahpa.org/> (accessed March 25, 2009).
17. Federal Food and Drugs Act of 1906, 1934. U.S. Department of Health and Human Services: FDA US Food and Drug Administration. <http://www.fda.gov/regulatoryinformation/legislation/ucm148690.htm> (accessed June 2010).
18. Palmer, P.; Jacobs, R.; Baker, P.; Ferguson, K.; Webber, S. Use of field-portable XRF analyzers for rapid screening of toxic elements in FDA-regulated products. *J. Agric. Food Chem.* **2009**, *57*, 2605–2613.
19. Dolan, S.; Nortrup, D.; Bolger, M.; Caper, S. Analysis of dietary supplements for arsenic, cadmium, mercury, and lead using inductively coupled plasma mass spectrometry. *J. Agric. Food Chem.* **2003**, *51*, 1307–1312.
20. Clark, S.; Menrath, W.; Chen, M.; Roda, S.; Succop, P. Use of a field portable X-ray fluorescence analyzer to determine the concentration of lead and other metals in soil samples. *Ann. Agric. Environ. Med.* **1999**, *6*, 27–32.
21. Levine, E.; Levine, M.; Weber, F.; Hu, Y.; Perlmutter, J.; Grohse, P. Determination of mercury in an assortment of dietary supplements using an inexpensive combustion atomic absorption spectrometry technique. *J. Autom. Methods Manage. Chem.* **2005**, *4*, 211–216.
22. Goldstein, S.; Slemmons, A.; Canavan, H. Energy dispersive X-ray fluorescence methods for environmental characterization of soils. *Environ. Sci. Technol.* **1996**, *30*, 2318–2321.
23. Saper, R.; Kales, S.; Paquin, J. Heavy metal content of ayurvedic herbal medicine products. *JAMA, J. Am. Med. Assoc.* **2004**, *292*, 2868–2873.
24. Saper, R.; Phillips, R.; Sehgal, A.; Khouri, N.; Davis, R.; Paquin, J.; Thuppil, V.; Kales, S. Lead, mercury, and arsenic in US- and Indian-manufactured ayurvedic medicines sold via the Internet. *JAMA* **2008**, *300*, 915–923.
25. Woolf, A.; Hussain, J.; McCullough, L.; Petranovic, M.; Chomchai, C. Infantile lead poisoning from an Asian tongue powder: A care report and subsequent public health inquiry. *Clin. Technol.* **2008**, *46*, 841–844.

# Editors' Biographies

## Mark A. Benvenuto

Mark A. Benvenuto is a Professor of Chemistry at the University of Detroit Mercy, in the Department of Chemistry & Biochemistry. His research thrusts span a wide array of subjects, but include the use of energy dispersive X-ray fluorescence spectroscopy to determine trace metal elements in land-based and aquatic plant matter, in relation to such materials being used in phyto-remediation of soils.

Benvenuto received a B.S. in chemistry from the Virginia Military Institute, and after several years in the Army, a Ph.D. in inorganic chemistry from the University of Virginia. After a post-doctoral fellowship at the Pennsylvania State University, he joined the faculty at the University of Detroit Mercy in 1993.

## Elizabeth S. Roberts-Kirchhoff

Elizabeth S. Roberts-Kirchhoff is Associate Professor of Chemistry and Biochemistry at the University of Detroit Mercy. Her research interests include the mechanism of action of cytochrome P450 enzymes including their role in the metabolism of drugs and natural products and the investigation of heavy metals in health supplements including kelp, clay, and protein powders.

Roberts-Kirchhoff received a B.S. in Chemistry from Texas A & M University and a Ph.D. in Biological Chemistry from the University of Michigan. After postdoctoral research at Wayne State University and The University of Michigan, she joined the faculty at the University of Detroit Mercy in 1997.

## Meghann N. Murray

Meghann N. Murray has a position and conducts research in the department of Chemistry & Biochemistry at University of Detroit Mercy. She received her B.S. and M.S. degrees in Chemistry from the University of Detroit Mercy and is certified to teach high school chemistry and physics. She has taught in programs such as the Detroit Area Pre-College and Engineering Program. She has been a judge and mentor with the Science and Engineering Fair of Metropolitan Detroit, FIRST Lego League and FRC Robotics. She is currently the chair of the Younger Chemists Committee and Treasurer of the Detroit Local Section of the American Chemical Society.

## Danielle M. Garshott

Danielle M. Garshott was born in Garden City and raised in Milford, Michigan. She attended the University of Detroit Mercy, where she received a B.S. in Biochemistry, Honors Program in 2011. She currently works as a research technician at Wayne State University's School of Medicine, Department of Pediatrics. Danielle intends to enter into a neuroscience doctoral program in the next year.

# Subject Index

## A

- AAS. *See* Atomic absorption spectrophotometer (AAS)  
AHPA. *See* American Herbal Product Association (AHPA)  
Aksarben soil, 6  
Alginate, 124  
Alkanethiolates, SAM on gold surfaces, 100  
American Herbal Product Association (AHPA), 129  
Antifouling surfaces  
  comparison, 102  
  copolymer, 102  
  polymer brushes, 101  
  SAM, 100  
Arsenate, 125  
Arsenite ion, 126  
ASA. *See* Standards of aspirin (ASA)  
*Ascophyllum nodosum*, 123  
Aspirin, 56  
Atomic absorption spectrophotometer (AAS), 39  
Atom transfer radical polymerization (ATRP), 101  
Atrazine  
  adsorption isotherms, 12  
  NNAT adsorption and desorption in soil at different pH levels, 13<sup>f</sup>  
  organic carbon partition coefficients, 13<sup>t</sup>  
ATRP. *See* Atom transfer radical polymerization (ATRP)

## B

- Balanus amphitrite*, 109  
BC. *See* Bioconcentration (BC) factors  
Betaine polymers, 102  
  copolymer formulation, 107<sup>s</sup>  
  functionalizable, 115  
  hydrolyzable, 116  
  releasing incorporated active agents, 117  
  structural design, 113  
Bioconcentration (BC) factors, 35, 45  
  Cd<sup>2+</sup> and Pb<sup>2+</sup> treatments, 30<sup>t</sup>  
Biofouling, 97  
1,3-Bisphosphoglycerate, 125  
*Brassica juncea*, 35  
  analysis, 39

- biomass experiment, 40  
  dried plant samples, 42  
  hydroponic growth experiments with “high Ca” or “low Ca”, 36  
  hydroponic tank experiments for growth experiments, 38<sup>t</sup>  
  hyperaccumulation, 36  
  observations and sampling, 38  
  plant harvest, 39  
  plant health and total biomass per tank, 41<sup>t</sup>  
  sample preparation, 39  
  treatment growth period, 37

## C

- Calcium ion, 35  
Castaic Lake Water Agency (CLWA), 65  
  fluorescence regional integration analysis, 73<sup>f</sup>  
  polarity rapid assessment method analysis, 72<sup>f</sup>  
  ultrafiltration (UF) analysis, 71<sup>f</sup>  
CHP. *See* Citrated human plasma (CHP)  
Citrated human plasma (CHP), 110  
CLWA. *See* Castaic Lake Water Agency (CLWA)  
Creative Scientific Inquiry Experience  
  class project, 54  
  GC-MS analysis, 56  
  materials and methods, 54  
  outcomes and assessment, 58  
  overview, 51  
  quantitative analysis, 52  
  water analysis project, 53  
Crude oil  
  equilibrate with Gulf of Mexico water, 92  
  photochemical transformation, 83

## D

- DBA. *See* Dibutylamine (DBA)  
DCM. *See* Dichloromethane (DCM)  
Deepwater horizon biodegradation, 82  
Deepwater horizon oil, 82  
  experimental materials and methods, 84  
  GC analysis, 88  
  GC-FID analysis, 89<sup>f</sup>



- irradiation time, 88*f*  
  loss of fluorescence, 91*f*  
  toxicity of water exposed to oil, 92*f*  
results and discussion, 86  
sampling location, 85*f*  
surface oil being collected, 87*f*
- DEET. *See* N,N-Diethyl-*m*-toluamide (DEET)
- Deionized (DI) water, 21
- Department of Health and Human Services (DHHS), 125
- DHHS. *See* Department of Health and Human Services (DHHS)
- DI. *See* Deionized (DI) water
- Dibutylamine (DBA), 9
- Dichloromethane (DCM), 84
- Dietary Supplement Health and Education Act of 1994 (DSHEA), 125
- Dinitrogen trioxide, 4
- Dissolved organic carbon (DOC), 66
- Dissolved organic matter (DOM), 62  
  characteristics, 68  
  fluorescence regional integration regions, 67*t*  
  illustration of binding behavior, 63*f*  
  natural water, 64  
  transformation, 62  
  ultrafiltration to measure size fraction, 66
- DOC. *See* Dissolved organic carbon (DOC)
- DOM. *See* Dissolved organic matter (DOM)
- DSHEA. *See* Dietary Supplement Health and Education Act of 1994 (DSHEA)
- E**
- E. coli* B bacteria, 21  
  mechanism of electrochemical disinfection, 22
- EDTA. *See* Ethylenediaminetetraacetic acid (EDTA)
- EEM. *See* Excitation-emission matrix (EEM)
- Environmental Protection Agency (EPA), 125
- EPA. *See* Environmental Protection Agency (EPA)
- EPS. *See* Extracellular polymeric substances (EPS)
- Escherichia coli*, 110
- Ethylenediaminetetraacetic acid (EDTA), 36, 37
- effect on plant uptake of toxic ions, health, and biomass, 42
- Excitation-emission matrix (EEM), 65
- Extracellular polymeric substances (EPS), 109
- F**
- FBS. *See* Fetal bovine serum (FBS)
- Fetal bovine serum (FBS), 110
- Fe-transporting chelators, 36
- Fibrinogen (Fg), adsorption values, 105*f*
- Fluorescence quenching, 68, 68*f*  
  determine KDOM, 74
- Fluorescence spectroscopy, 67
- Fucus vesiculosus*, 123
- Fulvic acid, 9
- G**
- GC-MS analysis, 56
- H**
- H. *See* Hydrogen (H)
- Herbicide atrazine, 5
- Herbicides, 5
- Hewlett-Packard, 85
- HOP. *See* Hydrophobic organic pollutants (HOP)
- HPLC analysis, 7
- Hydrogen (H), 22
- Hydrophobic organic pollutants (HOP), 62  
  analytical methods, 64  
  determination, 67  
  fluorescence spectroscopy, 67  
  illustration of binding behavior, 63*f*  
  KDOM analysis methods, 66  
  PRAM, 66  
  sample preparation, 65
- Hydroponic nutrient solutions, 36  
  measurement of selected ions, 39
- Hydroxyl radicals, 23
- Hyperaccumulators, 36
- I**
- IARC. *See* International Agency for Research on Cancer (IARC)

IBU. *See* Ibuprofen (IBU)  
Ibuprofen (IBU), 54  
International Agency for Research on  
Cancer (IARC), 125  
Ixtoc I exploratory well, 82

## K

KDOM analysis methods, 66  
Kelp food supplements  
concentration of arsenic, 130*t*  
details supplements, 128*t*  
experimental methods, 127  
farming, 124  
FDAs regulation, 125  
medicinal use, 124  
overview, 123  
results and discussion, 129

## L

LAL. *See* Limulus Amebocyte Lysate  
(LAL)  
*Laminaria digitata*, 123  
*Laminaria japonica*, 123  
LBWD. *See* Long Beach Water Department  
(LBWD)  
Limulus Amebocyte Lysate (LAL), 113  
Long Beach Water Department (LBWD),  
65  
fluorescence regional integration  
analysis, 73*f*  
polarity rapid assessment method  
analysis, 72*f*  
ultrafiltration (UF) analysis, 71*f*  
LS 55 luminescence spectrometer, 86

## M

Marine and hydrokinetic (MHK), 97  
MHK. *See* Marine and hydrokinetic (MHK)  
Microtox<sup>®</sup>, 86  
ModBlock digestion apparatus, 39  
Molecular weight cut off (MWCO), 66  
MWCO. *See* Molecular weight cut off  
(MWCO)

## N

N-Alkanes, boiling point and vapor  
pressure, 89*t*  
NAP. *See* Naproxen (NAP); Nitrosation  
assay procedure (NAP)  
Naproxen (NAP), 54  
*Navicula perminuta*, 109  
Nitric oxide (NO), 4  
Nitrosamines, 4  
Nitrosation, 4  
Nitrosation assay procedure (NAP), 6  
Nitrosonium ion, 4  
conversion of nitrite, 4*f*  
Nitrous acidium ion, 4  
NNAT. *See* N-Nitrosoatrazine (NNAT)  
N,N-Diethyl-*m*-toluamide (DEET), 56  
N,N-Dimethyl-*p*-nitrosoaniline (RNO), 21,  
23  
absorption spectra, 27*f*  
N-Nitrosamines, formation, 5*f*  
N-Nitrosoatrazine (NNAT), 3  
adsorption in soil, 7, 12, 14*f*  
aqueous solution, 14  
formation in soil, 11  
formation in solution, 8  
formation in water, 3  
HPLC analysis, 7  
reaction of atrazine and nitrite, 8*f*, 10*f*,  
11*f*, 12*f*  
soil, 16  
degradation, 16*f*, 17*f*  
stability in solution and soil, 7, 14, 15*f*  
water and soil, 6  
NO. *See* Nitric oxide (NO)  
Nonfouling materials, 98  
Non-steroidal anti-inflammatory drugs  
(NSAID), 54  
NSAID. *See* Non-steroidal  
anti-inflammatory drugs (NSAID)  
NSAID concentration, 51

## O

OEG. *See* Oligoethylene glycol (OEG)  
Oligoethylene glycol (OEG), 100  
OmniSolv, 84

## P

PAH. *See* Polycyclic aromatic  
hydrocarbons (PAH)

PDMS. *See* Polydimethylsiloxane (PDMS)  
 PerkinElmer, 86  
 Phytoremediation potential, 45  
 Phytosiderophores, 36  
 Plant shoot  
   ion concentration, 43*f*  
   total uptake of toxic metal, 44*f*  
 Polarity rapid assessment method (PRAM), 66  
 PolyCB acrylamides, 114  
 Polycyclic aromatic hydrocarbons (PAH), 62, 83, 86  
 Polydimethylsiloxane (PDMS), 66, 108  
 Polyethylene glycol (PEG)-based polymers, 98  
 Poly(2-hydroxyethyl methacrylate) (polyHEMA), 98  
 Polymer brushes, 101  
   gold surfaces, 102*s*  
   graft from method, 101  
   vs. random copolymers, 104  
   vs. SAM, 102  
 Poly(2-methyl-2-oxazoline) (PMOXA), 98  
 Poly(*N*-vinyl pyrrolidone) (PVP), 98  
 PolySBMA brushes, 104  
   diatom *Navicula* attached, 111*f*  
 PRAM. *See* Polarity rapid assessment method (PRAM)  
 Protein, resistance after PBS storage for 100 days, 112*f*  
 Protein-resistant coatings, marine organisms, 99*t*  
 Protein-resistant surfaces, 107*t*

**R**

Reference doses (RfD), 129  
 Relative standard deviation (RSD), 90  
 RfD. *See* Reference doses (RfD)  
 River Raisin  
   IBU peak area ratio, 58*f*  
   qualitative results for NSAID, 57*t*  
   sampling location, 55*t*  
 RNO. *See* *N,N*-Dimethyl-*p*-nitrosoaniline (RNO)  
 RSD. *See* Relative standard deviation (RSD)

**S**

*Salmonella typhimurium*, 21  
   bacteria count vs. disinfection time in ammonium sulfate solution, 29*f*  
   bacteria count vs. disinfection time in (NH<sub>4</sub>)<sub>2</sub>SO<sub>4</sub>, 25*f*  
   complete water disinfection time, 30*t*  
   electrolysis of aqueous solution, 26*t*  
   elimination rate constants, 28*t*  
   mechanism of electrochemical disinfection, 22  
   poultry rinsing water contaminated, 25  
   results and discussion, 24  
 SAM. *See* Self-assembled monolayers (SAM)  
 Self-assembled monolayers (SAM), 98, 100  
   fibrinogen adsorption, 103*t*  
   vs. polymer brushes, 102  
 Simazine, 9  
 Soil, 5  
   adsorption of NNAT, 7  
   properties, 6*t*  
   stability in solution, 7  
 Solid phase extraction (SPE), 66  
 Solid phase microextraction (SPME), 64  
 SPE. *See* Solid phase extraction (SPE)  
 Spectrophotometer, 23  
 SPME. *See* Solid phase microextraction (SPME)  
 SPR. *See* Surface plasmon resonance (SPR)  
 Standards of aspirin (ASA), 54  
 Sulfobetaine-based polymers, 107  
   antifouling performance in complex media, 110  
   different pendant groups and main chains, 115*s*  
   highly resist settlement of barnacle cyprids, 109  
   highly resist settlement of diatom cells, 109  
   highly resist the growth of ulva sporelings, 108  
   non-toxic to marine organisms and mammalian cells, 113  
   reduce strength of sporeling attachment, 108  
 Surface plasmon resonance (SPR), 100  
 Synchronous fluorescence scans, 86  
 Synchronous fluorescence spectra, 86

## T

TBT. *See* Tributyltin (TBT)  
 TEGDMA. *See* Tetraethylene glycol dimethacrylate (TEGDMA)  
 Tetraethylene glycol dimethacrylate (TEGDMA), 113

Tetramethylammonium hydroxide (TMAH), 55  
Titanium dioxide, 84  
TMAH. *See* Tetramethylammonium hydroxide (TMAH)  
Total ion chromatograms, 56  
Tributyltin (TBT), 97  
Trihalomethanes, 67  
    analysis before and after drinking water  
    treatment processes for CLWA and LBWD, 69<sup>t</sup>  
    formation potential, 68

## U

UC Davis Occupational Medicine Clinic, 126  
Ulva spores, SBMA coatings, 106<sup>f</sup>  
U.S. Bureau of Ocean Energy Management, 81  
U.S. Environmental Protection Agency (U.S. EPA), 62  
U.S. EPA. *See* U.S. Environmental Protection Agency (U.S. EPA)

USP. *See* US Pharmacopeia (USP)  
US Pharmacopeia (USP), 129

## V

Valentine soil, 12

## W

Water  
    analysis project, 53  
    electrochemical treatment, 22  
    laboratory electrochemical disinfection device, 24<sup>f</sup>  
    samples, 65

## Z

Zwitterionic betaine polymers, 98